Report

GNWT
Fort Good Hope Flood Study

March 31, 2026

CA0044345.8410

Distribution List

1 Electronic Copy: GNWT

1 Electronic Copy: WSP Canada Inc.
1721 8th Street East
Saskatoon, SK, S7H 0T4 Canada
(306) 665-7989:

Acknowledgements

Completion of this study was made possible with the financial support from the Government of Canada under the Flood Hazard Identification and Mapping Program (FHIMP) as well as financial support from the Government of the Northwest Territories (GNWT).

The project team at WSP Canada Inc. is grateful for technical guidance and support from staff at GNWT: Jad Saade, Michele Culhane, Anna Coles, and Benjamin Fisher; Apurba Das at Environment and Climate Change Canada, and Brian Perry at Natural Resources Canada.

We acknowledge the efforts of the members of K'ahsho Got'ı̨nę Foundation staff and all the Guardians who worked with the WSP field crew, Bernadette Weaver and Nathan Hoeve, to complete the field surveys on the Mackenzie River near Fort Good Hope. We would also like to thank the community members who attended engagement meetings and provided information for this study.

Numerous staff within WSP contributed to this study from proposal to completion. We would especially like to thank Laurence Bonin and Ed Hunt from Yellowknife office for stick-handling the bathymetry survey, Curtis Hallborg for his hydrology analysis, and Peter Thiede and team for their GIS and mapping expertise. Dr. Karl-Erich Lindenschmidt was a valuable team member throughout this study, contributing ice jam expertise and freely sharing his knowledge.

Table of Contents

TABLES

FIGURES

APPENDICES

Executive Summary

The Government of the Northwest Territories (GNWT) commissioned this flood study to update and improve understanding of flood hazards for the Charter Community of Fort Good Hope (Rádęyı̨ı̨ Kóę́), where spring breakup ice jam flooding has repeatedly threatened homes, infrastructure, and traditional lands. The study provides the technical foundation for new flood inundation and flood hazard maps to support emergency response, community planning, and climate resilient decision making. It incorporates new bathymetric/topographic survey data for the study area, information on floods and ice jams that have affected the community, advanced hydraulic and ice jam modelling methods, and considers potential impacts of climate change on ice jam floods.

Upstream of Fort Good Hope, ice jams usually occur at the Ramparts, where the Mackenzie River narrows into a steep, cliff-faced constriction that promotes ice accumulation. When these jams release, a large mass of ice moves downstream and can jam again just below Fort Good Hope. The recurring cause of major flooding at Fort Good Hope is backwater flooding generated by ice jams located around 5-10 km downstream of the community. The ice jam model developed in this study represents a scenario in which a jam downstream of the community impedes flow and produces upstream backwater that inundates Fort Good Hope. Historical records show at least five major ice jam floods have caused flooding in the community in the past 50 years (1961, 1976, 1982, 2005, 2021). The May 2021 flood, estimated at 33.8 m (CGVD2013) at Station 10LD001, is the highest on record and resulted from a long ice jam at the Ramparts releasing into an existing downstream jam.

A river survey was conducted in July 2025 to collect new Mackenzie River bathymetry data to improve the digital terrain model for the model area, and included 38 river cross sections over 120 km, plus surveys of hydraulic structures, highwater marks and ice scars. Observed ice scars were predominately located between Rabbit Skin River and 15 Mile Point, with a lesser number located on the side channel west of Manitou Island. Cross-section data were merged with 2020 LiDAR, Canadian Hydrographic Survey bathymetry, and the ArcticDEM to produce an enhanced digital terrain model for hydraulic modelling.

Historical hydrometric records at Fort Good Hope Station 10LD001 include water level monitoring during open water seasons; only sporadic open water flow records exist at this station. Because of this, hydrometric analyses required use of regional flow frequency curves derived from the Norman Wells and Arctic Red River gauges, with flows transposed to Fort Good Hope. Tributary flood frequency analyses were also completed using limited records for Rabbit Skin River and Jackfish Creek but these relatively small inflows have little effect on ice jam flood water levels at Fort Good Hope.

Hydraulic modelling for this study included open-water conditions and ice jam conditions. A one-dimensional (1D) HECRAS model was developed from Spruce Island (upstream of the Ramparts) to Anderson's Landing, about 80.4 km downstream of Fort Good Hope. Open-water hydraulics were calibrated using observed water levels for multiple flows, resulting in a riverbed Manning's n of 0.021.

Two recent ice jam events, May 20, 2021 and May 25, 2021, were used to calibrate and validate the ice-affected model, with the model successfully reproducing observed water levels at Station 10LD001 gauge (32.3 m and 33.8 m in CGVD13). For these ice jam conditions, key ice-specific parameters were implemented in the model. These parameters include river flow at time of breakup, ice thickness, ice Manning's n coefficient, porosity, friction angle, lateral stress ratio, maximum permitted velocity beneath the ice jam, and ice jam toe/head positions. Previous studies were reviewed to set a range of possible values for each of these ice-related parameters.

Furthermore, historical observed values were analyzed to define the appropriate frequency distribution for these parameters for which random values (2,000 values) were extracted from. Also, a Global Sensitivity Analysis was conducted to evaluate the influence of each parameter. The most sensitive parameters affecting water levels were flow, ice jam toe location, and ice Manning's n coefficient.

The HEC-RAS model was modified to enable Monte Carlo simulations in which different random input values were implemented in the model to obtain a set of ice jamming scenarios. Using HECRASController available in the Visual Basic of Applications (VBA) accessible through the macros in Microsoft Excel, the HEC-RAS ice jam model was able to run sequentially 2,000 cases involving different ice jams configurations and outputting water surface profiles along the Mackenzie River. Annual exceedance probability (AEP) water level profiles were then derived from the Monte Carlo simulations.

A Joint Probability Analysis was run as one of the 2,000 scenarios in which all parameters produce the maximum water levels, thus representing the case in which these extreme conditions occur simultaneously. The associated water surface profile has an exceedance probability of zero.

The Monte Carlo analysis generated the following annual exceedance probability (AEP) flood profiles:

- May 2021 flood (~20 year, 5% AEP): 33.8 m (CGVD2013) at Station 10LD001.
- 100-year flood (1% AEP): 34.8 m (CGVD2013) at Station 10LD001.
- 200-year flood (0.5% AEP): 35.0 m (CGVD2013) at Station 10LD001.

The main factors influencing future ice jam flood hazards include land cover changes in the Mackenzie River basin, changes in flows of the Mackenzie River and changes in river ice cover characteristics and behavior (i.e., timing, duration, and thickness). Land cover change and river flow projections were obtained from the MESH (Modélisation Environnementale Surface et Hydrologie – Surface and Hydrology Environmental Modelling) hydrological model, which was set up and calibrated by Elshamy et al. (2024a,b). River ice thickness changes were assessed based on data from an ensemble of statistically downscaled climate scenarios available from ClimateData.ca, which includes outputs from a total of 26 climate models each run for low, moderate and high emissions scenarios as part of AR6.

Climate change scenarios (mid century 2040–2065 and late century 2075–2100) show increasing spring flows and thinner ice, but the increased flows dominate, resulting in significantly higher future flood levels:

- 100-year flood (1% AEP): 36.6 m (mid-century), 37.4 m (late century) at Station 10LD001
- 200-year flood (0.5% AEP): 36.9 m (mid-century), 37.5 m (late century) at Station 10LD001

Flood extent increases modestly under climate change because the community's low lying area is confined by steep terrain. Flood hazard maps were developed for both current conditions and the mid-century climate change scenario. Results for late century conditions were analysed but not mapped.

The study confirms that Fort Good Hope is highly prone to ice jam flooding driven by interactions between the Ramparts ice jam, downstream jam formation, flow magnitude, and ice characteristics. The new bathymetry, hydrological data, and ice jam modelling provide a robust basis for flood hazard maps for the 100 year (1% AEP) and 200 year (0.5% AEP) ice affected floods, including future climate scenarios.

Key study findings include:

- The 2021 ice jam flood was close to a 20-year flood (5% AEP).

- The 2021 ice jam flood was close to a 20-year flood (5% AEP).
- Areas within the ice-affected floodway are more hazardous as they have water depths of at least 1 metre or are exposed to moving ice. The areas within the community susceptible to ice jam flooding include the same low-lying areas between the Mackenzie River and Jackfish Creek that flooded in May 2021, though the flooded extents are slightly larger. The floodway isolates the westernmost portion of the community including the RCMP building. During the 200-year (0.5% AEP) flood, at least 16 buildings are within the floodway and the bridge over Jackfish Creek is overtopped.
- Ice jam floods are projected to increase in severity under climate change.
- The change in 2024 from seasonal to continuous, year-round monitoring at the Fort Good Hope Station 10LD001 will improve data availability, though this gauge will still be exposed to ice on the river channel. Having a second station or instrumentation not exposed to ice (at the mouth of Jackfish Creek, for instance) would be helpful to avoid break-up data gaps in the future.
- Future monitoring of ice conditions at the entrance of the Ramparts, especially during ice jam and ice breakup seasons, using remote cameras and/or additional water level gauges would improve understanding of the release mechanisms and ice jam timing each year. A similar monitoring system (camera and gauge) is also recommended downstream of the community where the downstream ice jam forms. An enhanced hydrometric surveillance system of the Mackenzie River near Fort Good Hope would help with understanding and quantifying important ice phenomena such as passage of ice jam wave (jave) that currently can not be fully assessed, due to the scarcity of data and observations. Such a system would help with understanding the conditions leading to ice jam formation and enhance preparedness.

Overall, this study significantly advances understanding of ice jam flood hazards at Fort Good Hope and provides essential technical inputs for community emergency planning, land use planning, and climate adaptation.

1 INTRODUCTION

Flooding is the most common and costly natural disaster in Canada, resulting in average annual residential losses of $2.9 billion (Public Safety Canada 2022). While sparsely populated, northern Canada is not immune to flooding as most communities are located along major rivers, including the Charter Community of Fort Good Hope (also known as Rádéyílı Kóé), which is located on the eastern banks of the Mackenzie River. Furthermore, most floods in the Northwest Territories (NT), including ones along the Mackenzie River, are the result of ice jams during the spring breakup (GNWT 2025).

Ice jam floods on the Mackenzie River result from mechanical breakup of ice rather than thermal breakup and produce much higher flood water levels than open water conditions or due to backwater from stable ice conditions (Gray and Prowse 1993; Coles 2022a).

Updating flood hazard maps is warranted when a more severe event than the ones used for historical flood hazard assessment occurs or when numerous years have passed since the last study and additional data is available (NRCan 2023a; Lindenschmidt et al. 2024a). The most recent major ice jam flood event[1] occurred in May 2021, when Fort Good Hope and other communities along the Mackenzie River experienced record high flooding within the community that affected 13 homes and other buildings (GNWT 2021).

To help quantify and better prepare for floods, the GNWT, through the Department of Environment and Climate Change, is developing flood maps for Fort Good Hope. These maps and data will be a resource for emergency management, community planning, and flood mitigation purposes.

This study will provide updated flood mapping to define the current and future flood hazard at Fort Good Hope. It may also lead to improved understanding of local ice jam flood processes that will be useful to the community and the GNWT in planning for and responding to future events.

1.1 Project Objectives

This study is divided into two phases and the main objectives are to develop:

1) Flood Inundation Mapping at Fort Good Hope during the peak of the May 2021 ice jam flood event

2) Flood Hazard Mapping - under ice jam scenarios for two Annual Exceedance Probability (AEP) events including the 1% AEP (i.e., 100-year flood) and 0.5% AEP (i.e., 200-year flood).

This comprehensive report builds on the Phase 1 report (WSP 2025a) finalized in 2025. A description of the contents of each section is outlined as follows:

- Data and information collected, organized and reviewed is outlined in Section 2.
- New survey, river bathymetry and topographic data collected for this study in July 2025 is summarized in Section 3. Details were provided in a separate report (WSP 2026a).
- Flood hydrology including historical flood events affecting Fort Good Hope are provided in Section 4. This section also includes a summary of the ice breakup chronology of the May 2021 ice jam flood and the mechanisms responsible for it; the 2021 ice jam flood chronology was detailed in the WSP (2025c) flood chronology memorandum.

[1] A *flood event* refers to an actual event in which water levels have risen above normal water levels such that flooding has occurred. In this report, “100-year flood” denotes a theoretical flood event with a return period of 100 years.

- The overall modelling approach is outlined in Section 5.
- The setup, parameterization and calibration of the HEC-RAS 1D model for open water conditions is provided in Section 6.
- The setup and parameterization of the HEC-RAS 1D model for ice-affected and ice jam conditions is provided in Section 7.
- Ice jam flood calibration events and data is provided in Section 8.
- The Monte Carlo framework Global Sensitivity Analysis methods, joint probability analysis, and ice jam flood profile results are provided in Section 9.
- Climate change results are provided in Section 10.
- A description of flood inundation and preliminary flood hazard mapping for Fort Good Hope is provided in Section 11.
- Uncertainties in the study as it affects ice jam modelling are provided in Section 12.
- Recommendations to improve ice jam flood data at Fort Good Hope and reduce uncertainty for future flood events and studies is provided in Section 13.
- Feedback from the community and Indigenous governments from targeted in-person engagement was obtained by GNWT in February 2025 with a focus on the May 2021 flood inundation maps. The engagement input is summarized in Appendix A.
- Engagement with community and Indigenous governments also occurred virtually in February 2026 to review work completed and present the draft flood hazard maps. A short summary is provided in Appendix A.

This report provides the methods, analysis and results of the flood modelling and mapping study and incorporates community engagement information.

The purpose of this report is to summarize the hydrological and hydraulic analysis completed to support the development of the preliminary flood inundation map based on the May 2021 flood. This report summarizes the literature and data reviewed in support of Phase 1 of the study, and describes the methods, modelling tools, boundary conditions, assumptions and results. Uncertainties in the assessment and results and strategies for reducing these uncertainties is also discussed.

1.2 Study Area

The Charter Community of Fort Good Hope is located on the east bank of the Mackenzie River, near its confluence with the Hare Indian River[1] (Rabbit Skin River), and downstream of the Ramparts. At Fort Good Hope, the Mackenzie River is wide, with a width of about 1.6 kilometres (km). The community had a population of 507 in 2021 and there were 231 private dwellings in the community (Statistics Canada 2023). The community is home to the Fort Good Hope Dene Band and Fort Good Hope Métis Nation Local #54. Indigenous Guardians with the K'ahsho Got'ıné Foundation supported WSP field crews throughout surveys near Fort Good Hope and provided input at engagement meetings.

[1] Hare Indian River is the geographic name also used for the Water Survey of Canada hydrometric station on this river; however, the local name Rabbit Skin River is used throughout this report

There is a large island, Manitou Island, located within the Mackenzie River and west of the current Fort Good Hope community area, which was the location of the community until a flood in 1831 (Kriwoken 1983). From about 10 km to 14 km upstream of Fort Good Hope, the Mackenzie River is constricted within a narrow canyon, known as the Ramparts, with widths generally less than 0.5 km.

GNWT defined the study area for this flood study as shown in Figure 1-1, which includes the legal boundaries of the community of Fort Good Hope, and a reach of the Mackenzie River from below the Ramparts to the next bend in the river. GNWT with support from NRCan under the FHIMP program, obtained LiDAR data on October 8, 2020 (McElhanney 2021) for the study area to provide high resolution terrain data for flood mapping.

1.3 Study Basin

The Mackenzie River is the largest cold-region drainage basin in North America (de Rham et al. 2008). At Fort Good Hope, the Mackenzie River drains an area of 1,636,000 square kilometres (ECCC 2024a). Figure 1-2 shows the Mackenzie River watershed at Fort Good Hope.

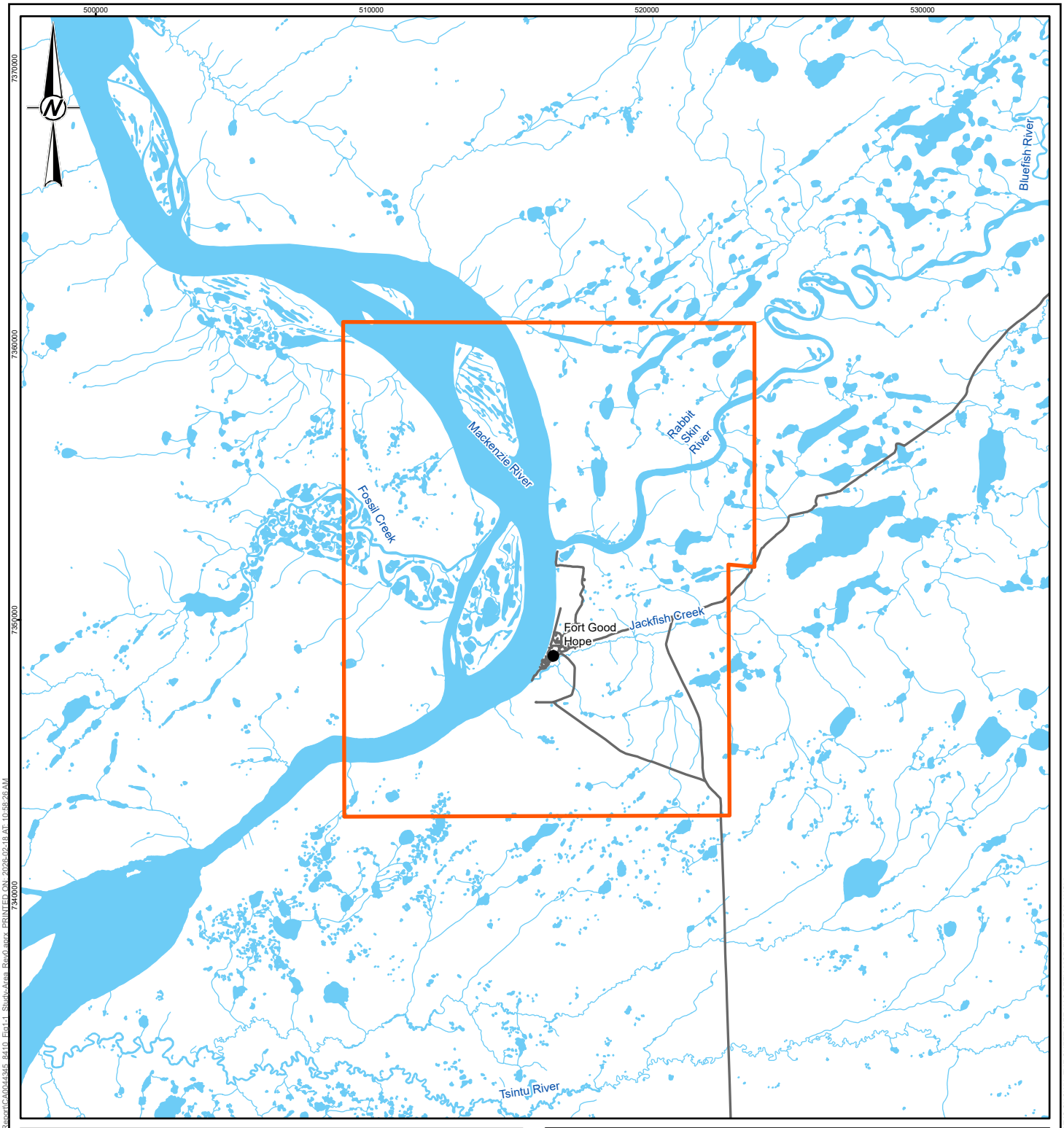

LEGEND

- COMMUNITY
- ROAD
- WATERCOURSE
- WATERBODY
- STUDY AREA

0 4 8

1:200,000 KILOMETRES

REFERENCE(S)

DIGITAL BASE DATA OBTAINED FROM GEOGRATIS, © DEPARTMENT OF NATURAL RESOURCES CANADA. ALL RIGHTS RESERVED.
PROJECTED COORDINATE SYSTEM: NAD 1983 UTM ZONE 9N

CLIENT

Government of Northwest Territories

Canada

PROJECT

FLOOD INUNDATION AND HAZARD MAPPING - FORT GOOD HOPE, NT

TITLE

STUDY AREA

CONSULTANT

wsp

YYYY-MM-DD	2026-02-18
DESIGNED	CH
PREPARED	PT
REVIEWED	JH
APPROVED	ML

PROJECT NO.	CONTROL	REV.	FIGURE
CA0044345.8410		0	1-1

LEGEND

- COMMUNITY
- PRIMARY HIGHWAY
- WATERCOURSE
- WATERBODY
- PROVINCIAL BOUNDARY
- MACKENZIE RIVER AT FORT GOOD HOPE WATERSHED

0 200 400

1:10,000,000 KILOMETRES

REFERENCE(S)

DIGITAL BASE DATA OBTAINED FROM GEOGRATIS, © DEPARTMENT OF NATURAL RESOURCES CANADA. ALL RIGHTS RESERVED.
PROJECTED COORDINATE SYSTEM: NAD 1983 UTM ZONE 9N

CLIENT

Government of Northwest Territories

Canada

PROJECT

FLOOD INUNDATION AND HAZARD MAPPING - FORT GOOD HOPE, NT

TITLE

MACKENZIE RIVER AT FORT GOOD HOPE WATERSHED

CONSULTANT

wsp

YYYY-MM-DD	2026-02-18
DESIGNED	CH
PREPARED	PT
REVIEWED	JH
APPROVED	ML

PROJECT NO.	CONTROL	REV.	FIGURE
CA0044345.8410		0	1-2

IF THIS MEASUREMENT DOES NOT MATCH WHAT IS SHOWN, THE SHEET SIZE HAS BEEN MODIFIED FROM: ANSI A

25mm

0

PATH: K:\CLIENTS\GOVERNMENT_OF_NWT\CA0044345_8410\Mapping\Hydrology\Phase 2 Report\CA0044345_8410_Fig1-2_Mackenzie_River_Fort_Good_Hope_Watershed_Rev0.aprx, PRINTED ON: 2026-02-18 AT 10:59:35 AM

2 DATA COLLECTION AND INFORMATION REVIEW

This section describes the collection, review and assessment of desktop information reviewed for this study are provided in Sections 2.1 to 2.4, while field studies are documented in Section 2.5. Section 2.6 summarizes Indigenous and local knowledge as it pertains to flooding at Fort Good Hope.

2.1 Previous Flood Mapping

Government flood line delineation mapping was completed for Fort Good Hope along with four other northern communities in 1983 (Kriwoken 1983). That report identified the highest extreme flood event as an ice jam flood in May 1961. The shapefiles representing flood lines were provided to WSP and represent about a 100-year flood as determined at the time from available information. See Section 4.1 for detailed flood history for Fort Good Hope.

2.2 Information Review

A summary of ice jam flood literature reviewed to date to support this study is provided in Table 2-1. Selected literature is incorporated into modelling approach described in Section 5. A full reference list is provided in the references section.

Table 2-1: Literature Reviewed

Purpose	References	Titles
Provides methods and/or regional case studies used in ice jam assessments	Beltaos 1983	River ice jams: theory, case studies and applications
	Beltaos 1995	River ice jams
	White 1999	Hydraulic and physical properties affecting ice jams
	Hawkes 2008	Joint probability analysis for estimation of extremes
	Zhang et al. 2019a	Variogram-based sensitivity analyses of a river ice model
	Lindenschmidt 2021	Rapid assessment of ice jam flooding at Fort Simpson along the Mackenzie River in the NWT
	Lindenschmidt et al. 2024a	Reach-Based Extrapolation to Assess the ice jam Flood Hazard of an Ungauged River Reach along the Mackenzie River, Canada
	Lindenschmidt 2024b	River Ice Processes and Ice Flood Forecasting – A Guide for Practitioners and Students (pp. 285-343). Switzerland AG: Springer Nature
Remote sensing data uses in ice jam modelling	Zhang et al. 2017	Using Remote Sensing Data to Parameterize Ice Jam Modeling for a Northern Inland Delta
	Zhang et al. 2019b	Potential of RADARSAT-2 to Improve Ice Thickness Calculations in Remote, Poorly Accessible Areas: A Case Study on the Slave River, Canada
Climate change impacts on ice jam floods	Zhang et al. 2022	Climate change impacts on ice jam behavior in an inland delta: a new ice jam projection framework
	Dehghani Sanij et al. *in press*	Shifts in ice jam flood hazard due to climate change along the Mackenzie River
Flood hydrology in northern rivers	Gray and Prowse 1993	Snow and floating ice. In Handbook of Hydrology
	Hicks and Beltaos 2007	River ice in Cold Regions. Atmospheric and Hydrologic Studies
	Burn 2008	Climatic influences on streamflow timing in the headwaters of the Mackenzie River Basin
	de Rham et al. 2008	Assessment of annual high water events for the Mackenzie River Basin, Canada

Guidelines, reports and drawings reviewed as part of this study are documented in Table 2-2.

Table 2-2: Guidelines, Reports and Drawings Reviewed

References	Purpose / Information Use
▪ NRCan 2023a. Federal hydrologic and hydraulic procedures for flood hazard delineation v.2.0 ▪ NRCan 2023b. Northwest Territories Ice Jam Flood Mapping Guidelines v1.0 ▪ NRCan 2023c. Northwest Territories Ice Jam Flood Mapping Case Studies v1.0	▪ GNWT Ice jam flood mapping guidelines ▪ GNWT Ice jam case studies includes two locations on the Mackenzie River ▪ Canadian flood mapping, hydrology and hydraulics guidelines, includes climate change and assessment methods and uncertainty
▪ GNWT Public Works and Highways (undated)	▪ Jackfish Creek bridge layout as-built drawing was referenced to support the bridge survey
▪ Kriwoken 1983. Historical flood review: Fort Simpson, Fort Norman, Fort Good Hope, Fort McPherson, Aklavik, Fort Liard, Nahanni Butte	▪ Flood history documentation including the 1931 flooding of the old site of the Fort on Manitou Island when an ice jam release at the Ramparts sent a mass of ice and water down upon the island. ▪ Subsequent breakup flooding in 1911, May 1961, and 1976 was attributed to ice jamming 7.5 km downstream of Fort Good Hope at an island below the mouth of the Rabbit Skin River. Backwater enters the community via Jackfish Creek and floods a low-lying areas along an abandoned channel. ▪ Benchmark elevations for 75T005 and 75T008 given in GSC vertical datum
▪ ECCC and GNWT. 2020. Hydrological analysis of Great Slave Lake in 2020	▪ Hydrological analysis documents reasons for record high water levels in Great Slave Lake in 2020 and potential water level conditions into 2021
▪ Coles 2022a. NWT flood events	▪ Flood history documentation
▪ GNWT 2021	▪ Sahtu Breakup reports dated May 12, 2021 to May 27, 2021 included daily status of breakup, movement of ice, hydrometric gauge data and photos, weather forecasts, GEM forecast maps, Planet imagery, Radarsat imagery, and Sentinel 2 imagery
▪ NHC 2025. Kátł odeh (Hay River) Flood Hazard Mapping Study	▪ Reviewed joint probability analysis methods used in this study.

Accounts of flooding by territorial and local governments and organizations and personal accounts are documented in Table 2-3.

Table 2-3: Accounts of Flooding Reviewed

Information Source	Details
K'ahsho Got'ine Guardians 2023	▪ Two videos taken from a canoe on May 25, 2021 (Time 18:13 and 18:23) in the flooded area of Fort Good Hope show water level on buildings
Online news articles: ▪ May 18, 2021, Fort Good Hope remains on flood watch as water levels waver (CBC News 2021) ▪ May 25, 2021, State of emergency declared in Fort Good Hope as flood waters rise (Brackenbury 2021a)May 26, 2021, Water recedes in Fort Good Hope, community remains alert (Brackenbury 2021b)	▪ May 18, 2021, article photo of Jackfish Creek – Mackenzie River evacuation trigger point stake – facing upstream ▪ May 25, 2021, article photo showing flooded area in Fort Good Hope; state of emergency called at 10:10. Siren sounded at 04:30. Video (length 1 minute:10 seconds) shows ice flowing past Fort Good Hope Photo from community member, date unknown ▪ Photo from community member in Fort Good Hope taken May 25, 2021
GNWT ECC Ice patrol (Emergency Operations Centres (EOCs) plans and photos (May 21, 2021)	▪ Oblique aerial photos from plane with notes of locations
GNWT Environment and Climate Change (ECC) Ice patrol report (May 21, 2021) provided by GNWT ECC Sahtu Regional Office and Sahtu Regional EMO – EOC Team	▪ Five-page report with Elder's description of breakup at the Ramparts and Fort Good Hope, and how breakup may progress, with aerial photos
Flood mapping project - February 12, 2025 engagement meetings in Fort Good Hope	▪ Observations are summarized in Appendix A

2.3 Hydrometric Data

This section summarizes the hydrometeorological data sources used in this study and summarizes some of the key findings.

Certain Water Survey of Canada (WSC) hydrometric gauging stations on the Mackenzie River and tributaries near Fort Good Hope provide key data for this project. Hourly and daily climate data are currently available at two stations at Fort Good Hope (ECCC 2025). Climate and hydrometric station data included in the study are provided in Table 2-4. The watersheds and gauge locations on the Mackenzie River are shown in Figure 2-1 and those for tributaries in the study area are shown in Figure 2-2. Stations within Fort Good Hope are shown on Figure 2-3.

Table 2-4: Climate and Hydrometric Station Data Details and Analysis

Station Name	Station ID	Period of Record	Data/Parameters	Data Purpose and Use
Mackenzie River at Norman Wells	10KA001	1943-1956; 1960-2026	▪ 5-minute and daily water level and discharge, data flags	▪ Open water flood frequency analysis ▪ Ice jam analysis
Mackenzie River at Sans Sault Rapids	10KD001	1962-1964; 1968-2026	▪ 5-minute and daily water level and discharge, data flags	▪ Open water flood frequency analysis ▪ Ice jam analysis
Mackenzie River at Arctic Red River	10LC014	1985-2026	▪ 5-minute and daily water level and discharge, data flags	▪ Open water flood frequency analysis ▪ Ice jam analysis

Station Name	Station ID	Period of Record	Data/Parameters	Data Purpose and Use
Mackenzie River at Fort Good Hope	10LD001	1963-2026	■ 5-minute and daily water level ■ Flow measurement using an Acoustic Doppler Current Profiler (ADCP) on July 27, 2010 ■ Remote camera images available in May 2021	■ Open water flood frequency analysis ■ Ice jam analysis
Rabbit Skin River near Fort Good Hope (Note: this station is named Hare Indian River on the Water Survey of Canada site)	10LD004	2005-2026	■ 5-minute and daily water level and discharge records, flags	■ Open water flood frequency analysis
Jackfish Creek near Fort Good Hope	10LD002	1980-1986	■ 5-minute and daily water level and discharge records, flags	■ Open water flood frequency analysis
Fort Good Hope A, Fort Good Hope CS	2201406 2201450	2018-2026 1998-2026	■ Hourly and daily climate data for both stations	■ Support ice jam analysis, for example estimating ice thickness

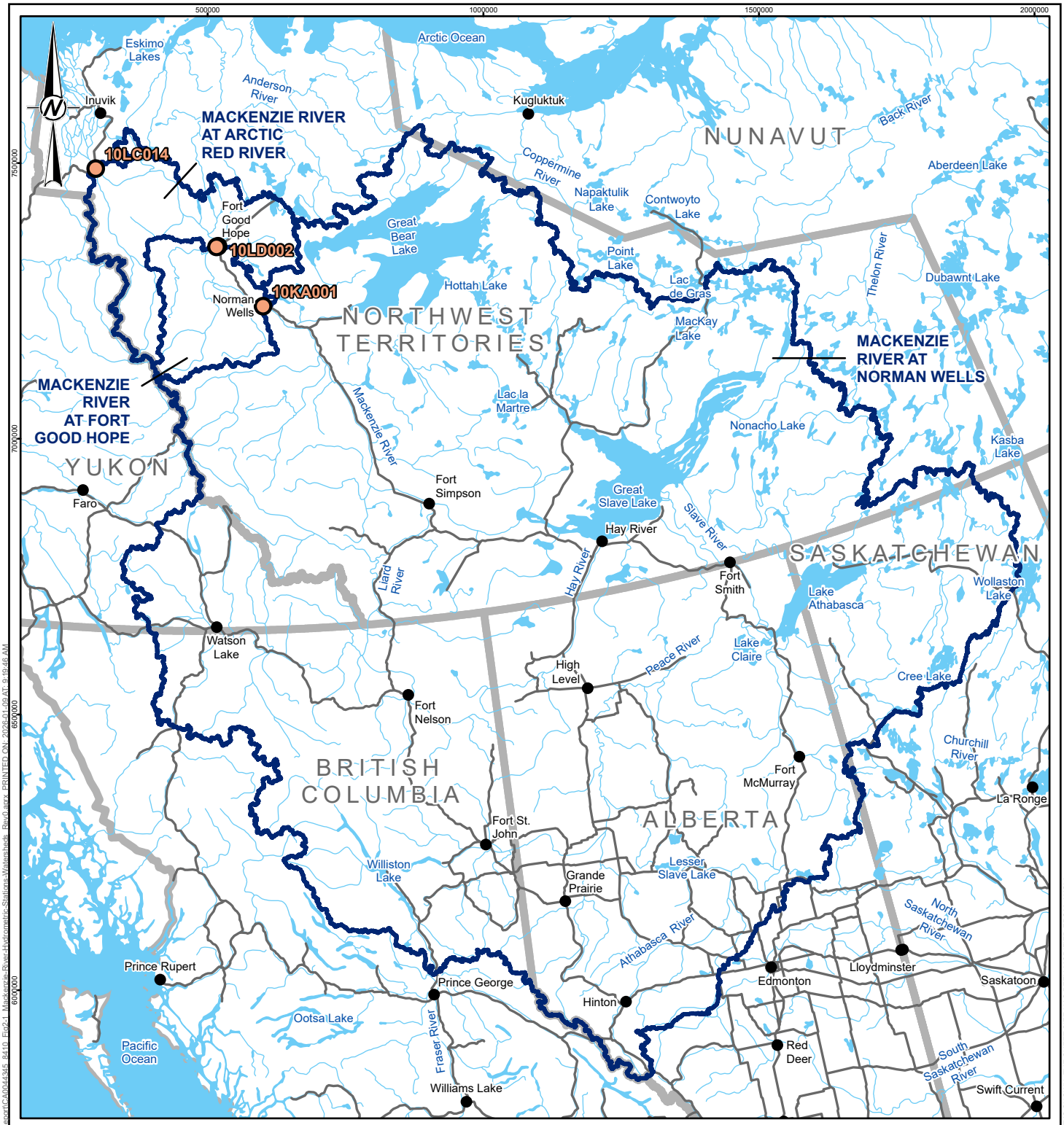

LEGEND

- COMMUNITY
- PRIMARY HIGHWAY
- WATERCOURSE
- WATERBODY
- PROVINCIAL BOUNDARY
- HYDROMETRIC STATION
- WATERSHED

0 200 400

1:10,000,000 KILOMETRES

REFERENCE(S)

DIGITAL BASE DATA OBTAINED FROM GEOGRATIS, © DEPARTMENT OF NATURAL RESOURCES CANADA. ALL RIGHTS RESERVED.
PROJECTED COORDINATE SYSTEM: NAD 1983 UTM ZONE 9N

CLIENT

Government of Northwest Territories

Canada

PROJECT

FLOOD INUNDATION AND HAZARD MAPPING - FORT GOOD HOPE, NT

TITLE

MACKENZIE RIVER HYDROMETRIC STATIONS LOCATIONS AND WATERSHEDS

CONSULTANT

wsp

YYYY-MM-DD	2026-01-09
DESIGNED	CH
PREPARED	PT
REVIEWED	JH
APPROVED	ML

PROJECT NO.	CONTROL	REV.	FIGURE
CA0044345.8410		0	2-1

IF THIS MEASUREMENT DOES NOT MATCH WHAT IS SHOWN, THE SHEET SIZE HAS BEEN MODIFIED FROM: ANSI A

25mm

0

PATH: K:\CLIENTS\GOVERNMENT_OF_NWT\CA0044345_8410\Mapping\Hydrology\Phase 2 Report\CA0044345_8410_Fig2-1_Mackenzie_River_Hydrometric_Stations_Watersheds_Rev0.aprx PRINTED ON: 2026-01-09 AT: 9:19:46 AM

LEGEND

- COMMUNITY
- ROAD
- WATERCOURSE
- WATERBODY
- PROVINCIAL BOUNDARY
- HYDROMETRIC STATION

WATERSHED

- 10LD002
- 10LD004

0 20 40

1:1,250,000 KILOMETRES

REFERENCE(S)

DIGITAL BASE DATA OBTAINED FROM GEOGRATIS, © DEPARTMENT OF NATURAL RESOURCES CANADA. ALL RIGHTS RESERVED.
PROJECTED COORDINATE SYSTEM: NAD 1983 UTM ZONE 9N

CLIENT

Government of Northwest Territories

Canada

PROJECT

FLOOD INUNDATION AND HAZARD MAPPING - FORT GOOD HOPE, NT

TITLE

TRIBUTARY LOCATIONS AND WATERSHEDS

CONSULTANT

wsp

YYYY-MM-DD	2026-01-09
DESIGNED	CH
PREPARED	PT
REVIEWED	JH
APPROVED	ML

PROJECT NO.	CONTROL	REV.	FIGURE
CA0044345.8410		0	2-2

IF THIS MEASUREMENT DOES NOT MATCH WHAT IS SHOWN, THE SHEET SIZE HAS BEEN MODIFIED FROM: ANSI A

25mm

0

PATH: K:\CLIENTS\GOVERNMENT_OF_NWT\CA0044345_8410\Mapping\Hydrology\Phase 2 Report\CA0044345_8410_Fig2-2_Tributary_Watersheds_Rev0.aprx PRINTED ON: 2026-01-09 AT: 10:8:32 AM

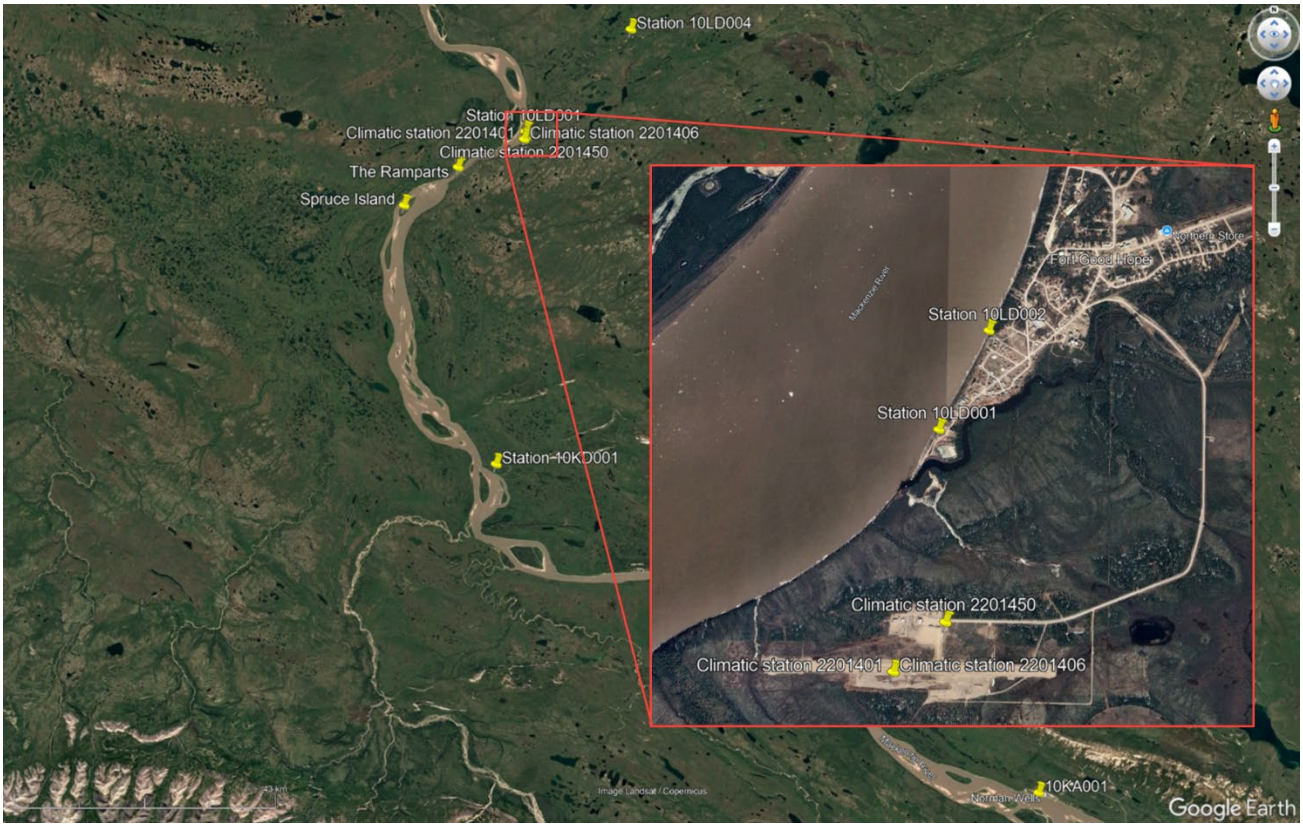

Figure 2-3: Locations of Hydrometric and Climatic Stations at Fort Good Hope

Results from the data review include the following main points:

- Discharge data is not collected at Station 10LD001 for the Mackenzie River at Fort Good Hope therefore this study relies on discharge derived at Station 10KA001 for the Mackenzie River at Norman Wells.
- As shown by the open water flood frequency results in Section 4.2, flood discharge at Fort Good Hope is estimated from the stations upstream (10KA001) and downstream of Fort Good Hope at Arctic Red River (10LC014). However, due to the presence of the Ramparts upstream of Fort Good Hope, peak flows moving through from Norman Wells may be attenuated and the Ramparts are susceptible to ice jams.
- Data gaps are common during the breakup period in the hydrometric records on the Mackenzie River. This is attributed to stations not being visited early enough to collect data during breakup and/or disturbance of the station instrumentation by ice, and/or stations not being reset again during breakup. As a result, data that could support ice jam modelling is missing. Data may also be missing if it is considered unreliable.
- During the ice jam flood at Fort Good Hope in May 2021, data recorded and gaps in the hydrometric records for the Mackenzie River include:
  - Station 10LD001 was in operation when peak water level occurred in the Community on May 25. However, for this event, the recorded levels can not be satisfactorily converted to geodesic using the conversion factor provided by WSC (+17.646 m). Using this factor results in a major peak water level underestimation for the May 2021 flood event.

- Elevations of water levels recorded from WSC gauge 10LD001 during the 2021 flood peak are about 2.8 m lower than flood elevations obtained from the high water mark survey performed by Ollerhead & Associates Ltd. in 2023, even though both have similar datum references. The 2020 LiDAR DTM was used as ground elevation reference for the 2023 survey and has been verified to be correct.
- The discrepancy between WSC water level readings and high water mark survey was investigated, and WSC was contacted for clarification. WSC indicated that the gauge may have been damaged, displaced or improperly calibrated. If damage occurred, it may have been caused by moving ice during breakup. As noted in Section 13, installing a water gauge at Jackfish Creek rather than along the Mackenzie River would reduce the likelihood of ice-related damage.
- WSP considers the WSC geodetic water levels from gauge 10LD001 to be unrealistically low, as no flooding would have occurred at the recorded elevations. To account for this error, the WSC levels used in this study for the event of May 2021 were adjusted by applying the 2.8 m offset.
- Station 10LD001 data was collected for a period of about nine days from May 19, 2021 at 17:55 to May 27, 2021 00:40 and restarted June 9, 2021 at 12:30. The 9-day record (May 19-27, 2021) is highly valuable as it provides information about the river dynamics before, during and after the highest flood peak on record.
  - Station 10KA001 (190 km upstream of Fort Good Hope) also had a data gap starting May 25, 2021, after 15:20, and restarted June 8, 2021, at 09:30.
  - Station 10LC014 (340 km downstream of Fort Good Hope) also had a short data gap on May 26, 2021, between 15:50 and 20:15.
- Bed elevations at Fort Good Hope were initially obtained from the WSC from an ADCP discharge measurement completed on July 27, 2010; however this data was superseded by the detailed bathymetry survey conducted under this project in July 2025.

2.4 Geospatial Data

Geospatial data used in this study, its purpose, and references are included in Table 2-5.

Table 2-5: Geospatial Data Details and Analysis

Category	Dataset Reference	Data Purpose and Use
Imagery / Terrain/Elevation / Base Layer	McElhanney Ltd. 2021	▪ LiDAR data was collected October 8, 2020 for an area of 237 km^2. It was used as terrain layer for flood mapping in the Study Area, various formats provided and a summary report ▪ Orthophoto provides a base map with 20 cm resolution.
	GNWT ArcGIS MapServer (GNWT 2015-2016)	▪ Base data layers
	Digital Surface Model (DSM) published by Natural Resources Canada (NRCan 2025a)	▪ Used to estimate river surface slopes

Table 2-5: Geospatial Data Details and Analysis

Category	Dataset Reference	Data Purpose and Use
River Ice Monitoring and Analysis	NRCan 2020; Government of Canada 2025a	▪ Radarsat Constellation Mission (RCM-3) derived ice-cover conditions ▪ Shows river ice extent and ice jam roughness at the Ramparts for ten captures/dates between May 5, 2021, and May 26, 2021
	Sentinel-1 C-Band images, Sigma/Gamma intensity (Government of Canada 2025b)	▪ Shows ice jam and open water areas ▪ Tracks ice front on cloudy days
	Sahtu ice break-up reports (GNWT 2021)	▪ Planet optical imagery shows ice-cover conditions based on Planet satellite images ▪ Sentinel 2 imagery shows ice-cover extent ▪ RCM-3 imagery shows ice extent and roughness ▪ Oblique aerial photos of flood extent taken May 25, 2021
	PlanIt North 2023	▪ One aerial photo of flood extent in Fort Good Hope

Results from the data review include the following:

- The 2020 LiDAR DSM is referenced to the CGVD2013 datum, and one control point was published with the report (McElhanney 2021).
- RADARSAT Constellation Mission third generation (RCM-3) images (Government of Canada 2025a) were available on the Earth Observation and Data Management System (EODMS) for the May 2021 flood on the Mackenzie River and showed where the ice covered versus open water areas were and roughness of ice cover indicating ice jams. Product details are provided in NRCan (2020). The river ice breakup condition products are derived from RADARSAT-2 images with a system developed and operated by the Canada Center for Mapping and Earth Observation of Natural Resources Canada, Department of Natural Resources Canada. All rights reserved.
- Planet, Sentinel 2, and RCM-3 imagery for the Fort Good Hope area between May 11, 2021, and May 25, 2021, were included in various Sahtu Break-up reports (GNWT 2021). These show visible ice-cover conditions and extent.
- Aerial photos of the flood extent in Fort Good Hope taken on May 25, 2021, were provided by the ECC Sahtu Regional Superintendent. These were included in the Sahtu Break-up reports (GNWT 2021) on May 26, 2021, and one image was included in the PlanIt (2023) report.

2.5 Field Data

This section summarizes the field data available and how it was used in this report (Table 2-6). This includes the high water mark survey by Ollerhead & Associates Ltd. in 2023 (Ollerhead 2023). Some flood photos were provided to WSP after the February engagement.

Table 2-6: Field Data Details and Analysis

Dataset Reference	Data Purpose and Use
Ollerhead 2023	■ Established control for WSC benchmarks in CGVD2013 and CGVD28, and collected 17 high water marks for the May 2021 ice jam flood event in Fort Good Hope. ■ This survey was informed by field notes and photos documenting 2021 and 2023 high water levels commissioned through the K'asho Got'ine Housing Society with support by PlanIt North and the K'ahsho Got'ine Foundation.
Fort Good Hope EMO emergency plan and 2021 flood photos with documented dates and times	■ Provide information on 2021 flood chronology and flood monitoring and response.
WSP Canada Inc. 2026b	■ Fort Good Hope Survey Bathymetry Memorandum documents survey data collected in July 2025 for this study to improve river bathymetry, and obtain ice scar and high water mark elevations in the study area.

Results from the data review include the following main points:

- The flood extent captured in May 2021 aerial photographs of Fort Good Hope compared very well with the flood extent derived from plotting the high water mark survey results (Ollerhead 2023) on the 2020 LiDAR DTM.
- Three WSC benchmarks were surveyed by Ollerhead and Associates and both CGVD28 and CGVD2013 elevations were obtained.
- WSP's survey results are summarized in Section 3. Elevation results aligned with Ollerhead and Associates survey results as well as the October 8, 2020 LiDAR data (McElhanney 2021).

2.6 Indigenous and Local Knowledge

Indigenous and local knowledge play a vital role in understanding flood history, providing insights beyond scientific data, that can help inform flood hazard mapping studies. This has included local observations of past floods and the timing of ice runs or jams, relative severity of different flood events, changes in river flow, and the effects of climate on traditional lands and communities (see Appendix A for details). The importance of this knowledge is particularly true for the NWT where datasets are often short and sparse.

Historical knowledge of past floods documented by the Hudson Bay Company and the Roman Catholic Church also provided valuable information for this study (Kriwoken 1983).

3 BATHYMETRIC AND TOPOGRAPHIC FIELD SURVEY

In July 2025, WSP performed bathymetric and topographic surveys to address spatial data gaps for the Mackenzie River, Rabbit Skin River, and Jackfish Creek and their overbank areas to develop a hydraulic model to simulate ice jam floods, and to collect observations and data to calibrate that model. K'ahsho Got'ıné Guardians supported WSP field crews throughout surveys near Fort Good Hope. Survey results are summarized in a separate memorandum (WSP 2026a) and are provided in this section.

Bathymetric and topographic field surveys were completed along the Mackenzie River, Rabbit Skin River and Jackfish Creek (Figure 2-2 and Figure 2-3).

3.1 Survey Methods

As described in WSP (2026a), surveys were conducted using Trimble R12i real-time kinematic (RTK) equipment. Bathymetric surveys were performed using a Hydrolite Plus echosounder equipped with RTK survey equipment mounted to a boat. Land-based topographic surveys, and surveys of features in shallow water, were performed using the RTK equipment mounted to a pole. The areas and features surveyed are described in detail in the following subsections and selected photos are provided in Appendix B.

All surveyed data are referenced to the NAD83 CSRS horizontal datum projected using the UTM Zone 9N coordinate system, with vertical datum CGVD2013 (Mean Sea Level). For completeness, elevations relative to the vertical datum CGVD28 are provided, but elevations relative to the more current datum of CGVD2013 are used and presented preferentially.

Bathymetric and topographic surveys were completed by WSP from July 4 to 18, 2025 and included the Mackenzie River, Rabbit Skin River, and Jackfish Creek. The survey data includes river cross sections, high water marks and ice scar elevations and locations, and hydraulic structure data.

The survey collected the following information in the study area:

- 38 cross sections over approximately 120 km of the Mackenzie River at Fort Good Hope
- 9 cross sections on the Rabbit Skin River
- 7 cross sections on Jackfish Creek
- Topography of Jackfish Creek bridge deck, approaches, abutments, and low chord elevation
- 21 culverts in Fort Good Hope
- Topography of 12 cabins, including two cabins with documented impacts from the 2021 flood
- 38 ice scars on trees and eight other high water marks (HWMs) (deposited debris)

Data from river cross sections was used to update geometry of the hydraulic model. The HWMs were used to calibrate the hydraulic model.

3.2 Survey Accuracy and Error

The RTK base station was set up over a temporary control point comprising of a rebar pin embedded into the ground. Temporary check points comprising a rebar pin embedded into the ground were set up near the temporary control point. At the start and end of each base station set up, the check points were surveyed to confirm acceptable survey closure. Acceptable survey closure was achieved at the end of each base station survey as the position of check points were consistently within 0.03 m. This is within the accuracy of 0.05 m required for this study.

The position assigned to the base station was corrected using the Canadian Spatial Reference System Precise Point Positioning (CSRS-PPP) service. The horizontal and vertical position delta (difference between the initial and corrected base station position) was applied to all points collected during that base survey to correct those data.

Control points with known three-dimensional position or known elevation in Fort Good Hope were included in surveys. These control points were established by Canada Lands Surveys and Water Survey of Canada and were

recently surveyed by Ollerhead & Associates (2023) and by WSP (2025) (Table 3-1). Comparing to coordinates recorded by WSP, values were within the accuracy of 0.05 m specified in the terms of reference.

Table 3-1: Survey Control Point Positions Reported by Ollerhead & Associates and WSP

Control Point Name	Northing (m)		Easting (m)		Elevation (CGVD2013; m)		Elevation (CGVD28; m)	
	Ollerhead[1]	WSP	Ollerhead[1]	WSP	Ollerhead[1]	WSP	Ollerhead[1]	WSP
75T005	7,348,027.90	7,348,027.89	516,012.45	516,012.48	39.84	39.79	39.88	39.85
82-1	7,347,990.70	7,347,990.69	515,919.48	515,919.49	39.01	38.95	39.04	39.01
NT05-146	7,347,991.14	7,347,991.12	515,921.09	515,921.08	38.98	38.93	39.02	38.98

[1]Ollerhead & Associates (2023).

After survey data were corrected, some data points were screened out. Some data points were flagged by the field crew to be screened out due to poor satellite signal in the field. Most points that were screened out were from the bathymetric survey when the boat pitched or rolled during manoeuvring or acceleration, resulting in erroneous depth and riverbed elevations.

3.3 Cross Section Survey

The bathymetric surveys were performed in the following three main areas (Figure 3-1) and included:

- 38 cross sections on Mackenzie River, over approximately 120 km of river reach
- 9 cross sections on Rabbit Skin River
- 7 cross sections on Jackfish Creek

Cross sections of the Mackenzie River and Rabbit Skin River were accessed using boats launched from Fort Good Hope. Two boats were available and were selected at the start of the day based on expected river conditions. The bigger boat was the primary boat for the Mackenzie River cross sections and the smaller boat with a shallower draft was used to access the Rabbit Skin River cross sections and cross sections of the Mackenzie River that were too shallow to access with the bigger boat. In some areas of the Mackenzie River, an inflatable kayak was used to access and survey shallow side channels that were separated from the main channel by bars. Jackfish Creek was not accessible by a motorboat, thus a canoe was used to collect bathymetric data, with a combination of mounting the depth sounder to the canoe and collecting points using the RTK mounted to a survey pole.

At all cross section locations, water levels were surveyed on both shorelines using the RTK mounted to a survey pole. At cross sections where the river edge had a low slope that allowed safe access by the survey team, ground elevations were surveyed to extend the cross section overland. In areas where the river edge had a steep or vertical slope, or was otherwise unsafe to disembark, ground elevations were not surveyed.
Cross sections were extended on land until one of the following conditions was reached:

- surveyed points extended 5 m horizontally past the bank crest
- until passage became unreasonable (e.g., dense vegetation)
- until 25 m horizontally was surveyed

The overland extension of cross sections served to facilitate merging surveyed data with available digital elevation models to be used in hydraulic and ice jam modelling, and surveyed cross sections will be used as geometry in the hydraulic model.

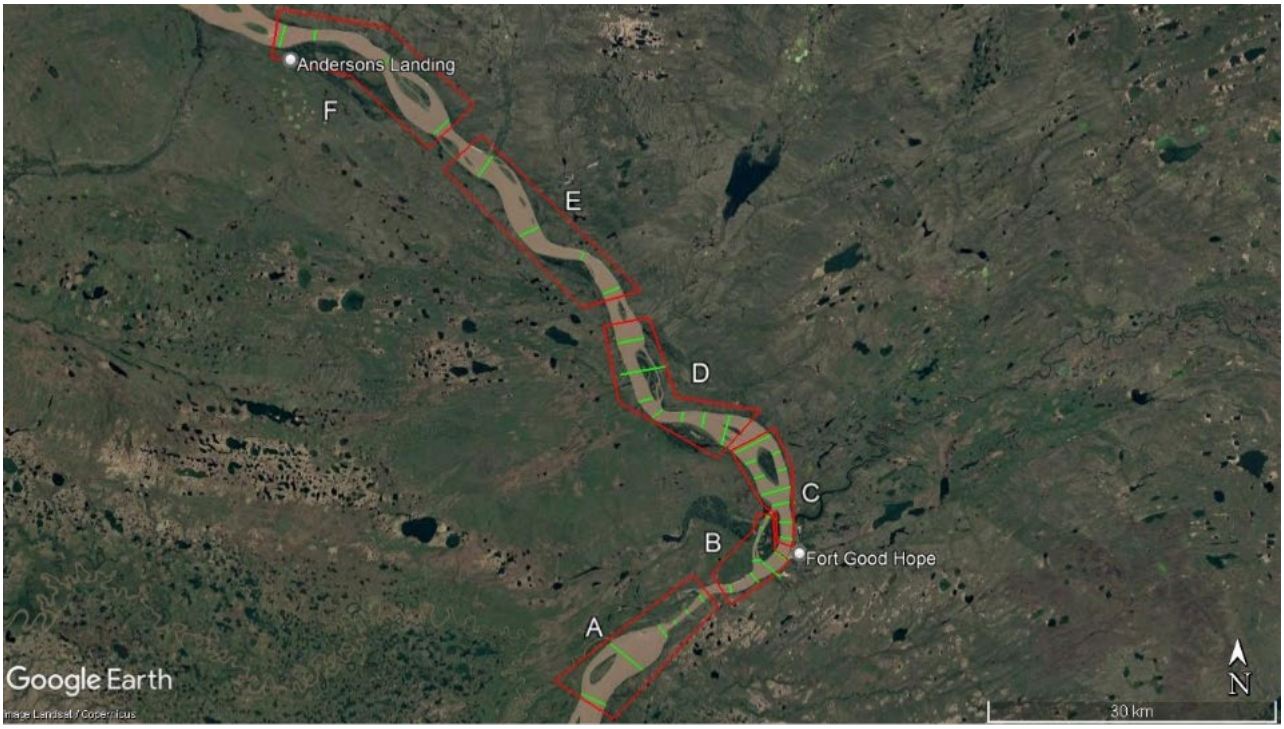

Figure 3-1: Bathymetry Survey Data Collection Areas A to F

3.4 Hydraulic Structures

Hydraulic structures within the study area include the Jackfish Creek Bridge and 21 culverts within Fort Good Hope. These structures were all surveyed in July 2025, results were provided as a data point file as outlined in WSP 2026a. Selected photos of the bridge are provided in Appendix B.

The Jackfish Creek Bridge was surveyed, including approaches, and abutments comprising binwalls and gabion baskets. The deck elevation was measured to be 35.8 m. The lower chord of the bridge could not be directly surveyed due to poor signal when using the RTK under the bridge. Instead, the lower chord was measured using a measuring tape relative to the elevation of the top of the binwall. The elevation of the low chord was measured to be 34.70 m, referenced to CGVD2013.

Jackfish Creek geometry and inflow was not explicitly represented in the hydraulic model because the inflow used was estimated using a watershed that includes Jackfish Creek's watershed. Incorporating the creek directly into the model would therefore have resulted in double-counting its contribution and overestimating the total inflow.

The surveyed Jackfish Creek Bridge's elevation data were used to determine the flood magnitude at which the bridge would become overtopped. Extreme flood conditions next to the bridge are governed by the backwater flow from the Mackenzie River; and therefore, the creek itself did not need to be explicitly modelled.

A total of 21 culverts were surveyed, primarily around the community park and the main street, but also including larger culverts along the road between the main portion of the town and the water treatment plant. Culvert diameters varied between approximately 0.3 m to approximately 1.2 m. A list or inventory of culverts was not

provided, and consequently the culverts observed by WSP is not necessarily complete or exhaustive. None of the culverts were included in the hydraulic model because WSP considered that their implementation would not meaningfully influence overall flood levels, while significantly increasing computational demands, which are already high. Adding the culverts would make the model heavier and less efficient, particularly given the additional complexity introduced by ice jams and the Monte Carlo simulations. The culverts do not impact the computed river flood extents which are limited to the low-lying part of the Community.

3.5 High Water Marks and Ice Scars

During the July 2025 survey, a total of 38 ice scars were recorded: 27 were measured directly and 11 were measured indirectly by recording the relative distance from the point of observation to the ice scar using a Leica DISTO Laser Distance Meter (WSP 2026a). When ice scars are measured indirectly, the reported precision is reduced to the nearest metre for horizontal coordinates, and the nearest decimetre for elevation. Observed ice scars were predominately located between Rabbit Skin River and 15 Mile Point, with a lesser number located on the side channel west of Manitou Island. Two ice scars were observed upstream of the Ramparts.

A total of eight HWM's were recorded. All observed HWM's were lines of debris deposited on the banks, and all were observed incidentally when surveying cabins. Ice scars and HWM's that were surveyed are not exhaustive for any areas, and the absence of observations of ice scars or HWMs is not indicative of the absence of those marks in any areas. Selected photos are provided in Appendix B.

3.6 Digital Terrain Model

The digital terrain model (DTM) to be used for the hydraulic model is based on the following datasets:

- NRCan HRDEM based on the Arctic DEM (NRCan 2025)
- LiDAR data for Fort Good Hope (McElhanney 2021)
- Canadian Hydrographic Service Non-Navigational (CHS NONNA) bathymetry data (DFO 2025)
- CHS Nautical Charts 6421 and 622 for the Mackenzie River near Fort Good Hope (DFO 2024)
- Bathymetry survey results obtained in July 2025 (WSP 2026a)

The WSP bathymetry survey data were validated by comparing them to the CHS NONNA bathymetry data (DFO 2025) and the CHS Nautical Chart data. Figure 3-2 a, b, and c. compare the DTM without the surveyed bathymetry data (original DTM) and the DTM with the surveyed bathymetry data (new DTM). The DTM includes Jackfish Creek but not the Rabbit Skin River.

Figure 3-2 illustrates the good agreement between the surveyed bathymetric data and the DTM obtained from CHS NONNA and Nautical Charts. This figure indicates that the riverbed did not change much at this location and the surveyed bathymetric data is considered reliable. These data are merged to the original DTM and will be used as the new DTM implemented in the updated version of the HEC-RAS model.

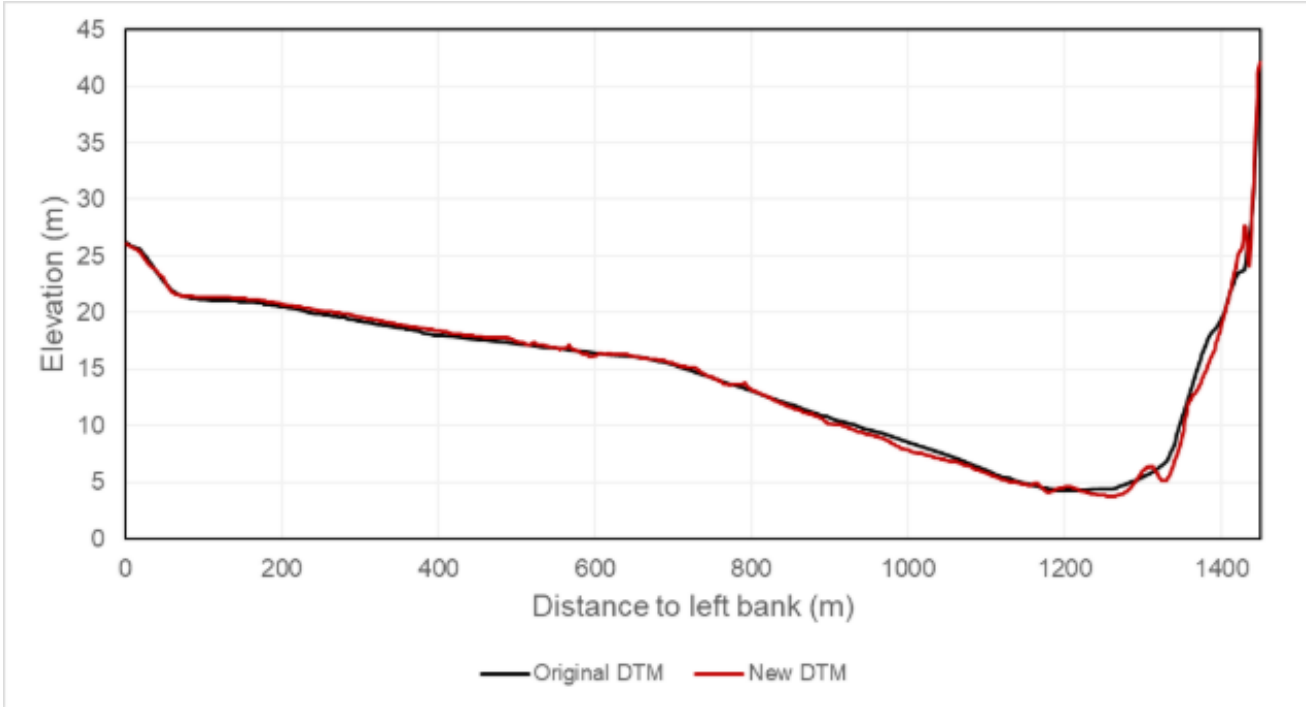

a. Cross section 2.3 km upstream of Fort Good Hope

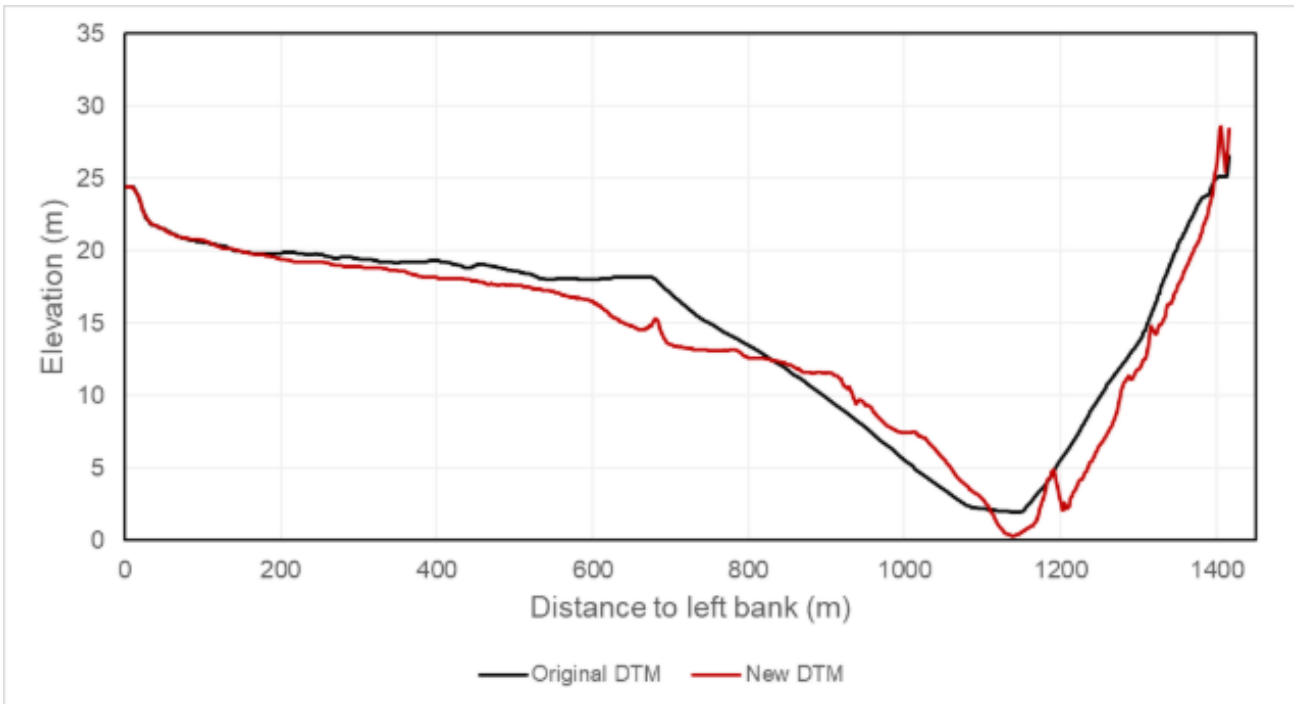

b. Cross section at Fort Good Hope

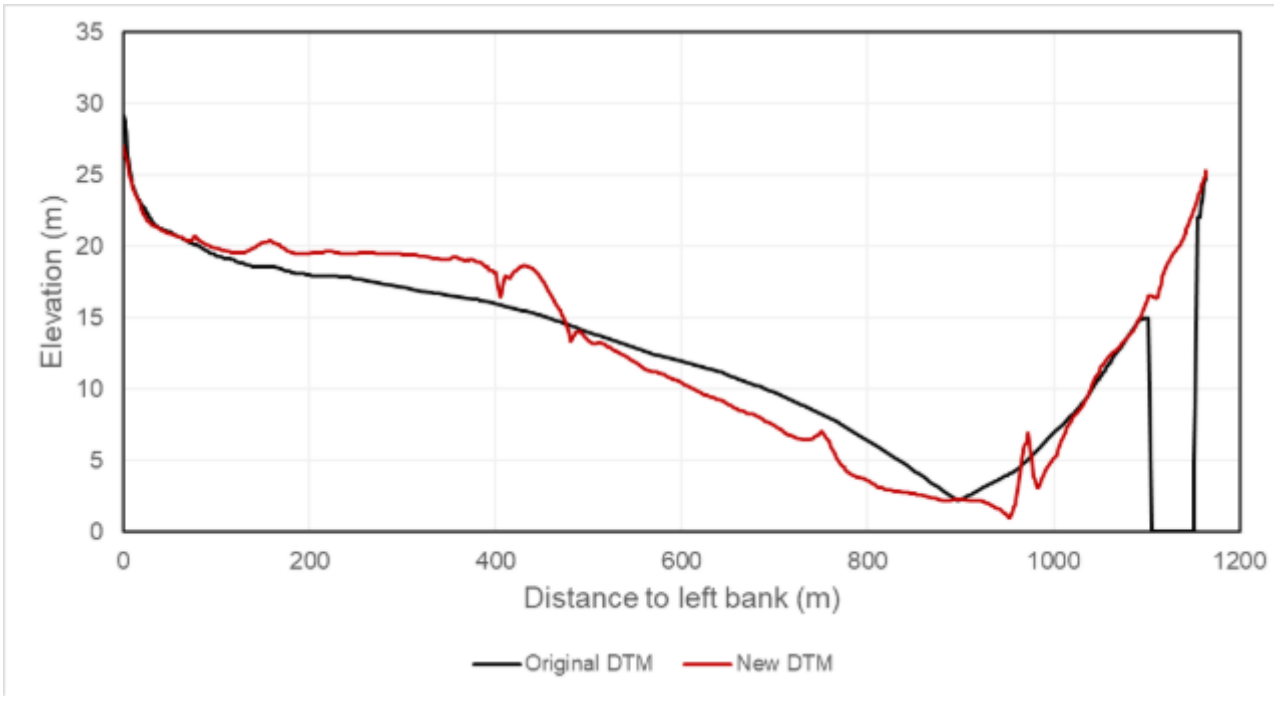

c. Cross section 2 km downstream of Fort Good Hope

Figure 3-2: Comparison between the Original DTM (without surveyed data from data obtained in 2021, 2024, and 2025) and the New DTM (with surveyed data obtained in 2025) at Three Cross Sections near Fort Good Hope

3.7 Survey and Model Stationing

Table 3-2 shows the coordinates of the center points at each cross section used in the HEC-RAS model on the Mackenzie River sorted from upstream to downstream.

HEC-RAS automatically assigns a stationing number to each cross section, with the most upstream cross section having the highest value. Some of these cross sections coincide with the field survey cross sections while others are added by the modeler. For these cross sections, the corresponding field survey names are provided alongside them.

Cross section 4384 is the one nearest to Fort Good Hope. Downstream of cross section 349, the Rabbit Skin River is modelled as a tributary to the Mackenzie River. HEC-RAS splits the Mackenzie River in an upper and lower reach, which is why the stationing sequence changes. In the upper reach, station numbers decrease downstream until station 349. Beyond this point, the lower reach begins with its own independent numbering sequence.

Similarly, Table 3-3 presents the coordinates of the center points at each cross section used in the HEC-RAS model on Rabbit Skin River from upstream to downstream.

Table 3-2: Centre Point Positions of each Cross Section used in the Model on the Mackenzie River – from Upstream to Downstream

Cross Section Stationing	Easting[(a)]	Northing[(a)]
Most upstream cross section on the Mackenzie River		
29401	496,390	7,333,391
27149	496,972	7,335,647
25265	498,190	7,337,238
23413 – Cross section A2	499,564	7,338,832
21717	501,014	7,339,677
20476	502,137	7,340,101
18644 – Cross section A3	503,509	7,341,274
17345 – Cross section A4	504,631	7,341,972
15445 – Cross section A5	506,128	7,343,120
13008 – Cross section A6	507,825	7,344841
10530 – Cross section B1	510,170	7,345,340
7735 – Cross section B2	512,564	7,346,588
5891 – Cross section B3 and B5	513,724	7,348,222
5184	514,049	7,348,745
4384	514,311	7,349,194
3861 – Cross section B4 and B6	514,523	7,349,481
3239	514,685	7,349,856
2036 – Cross section B7 and C1	514,959	7,350,666
349 – Cross section B8 and C2	515,196	7,352,201

Table 3-2: Centre Point Positions of each Cross Section used in the Model on the Mackenzie River – from Upstream to Downstream

Cross Section Stationing	Easting[(a)]	Northing[(a)]
Inflow junction from Rabbit Skin River		
84283 – Cross section C3	515,571	7,354,047
82748 – Cross section C4	515,246	7,355,381
80825 – Cross section C5 and C8	514,535	7,357,327
79219 – Cross section C6 and C9	513,849	7,358,949
77118 – Cross section C7	512,604	7,360,463
73442 – Cross section D1 and D2	510,481	7,361,743
70424 – Cross section D3	507,662	7,362,778
68216 – Cross section D4	505,505	7,363,040
66159 – Cross section D5	503,446	7,363,140
63551 – Cross section D6	501,750	7,364,686
62067	501,126	7,365,946
60908	500,802	7,367,031
58487 – Cross section D7	499,941	7,369,351
54647	499,509	7,372,262
52364	498,781	7,374,416
50292 – Cross section E1	497,896	7,376,249
48727	497,172	7,377,347
45549 – Cross section E2	495,039	7,379,642
42220	491,821	7,380,340
39991 – Cross section E3	490,038	7,381,313
37904	489,090	7,383,060
36093	488,279	7,384,590
34657	487,780	7,385,829
31097 – Cross section E4	485,385	7,388,585
28696	483,452	7,389,995
26035 – Cross section F1	481,668	7,391,916
22089	479,361	7,394,759
19450	477,876	7,396,356
14678 - Cross section F2	474,521	7,399,674
11470	471,989	7,401,557
6905- Cross section F3	467,810	7,402,505
3572- Cross section F4	464,417	7,402,443
Most downstream cross section on the Mackenzie River		

(a) Coordinates are in NAD83(CSRS)/UTM Zone 9N.

Table 3-3: Centre Point Positions of each Cross Section used in the Model on Rabbit Skin River – from Upstream to Downstream

Cross Section Stationing	Easting[(a)]	Northing[(a)]
6816 – Cross section RSR5	521,015	7,355,397
4848 – Cross section RSR4	519,749	7,354,408
3323 – Cross section RSR3	519,528	7,352,924
1791 – Cross section RSR2	518,096	7,352,761
470 – Cross section RSR1	516,840	7,352,724
Junction to the Mackenzie River		

(a) Coordinates are in NAD83(CSRS) UTM Zone 9N.

3.8 Additional Data

Selected photos of key features in the study area that were surveyed in July 2025 are provided in Appendix B.

4 FLOOD HYDROLOGY

4.1 Flood History

Larger floods at Fort Good Hope that were recorded at gauges (WSC 2024) and/or documented through historical accounts (Selwyn 1980; Karamanski 1953; Kriwoken 1983; Coles 2022a) are provided in Table 4-1 (Coles 2022b). The May 2021 flood is considered the highest on record; more detail on this event is provided in the Fort Good Hope 2021 Flood Chronology memorandum (WSP 2026b).

Ice jams usually occur at the Ramparts, where the Mackenzie River narrows into a steep, cliff-faced constriction that promotes ice accumulation. When these jams release, a large mass of ice is driven downstream and often jams again just below Fort Good Hope. The recurring cause of major flooding at Fort Good Hope is backwater flooding generated by ice jams located around 5-10 km downstream of the community. The ice jam model developed in this study represents a scenario in which a jam downstream impedes flow and produces upstream backwater that inundates Fort Good Hope. It is important to note that the model simulates the backwater effects of a stable jam only and does not simulate the jam release.

Table 4-1: Flood History of Fort Good Hope

Flood Event – Date of Peak	Details
May 26-28, 1831 (or 1836)	Fort Good Hope was located on Manitou Island from 1804 to 1831, when they experienced an ice jam flood. A release of an ice jam at the Ramparts sent a mass of ice and water downstream upon Manitou Island so it was completely under water, and 3 feet (ft) over bankfull stage. The community was destroyed and subsequently moved to its present location on the east bank of the Mackenzie River. Flood chronology provided by Kriwoken (1983, from Hudson Bay Company [HBC]): ▪ May 24: Water level rising; ice breaks up moves for one hour downstream then stops. ▪ May 26: Water at bankfull. At sunrise, Upper Ramparts ice comes down with great velocity; soon after water was rushing into the fort, reaching 3 ft in the stores and houses. By noon, water drops 2 ft, drawing off gradually. ▪ May 27: Water rises a second time, again rushing into the fort. ▪ May 28: Ice piled high (20 ft) on banks. ▪ May 30: Water receding fast.

Flood Event – Date of Peak	Details
	Other sources, including GNWT's culture and heritage team in the ECE (Education, Culture, and Employment) department, reference ice destroying the Manitou Island fort in 1836. An ambiguity exists on the exact date at which flooding occurred, with evidence pointing to either 1831 or 1836 (Saade 2025).
May 17, 1911	1911 was the lowest of three extreme flood events that flooded Fort Good Hope as noted in Kriwoken (1983). Estimated flood peak of 32.5 masl (GSC) exceeded the bankfull stage of Jackfish Creek abandoned channel. Flood chronology provided by Kriwoken (1983, from HBC): ▪ May 7: Ice/water level started to rise on the Mackenzie ▪ May 16: The Ramparts ice comes down and jams downstream. May 17: Ice moves and the river cleared: at 19:30 water level rises fast and flooded via the low point at the mission, at 22:00 Mackenzie River ice went down and was all broken.
May 1961 (date unknown)	The highest of three extreme flood events at Fort Good Hope as noted in Kriwoken (1983). Flood levels were surveyed at three locations that ranged from 33.4 masl to 33.7 masl (CGVD28). The maximum flood level was mapped. Backwater from Mackenzie River overtopped Jackfish Creek banks and flooded the low-lying gully located northeast of HBC store. Believed to be caused by the ice jam 5 km downstream of Fort Good Hope at the mouth of Rabbit Skin River. No evidence available on extreme ice shove limits.
May 1976 (May 8 based on community knowledge, see community engagement Feb 2025)	The second-highest of three extreme flood events that flooded Fort Good Hope as noted in Kriwoken (1983). Flood levels were surveyed at three houses in the gully and ranged from 33.0 to 33.5 masl (CGVD28). Backwater from Mackenzie River overtopped Jackfish Creek and flooded the low-lying part of the community northeast of HBC store. Ice jam noted to be 8 km downstream at the island (Coles 2022a).
May 1982 (date unknown)	Break-up flooding in May at a river level 20 metres above the river level of 21.28 m (GSC) surveyed on July 18, 1982. It was due to ice jamming 7.5 km downstream at an island below the mouth of the Rabbit Skin River. Backwater enters Fort Good Hope via Jackfish Creek, flooding the low-lying gully northeast of the HBC store; this gully was a past channel of Jackfish Creek (Kriwoken 1983).
May 11-14, 2005	Jackfish Creek and Rabbit Skin River rose to the point that 50 people were evacuated from Fort Good Hope. A state of emergency was declared. Estimated Total Cost: $920,000 (GNWT 2014) The maximum flood level is estimated as 33.5 m (see Section 4.2)
May 25, 2021	Ice released from the Ramparts began to move in Fort Good Hope the evening of May 24, 2021 and continued through May 25, 2021. There was still an ice jam starting 6 km downstream of Fort Good Hope after the peak had passed (GNWT 2021). An evacuation alarm was issued for Fort Good Hope Community at 04:30. When water levels exceeded 12 m, an evacuation was triggered, a state of emergency was declared at 10:10 on May 25, 2021. Flood waters neared the 17 m mark on Tuesday evening, May 25, 2021 (Arthur Tobac, Fort Good Hope public information officer). Record ice jam related flooding which peaked on May 25, 2021 at 17:30 based on stage records and were slowly receding thereafter (GNWT 2021). The EMO officer, Roger Plouffe, observed water level dropped about 2.5 m at 19:30 Monday (date assumed to be following Monday) when the downstream ice blockage broke up. The hydrometric water level gauge recorded photographs during the spring flood on May 24 and 25, 2021 (GNWT 2021) The maximum flood level is estimated as 33.8 m based on land surveys.

HBC = Hudson Bay Company, GSC = Geological Survey of Canada, GNWT = Government of Northwest Territories, EMO = Emergency Management Office.

4.2 Recent Ice Jam Flood Events

Two major ice jam flood events occurred in the last 20 years at Fort Good Hope: in May 2005 and May 2021. Figure 4-1 compares the flood extent in May 2005 and 2021. Four buildings (a, b, c, and d) are pointed out on both images to ease the comparison.

(a) May 2005 (b) May 2021

Source: GNWT 2014

Figure 4-1: Flood Extent Comparison: May 2005 and May 2021 (aerial images; flood extents are indicated by a dashed line)

May 2021 maximum flood level was evaluated based on land surveys: 33.8 m (CGVD 2013). Unfortunately, no water level record or maximum flood level estimate is available for May 2005 event.

Based on flood images comparison, it appears that maximum flood height was similar during both events, in 2005 and 2021. The image comparison indicates that the 2005 maximum flood height was slightly lower in 2005 than in 2021. For instance, the flood line around house “d” (Figure 4-1) is on one side in 2005 and on the other in 2021. The height difference is estimated as -0.3 m, based on LiDAR ground information (McElhanney 2021). Thus, the May 2005 maximum flood level is estimated as 33.5 m.

Figure 4-2 shows the ice on the Mackenzie River and the flooding at Fort Good Hope in May 2005.

Figure 4-2: Ice on the Mackenzie River and Flooding at Fort Good Hope in May 2005

4.3 Open Water Flood Frequency

Using the flood frequency analysis results for the Norman Wells and Arctic Red River gauges, a regional flood frequency curve for the Mackenzie River was developed by plotting flood frequency results against drainage area (Table 4-2). The location of the regional hydrometric gauges is provided in Figure 4-3. The regional curve was then used to estimate annual exceedance probability (AEP) flows for the Mackenzie River at Fort Good Hope (Figure 4-3). Attenuation of larger peak flows is noticeable in records between Norman Wells and Arctic Red River gauges, and this may be due in part to the Ramparts – a distinct narrow reach that can behave like a hydraulic control that can raise levels locally or upstream and constrict flow further downstream (WSP 2025).

Table 4-2: Mackenzie River at Fort Good Hope (10LD001) Open Water Flood Frequency Estimates - Flows

Annual Exceedance Probability	Average Return Period (years)	Peak Mean Daily Flow (m^3/s)
20%	5	27,000
10%	10	29,000
4%	25	31,000
2%	50	32,000
1%	100	33,000
0.5%	200	34,000
0.2%	500	36,000

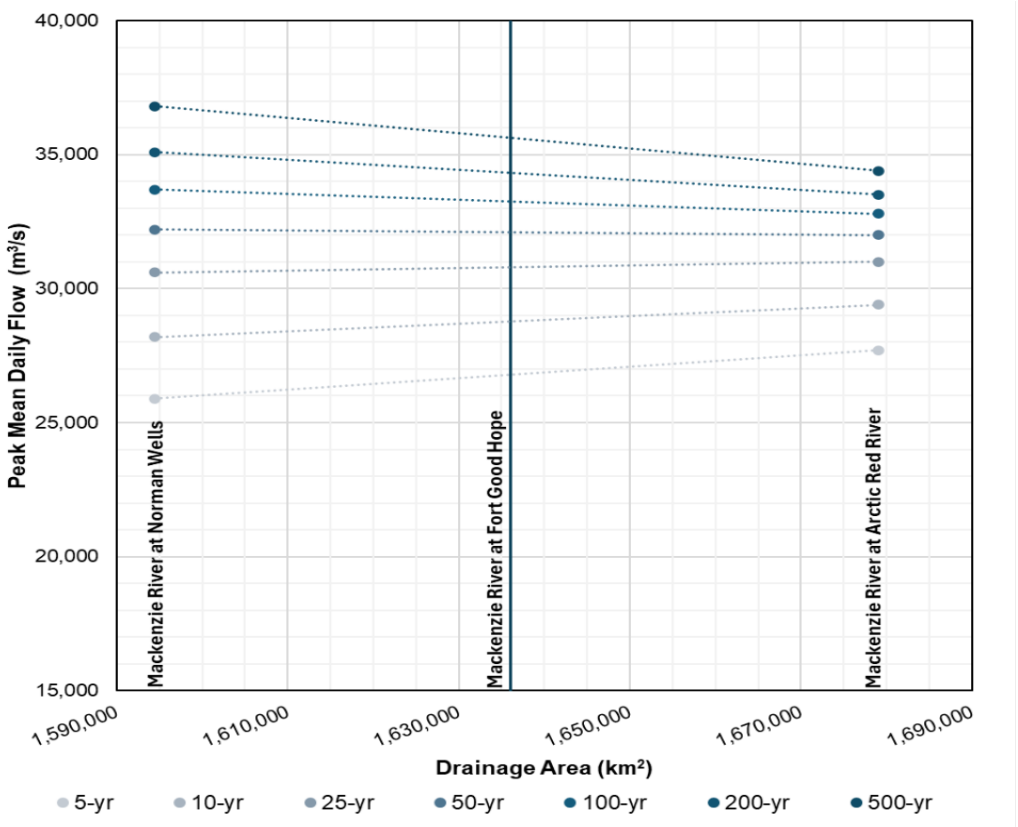

Figure 4-3: Mackenzie River Regional Frequency Curve

A flood frequency analysis was completed for the two tributaries of the Mackenzie River in the study area. Both the Rabbit Skin River and Jackfish Creek (the latter has only 7 years of data for annual peaks) have shorter records which introduces a large amount of uncertainty to this analysis. Details are provided in WSP (2025). Flood frequency analysis results based on annual peak daily values are summarized in Table 4-3.

Table 4-3: Open Water Flood Frequency Analysis Results – Tributaries of Mackenzie River

Annual Exceedance Probability	Average Flood Event (years)	Peak Mean Daily Flow (m^3/s)	
		Rabbit Skin River at Fort Good Hope (10LD004) [a]	Jackfish Creek at Fort Good Hope (10LD002) [b]
50%	2	390	3.9
20%	5	680	4.5
10%	10	860	4.8
4%	25	1,100	5.0
2%	50	1,200	5.1
1%	100	1,400	5.2
0.5%	200	1,500	5.3
0.2%	500	1,700	5.4

(a) Weibull distribution was best fit for Rabbit Skin River annual peak data.

(b) 3-Parameter Log-normal distribution was best fit for annual peak data for Jackfish Creek to obtain these results.

Four flow magnitudes were selected in the HEC-RAS model for calibration and validation purposes. These flows have corresponding water surface elevations recorded at gauge 10LD001 on the Mackenzie River at Fort Good Hope. A discharge of 25,445 m^3/s measured on June 3rd, 2022 was used to calibrate the riverbed Manning's n coefficient. The model was then validated using the three additional flows: 19,597 m^3/s, 31,498 m^3/s, and 33,345 m^3/s.

4.4 Ice Regime

The Community of Fort Good Hope is located 10 km downstream of a narrow reach of the Mackenzie River, called the Ramparts. The river at the Ramparts is approximatively 0.5 km wide. Upstream of the Ramparts, up to Norman Wells (175 km-long reach), the river is wider; between approximately 1.0 and 4.5 km.

Another narrow reach and bend, called 15-Mile Point, is located 22 km downstream of Fort Good Hope.

Both sites (the Ramparts and 15-Mile Point) are prone the ice jamming. The timing of ice jams and releases upstream and downstream of the Ramparts dictates the severity of the ice jam flood at Fort Good Hope. Typically, the ice accumulation downstream of the community clears first, which leaves room for incoming ice run when the Ramparts ice jam releases second. In this frequent situation, the resulting water levels do not cause flooding at Fort Good Hope.

In some years (as in 1911, 1961, 1976, 2005, and 2021), it is believed that the Ramparts ice jam releases first, which creates an ice run that passes in front of Fort Good Hope and adds ice volume to the downstream jam. In this situation, the resulting water levels usually rise rapidly and lead to land-flooding at Fort Good Hope. This ice jam flooding scenario is the one analyzed in this study because it is considered to have caused the most extreme flood impacts for the community.

To illustrate the general ice jam and release processes on the Mackenzie River, WSP has analyzed the historical water level data at Norman Wells. Appendix C shows the daily water level recorded at Station 10KA001 (Mackenzie River at Norman Wells) for years 2002 to 2023 (22 years).

For all years analyzed, the maximum annual water level always occurred during the month of May, at time of breakup. Most of the years shows similar patterns at breakup:

1) Sudden water level rise (R1)

2) Sudden water level drop (D1), a few days (1-4 days) after the rise R1

From our understanding, the sudden rise R1 observed at Norman Wells is caused by ice jam formation and resulting backwater effect. The sudden drop D1 is associated with ice jam consolidation and potentially ice jam release. Historical data shows that the drop D1 can sometime be followed by a second one (drop D2).

In May 2021, the water level at Norman Wells rose rapidly on May 17 (+3.0 m in 1 day), then dropped on May 18 (-2.9 m in 1 day). The water level remained constant for 5 days before dropping again on May 24 (-1.6 m). Discharge recorded at Station 10KA001 during the same period (May 17 to 24) was stable, ranging between 18,400 and 22,700 m^3/s.

The sudden rise and drop sequence (R1, D1) observed almost every year indicates that ice jams form almost every year on the Mackenzie River near Fort Good Hope. Therefore, ice jam potential is present every year.

The Ramparts is a natural barrier that promotes ice jam formation upstream of Fort Good Hope, thus reducing the frequency of ice jam flooding for the community. However, in some years (as in 2021), the ice jam formed at the Ramparts may release first and combine with ice jam downstream, leading to significant ice jam flooding in the Community.

4.5 River Ice Thickness

ADCP surveys were carried out at Norman Wells by the Water Survey of Canada to measure under-ice flows from 2004 to 2021. During this campaign, ice thickness was measured in situ in 2013, 2015, and 2016. Table 4-4 shows the average ice thickness of each of these measurements.

Table 4-4: Average Ice Thickness at Norman Wells from ADCP surveys

Date	Average Ice Thickness (m)
March 5, 2013	1.84
March 12, 2015	0.51
January 28, 2016	1.08
April 15, 2016	1.19

The ice thickness on March 12, 2015 is low compared to the other ice thicknesses. The cumulative degree-days of freezing (CDDF), discussed in more details in Section 7.1, indicate that this year has a below average CDDF. This suggests that the winter of 2014-2015 is a comparatively a mild year.

Ice thickness data were also found from the Original Ice Thickness Program which is a data collection of ice thicknesses in different regions in Canada (ECCC 2024b). Ice thicknesses at certain days in winter from 1959 to 2000 are provided as measured at Norman Wells. The box plot shown in Figure 4-4 illustrates the mean and median ice thickness, along with the minimum and maximum values, as well as the first and third quartiles.

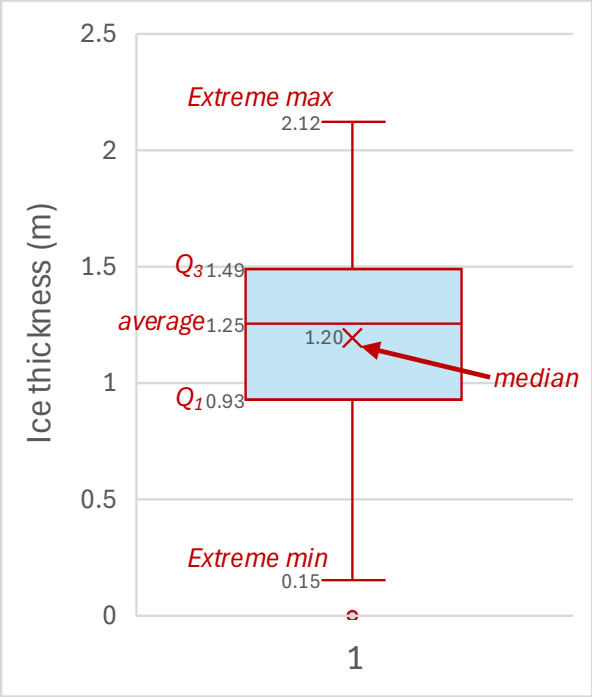

Figure 4-4: Box Plot of the Ice Thicknesses Obtained from the Original Ice Thickness Program

Ice thickness during break-up will be estimated using measurements taken around the dates of peak ice jam staging.

Another method that will be used to assess ice thickness will be to calculate it using the Stefan equation as presented in Equation 7-1 of Section 7.1. The measured ice thicknesses will be used to adjust the ice thickness estimation from the Stefan equation.

4.6 Ice Jam Flood Frequency

Recent historical data (Table 4-1) shows that the low-lying part of the community was flooded in 1961, 1976, 1982, 2005, and 2021. Thus, ice jam floods occurred at least five (5) times over the last 50 years, which corresponds to an annual flood frequency of about 10%.

Ice jam modeling results (Section 9.4) provide more detailed ice jam flood frequency estimates.

4.7 Concurrent Ice Jams

For ice jam flooding to occur at Fort Good Hope, an ice jam must form downstream of the community and cause significant backwater. Three types of downstream jam are possible:

- Type 1: accumulation of local ice formed downstream of the Ramparts
- Type 2: ice run coming from upstream of the Ramparts that stopped by itself downstream
- Type 3: ice run coming from upstream of the Ramparts that was impeded by an existing jam

A Type 1 jam is less likely to cause flooding at the community because the ice volume is limited. For instance, the river length between the Ramparts and 15-Mile Point is 35 km.

An ice run initiated at the Ramparts is unlikely to stop by itself on its way down (Type 2) unless it is impeded by an existing ice jam (Type 3).

A Type 3 jam occurs when an upstream ice jam (at the Ramparts) releases while a downstream ice jam is in place. This type of jam is the one associated with higher flooding magnitude.

The Ramparts is a region prone to ice jam formation. Its narrow section creates a major flow contraction. The Ramparts is the most constrictive river morphologic feature in the area. Thus, ice that makes its way through the Ramparts will likely run freely downstream, even through the river bends, islands and channels. This explains why Type 2 downstream jams are unlikely. Because of the major constriction at the Ramparts, an upstream jam is more likely to release after a downstream one; thus, reducing the likelihood of Type 3 downstream jam. Although, in certain conditions, an upstream jam may release first and the resulting ice run may be impeded by the presence of a downstream jam, as was observed in May 2021.

In theory, the ice floes produced by a release at the Ramparts are small enough to be carried downstream by the flow without causing major ice jams. Such occurrences were observed from satellite images (available since 2017), where for 9 winter seasons, the release of the upstream ice jam has not caused jamming downstream. Instead, once the ice jam at the Ramparts is released, the downstream ice typically releases before, or simultaneously, along the Mackenzie River, causing no flooding at Fort Good Hope.

For instance, on May 17, 2024, two concurrent ice jams were observed both upstream and downstream of Fort Good Hope, as shown in Figure 4-5. The upstream jam extended roughly 9 km upstream of the Ramparts. The next available satellite image, dated May 22, 2024, shows that both jams had fully cleared. No flooding occurred that spring.

(a) Satellite imagery from Copernicus (2025) on May 17, 2024 at near Fort Good Hope

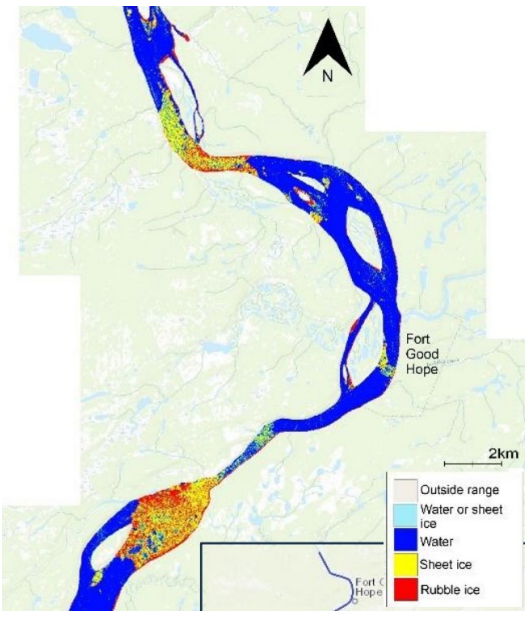

(b) River ice classification of the Mackenzie River near Fort Good Hope 2024-05-17 20:00 MDT (GNWT 2024)

Figure 4-5: Concurrent Ice Jams Observed on May 2024 from both Satellite Imagery and River Ice Classification

A similar situation occurred on May 21, 2021, when satellite imagery again shows concurrent ice jams upstream and downstream of the community, as illustrated in Figure 4-6. The RADARSAT image (Figure 4-6b) shows the ice condition on that day. The upstream jam is made of smoother rough and rough ice, as shown the orange and red colours. The downstream jam is made up of a mix of smooth ice, rougher smoother, smoother rough, and rough ice. On May 21, 2021, the upstream jam was approximately 100 km long. The large volume of ice released from the Ramparts subsequently jammed downstream of Fort Good Hope, producing one of the most severe floods on record.

These observations suggest that the length of the upstream ice jam at the Ramparts may influence whether its release will trigger downstream jamming near Fort Good Hope. Other factors also contribute to the probability of ice-related flooding at Fort Good Hope. These include the flow magnitude and the rate of snow and ice melt. Low flows generally pose a low flood risk on the community. A high rate of snow and ice melt might be the cause of high flows, but at the same time, might favor early jam release, thus reducing the risk of flooding.

Freeze-up levels also influence the stability of the jams and the likelihood of ice jam flooding for the community. A jam formed at higher elevation will have more room underneath to pass the incoming flow, while remaining stable. If the jam downstream of the community is more stable, it is more likely to stay in place longer and cause more backwater effect and associated flooding when the upstream jam releases. Observations show that the freeze-up and winter water levels on the Mackenzie River prior to breakup in May 2021 were historically high.

In sum, forecasting flooding at Fort Good Hope is not a linear and simple task that relies on a single variable. The phenomenon results from the interaction of multiple, interdependent factors, and additional data are required to improve our understanding of the conditions that lead to flooding and those that do not.

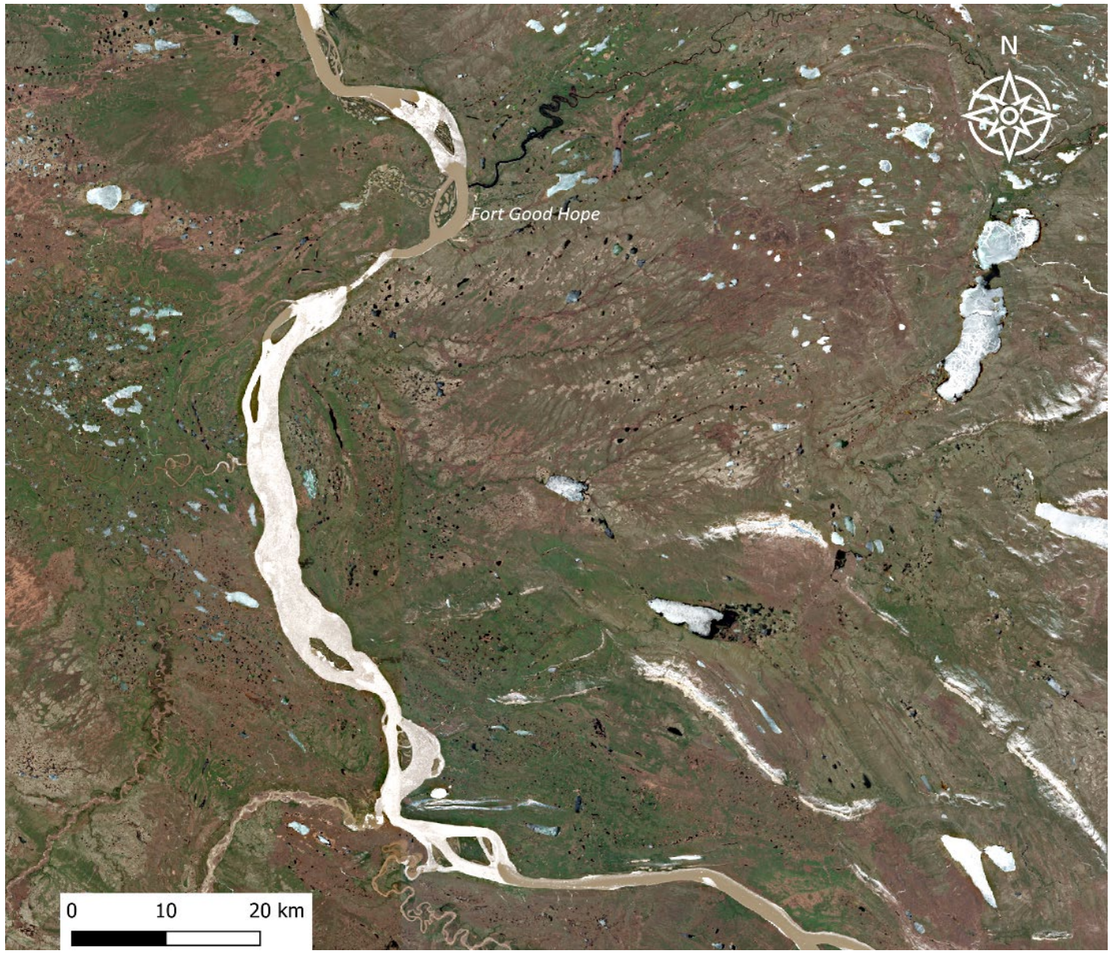

(a) Satellite image on May 21, 2021 near Fort Good Hope (Copernicus 2025)

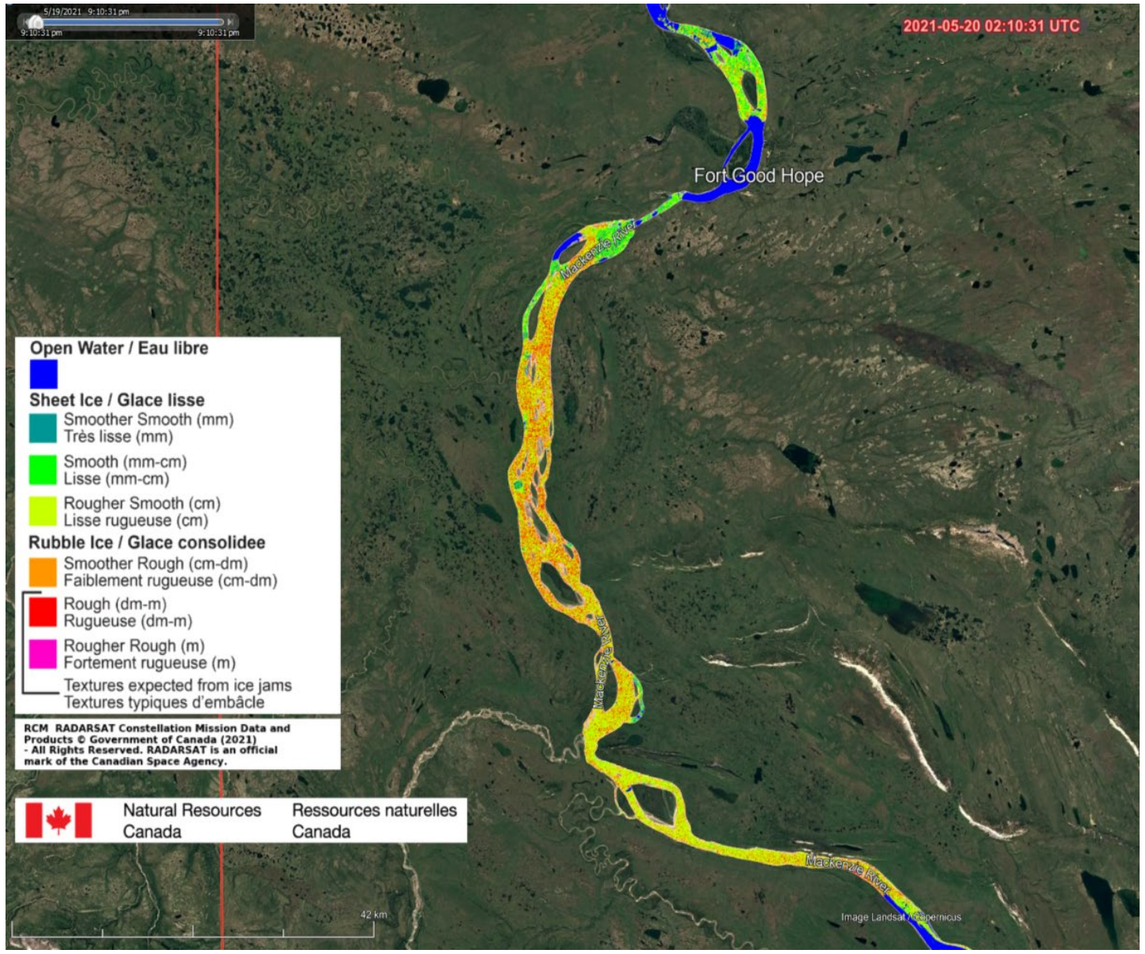

(b) RCM RADARSAT Constellation Mission Data of the ice conditions on May 20, 2021 02:10:31 UTC near Fort Good Hope (NRCan 2021)

Figure 4-6: Concurrent Ice Jams near Fort Good Hope on May 21, 2021

5 MODELLING APPROACH

This section describes the modelling methodology followed for this study and includes the following:

1) Set up the HEC-RAS model by incorporating the digital terrain model described in Section 3 (which combines online data with field surveyed data) and defining cross sections along the Mackenzie River and Rabbit Skin River.

2) Calibrate the HEC-RAS model for open water condition by adjusting the riverbed's Manning's n coefficient using an event for which the flow and the corresponding water elevation at Fort Good are known. Validate the model in open water condition with three other events (Section 6).

3) Calibrate the HEC-RAS model for ice jam conditions. Section 7 describes ice-specific parameters used in the model such as ice thickness, ice Manning's n coefficient and ice jam toe and head locations. Section 8 presents the calibration of the ice jam model for the May 20, 2021 and May 25, 2021 which were ice jam conditions.

4) Perform the Monte Carlo Analysis as explained in Section 9. This involves defining hydraulic and physical properties that affect ice jam conditions such as flow, ice thickness, and ice Manning's n coefficient. Historical observed values are analyzed to define the appropriate frequency distribution for these parameters from which random values (2,000 values) are be extracted from. A global sensitivity analysis is also carried out to evaluate the influence of each parameter. Furthermore, a joint probability analysis is performed to determine the consequences of extreme values occurring at the same time.

5) Implement these parameters obtained from the Monte Carlo Analysis in the HEC-RAS ice jam model. This step is performed using HECRASController, which automatically runs these 2,000 case scenarios sequentially. HECRASController is available in the Visual Basic of Applications (VBA) accessible through the macros in Microsoft Excel. The relevant exceedance probabilities are calculated, and the corresponding water surface profiles are plotted.

6) Consider climate change (Section 10) for which future projected of peak ice thicknesses and flows are estimated and implemented in the ice jam model for mid-century (2050s) and end-of-century (2080s) future periods.

7) Provide flood mapping with and without climate change for the 1% and 0.5% AEPs.

6 OPEN CHANNEL HYDRAULICS

Flooding events for the Mackenzie River near Fort Good Hope were simulated using a 1D model with HEC-RAS (version 6.6) developed by the US Army Corps of Engineers (USACE 2024). This section presents the model setup as well as its calibration for different historical water level records.

6.1 Open Water Model Setup

The digital terrain model (DTM) used in this hydraulic model is a combination of existing bathymetry data and surveyed ground data as presented in Section 3.6. The model extends from just upstream of Spruce Island to Andersons Landing with 56 cross sections spaced at intervals ranging from 0.5 to 3 km, as shown in Figure 6-1. A portion of these cross sections corresponds to those collected during the 2025 field survey, while others were added by the modeller.

Figure 6-1: 1D HEC-RAS Model Extent from Spruce Island to Anderson's Landing

The flows measured at Norman Wells and the water levels recorded at Fort Good Hope (in CGVD13) were used to calibrate the model.

The flows measured at Norman Wells from Station 10KA001 are transposed at Fort Good Hope by multiplying them by the drainage area ratio of 1.026. This ratio is obtained by dividing the Fort Good Hope drainage area (1,636,000 km^2) to the Norman Wells drainage area (1,594,500 km^2). The drainage area at Fort Good Hope includes Jackfish Creek and its watershed. This implies that the flow at Fort Good Hope already includes the flows coming from Jackfish Creek, and so, there is no need to include it again in the model. Therefore, no junction was included at that location.

On the other hand, the Rabbit Skin River is included in the model, with a junction connecting it to the Mackenzie River, and its flow measurements were obtained using Station 10DL004 on Rabbit Skin River (see Figure 2-3).

The water levels at Fort Good Hope (Station 10LD001) were converted from the local zero datum to CGVD13 using a conversion factor of +17.609 m. This conversion factor was obtained by knowing that the correction factor between the local zero datum and CGVD28 is +17.646 m (WSC 2025) and that the correction factor from CGVD28 to CGVD13 is -0.037 m (Ollerhead 2023). Figure 6-2 shows the water levels measured at Station 10LD001 from 2011 to 2023. The two years with the highest non-ice-related elevations, 2012 and 2022, were selected for the calibration of the open-water model. The peak observed in 2021 is ice-related and was therefore not considered for this calibration.

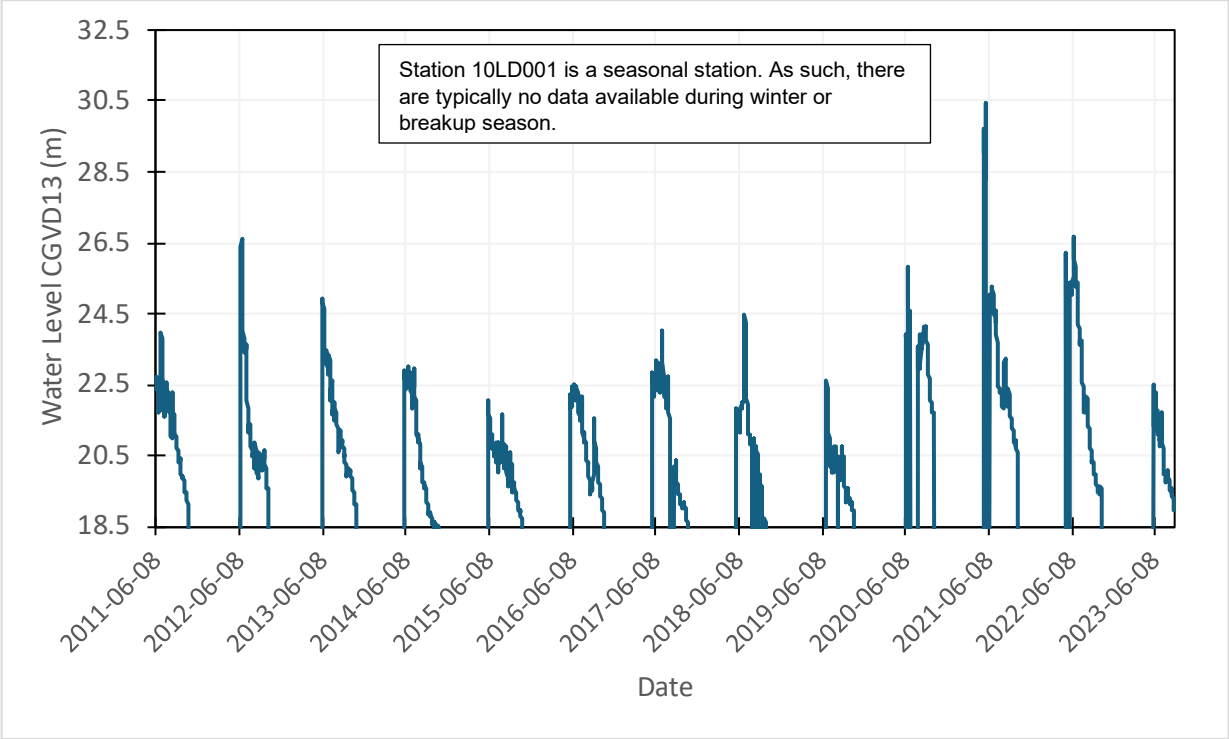

Figure 6-2: Water Levels Gauged at Fort Good Hope at Station 10LD001 in CGVD13 from 2011 to 2023

The peak elevations in 2012 and 2022 were the same at 26.6 m with flows corresponding to 33,345 and 31,498 m³/s, respectively. These peaks were preceded and followed by stable water elevations as shown in Figure 6-3 and Figure 6-4. In 2012, a stable water elevation at 23.4 m was attained after the peak elevation, with a corresponding flow of 19,597 m³/s. In 2022, a stable water elevation at around 25.1 m was reached before the increase in water levels. These stable water elevations were also considered in the open-water model calibration. Table 6-1 summarizes these chosen water elevations and flows.

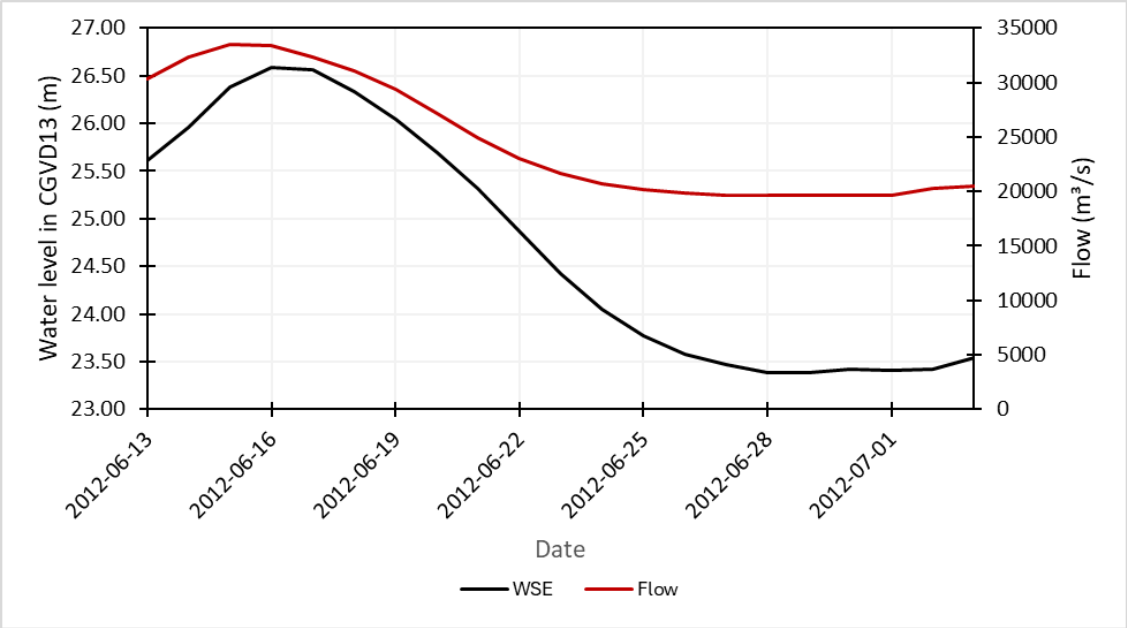

Figure 6-3: Water Levels at Fort Good Hope at Station 10LD001 around the 2012 Peak Elevation

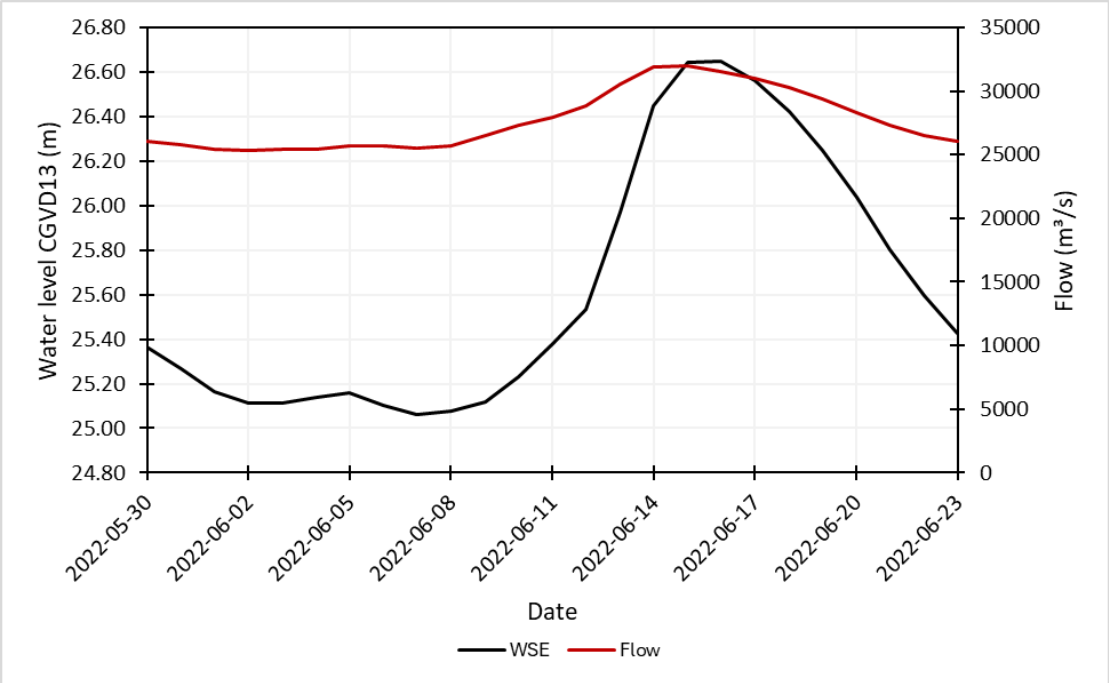

Figure 6-4: Water Levels at Fort Good Hope at Station 10LD001 around the 2022 Peak Elevation

Table 6-1: Water Levels in CGVD13 (m) at Station 10LD001 and Flows (m³/s) at Station 10KA001 Transposed at Fort Good Hope for the Open-Water Model Calibration

Date	Water level in CGVD13 (m)	Flow (m³/s)
2012-06-16	26.6	33,345
2012-06-29	23.4	19,597
2022-06-03	25.1	25,445
2022-06-16	26.6	31,498

Furthermore, a rating curve was calculated using measured water levels and flows. The ice-related events were not considered in the rating curve.

Figure 6-5 shows the rating curve of the water levels from Station 10LD001 and flows at Fort Good Hope (transposed from Station 10KA001) in red.

The blue line shows the rating curve obtained from observed water levels and flows at Norman Wells (Station 10KA001). The comparison between the two rating curves shows that the water levels at Fort Good Hope are most sensitive to flows than those at Norman Wells.

The orange points represent the ice-related water levels, which were not considered in determining the equation of the rating curve shown in the figure. The blue point shows the maximum ice jam related flood level that occurred in May 2021 as surveyed by Ollerhead & Associates in 2023.

The green points show the four points from Table 6-1 used for the open-water calibration.

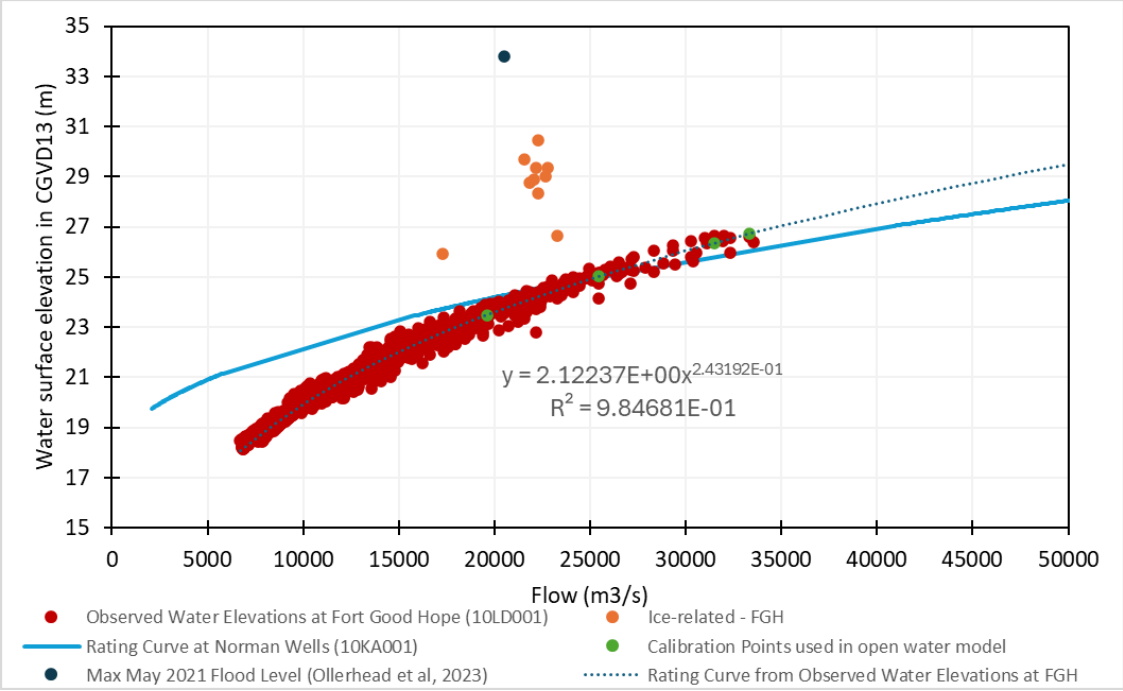

Figure 6-5: Rating Curves at Fort Good Hope and Norman Wells for Open-Water Conditions

Table 6-2: Difference between the Rating Curve and the Observed Water Levels (WL) at Station 10LD001

Flow at FGH (m^3/s)	WL from Rating Curve (m)	Observed WL at Station 10LD001 (m)	Absolute Difference (cm)
19,597	23.5	23.4	10
25,445	25.0	25.1	10
31,498	26.3	26.6	30
33,345	26.7	26.6	20

Since the difference between the observed water levels and those derived from the rating curve reach up to 30 cm, this value is considered the tolerance for our analysis. This value corresponds to the tolerance found in some studies involving hydraulic modeling calibration and validation (Loney 2021; HDR Alaska 2015).

6.2 Model Parameters

In open channel flow where no ice is considered, the main parameter that was calibrated is the Manning's n roughness coefficient of the riverbed.

6.3 Open Water Model Calibration

The Manning's n coefficient of the riverbed was calibrated to 0.021 and the Manning's n coefficient of the floodplain was set to 0.07. The upstream boundary condition is governed by the flows presented in Table 6-2 while downstream boundary condition was set to a normal depth of 0.0001. Table 6-3 shows the absolute difference (in cm) between the observed water levels and those calculated with HEC-RAS. A maximum absolute difference of 29 cm is obtained for a flow of 31,498 m^3/s. This difference falls within the tolerance from Table 6-2. The water levels calculated with HEC-RAS were also compared to those obtained from the rating curve in Table 6-4. A maximum absolute difference of 16 cm was obtained from Table 6-4, which according to the tolerance of 30 cm, is deemed acceptable.

The observed water levels are daily mean elevations recorded since 2011. Although the rating curve captures the overall trend, natural variability in the observed levels creates a range of possible elevations around it. This greater variability explains the larger differences between the observed water levels and those calculated with HEC-RAS.

Table 6-3: Difference between the Observed Water Levels (WL) and those Calculated with HEC-RAS

Flow (m^3/s)	Observed WL (m)	WL from HEC-RAS (m)	Absolute Difference (cm)
19,597	23.39	23.61	22
25,445	25.11	25.11	0
31,498	26.65	26.46	19
33,345	26.59	26.88	29

Table 6-4: Difference between Water Levels (WL) from the Rating Curve and those Calculated with HEC-RAS

Flow (m^3/s)	WL from Rating Curve (m)	WL from HEC-RAS (m)	Absolute Difference (cm)
19,597	23.48	23.61	13
25,445	25.02	25.11	9
31,498	26.35	26.46	11
33,345	26.72	26.88	16

Figure 6-6 presents the calibration results for the four flows scenarios, showing the water surface profiles computed with HEC-RAS compared to the observed water surface elevations from Station 10LD001. Furthermore, a sensitivity analysis indicates that flows coming from the Rabbit Skin River do not influence water levels at Fort Good Hope. This is because the inflow from the Rabbit Skin River is located downstream of Fort Good Hope.

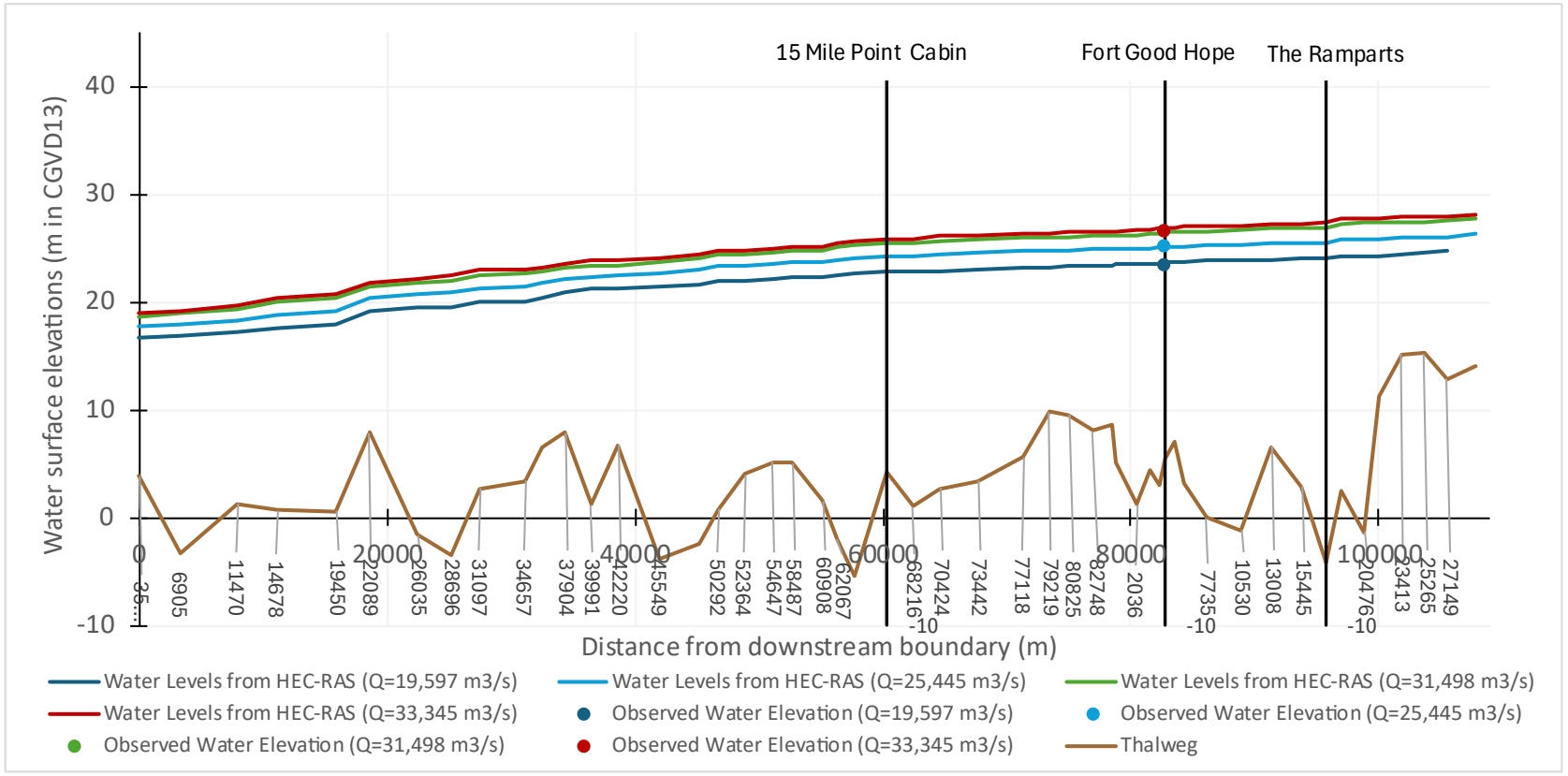

Figure 6-6: Calibration Results of the Open-Water Model in HEC-RAS

7 ICE-SPECIFIC MODEL PARAMETERS

The main ice-specific parameters considered in this model are:

- Ice thickness
- Ice Manning's n coefficient
- Ice specific gravity
- Friction angle
- Porosity
- Stress k1 ratio (default at 0.33)
- Maximum velocity (default at 1.524 m/s)
- Ice jam toe and head locations

7.1 Ice Thickness

The initial ice thickness of the ice jam was determined using the Stefan equation (Michel 1971):

$$h = \alpha\sqrt{CDDF} \quad \text{(Eq. 7-1)}$$

Where *h* is the ice thickness (m), α is a site-specific ice growth coefficient that can be determined from Table 7-1, and *CDDF* is the cumulative degree-day of freezing calculated from the beginning to the end of each winter period (°C-d). These dates were defined by identifying five consecutive days having temperatures below zero for the start period and five consecutive days above zero for the end periods.

Table 7-1: Value of Ice Growth Coefficient in the Stefan Equation (Michel 1971)

Snow and wind conditions	Coefficient α ($m/°C^{1/2}day^{1/2}$)
Theoretical value	0.035
Windy lakes with no snow	0.027
Average lake with snow	0.017 to 0.024
Average river with snow	0.014 to 0.017
Sheltered small river with rapid flow	0.007 to 0.014

In this study, a value of 0.017 was selected because the study is carried out on a river. The upper bound of the recommended range was taken because the Mackenzie River is a wide river. The CDDF is obtained using the temperature data measured at Station 2201450 located at the Fort Good Hope Airport and that offers daily data from 1998 to 2025. The years 2010, 2011, 2018, and 2024 were not considered in the analysis due to too many missing data. In total, 23 years were considered in the analysis.

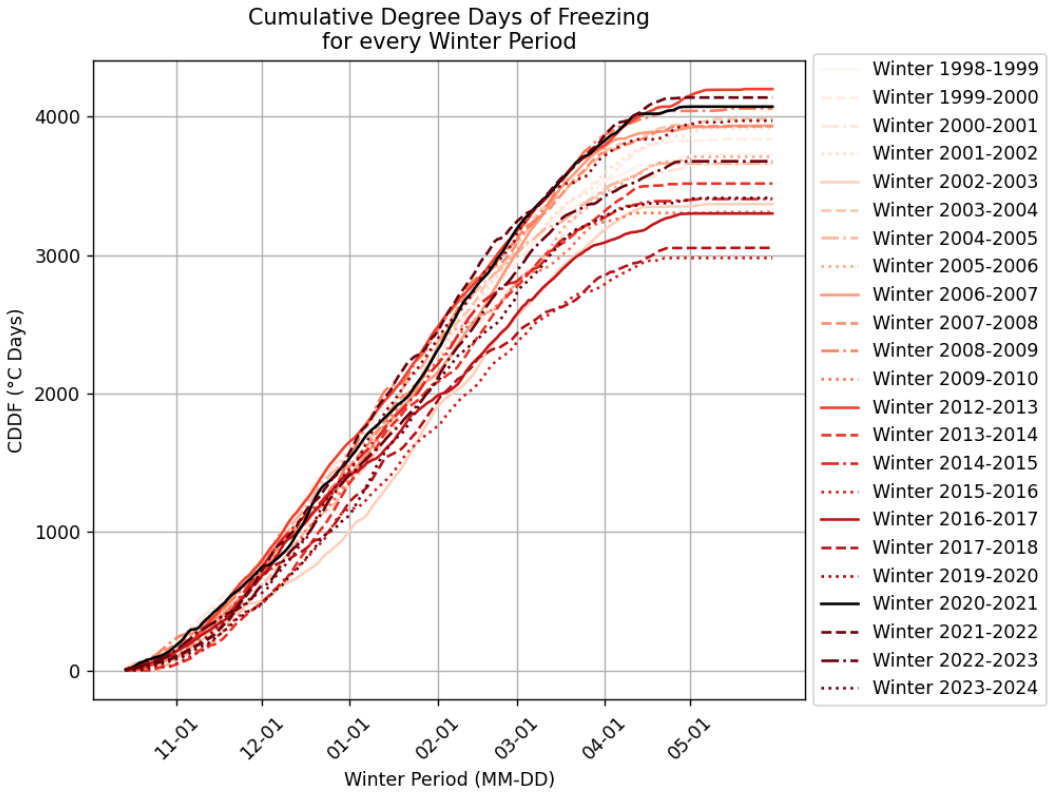

Figure 7-1: Cumulative Degree Days of Freezing for 23 Winter Periods from 1998 to 2024 Obtained from Station 2201450 at Fort Good Hope Airport

Figure 7-1 illustrates the evolution of the cumulative degree days of freezing throughout each winter. The CDDF for the 2020-2021 winter, in which the flooding occurred, is shown in black and is 4,071°C-d. From November to end-of-March, the CDDF remained mostly above average, and towards the end of the season, it increased further, ranking among one the highest recorded values.

The maximum, average and minimum CDDF were 4,198 °C-d, 3,687 °C-d, and 2,978 °C-d, respectively.

The ice thicknesses calculated from these CDDF are in Table 7-2.

Table 7-2: Ice Thicknesses Calculated using the Stefan Equation and the Maximum, Average, and Minimum CDDF Calculated using Climatic Data from Station 2201450

Statistic	CDDF (°C-d)	Ice thickness (m)
Maximum	4,192	1.3
Average	3,687	1.2
Minimum	2,978	1.1

The average ice thicknesses obtained from the ADCP survey carried out by Water Survey of Canada at Norman Wells presented in Table 4-4 and the median ice thickness obtained from the Original Ice Thickness Program presented in Figure 4-4 were both 1.2 m. The initial thickness (prior to jamming) calculated using the Stefan equation corresponding to these ice thicknesses corresponded to the one obtained using the average CDDF. This thickness was taken as the initial ice thickness of the ice jam for ice jam model.

7.2 Ice Manning's n Coefficient

The ice Manning's n coefficient represents the roughness of friction underneath the ice cover or the ice jam. Table 7-3 shows the typical ice Manning's n coefficients as proposed by USACE (2025), the developer and primary user of HEC-RAS.

Table 7-3: Suggested Range of Manning's n Values for Ice Jams (USACE 2025)

Thickness		Manning's n Coefficient Values		
ft	m	Loose frazil	Frozen frazil	Sheet ice
0.3	0.09	-	-	0.015
1.0	0.30	0.01	0.013	0.04
1.7	0.52	0.01	0.02	0.05
2.3	0.70	0.02	0.03	0.06
3.3	1.01	0.03	0.04	0.08
5.0	1.52	0.03	0.06	0.09
6.5	1.98	0.04	0.07	0.09
10.0	3.05	0.05	0.08	-

The ice Manning's n coefficient was calibrated in the ice jam model using two water levels recorded during the ice-related flooding event of 2021. In the Monte Carlo Simulation, a range of ice Manning's n coefficients was determined using the typical ice Manning's n coefficients from Table 7-3 and the calibrated ice Manning's n coefficients.

7.3 Ice Specific Gravity

The ice specific gravity is the ratio of the density of ice to the density of water. This parameter was kept at the default value of 0.916.

7.4 Friction Angle

The internal friction angle of the jam is the strength of the ice jam as a granular material (USACE 2025). The default value is 45°.

7.5 Porosity

The ice jam porosity represents the fraction of the ice jam that is filled with water (USACE 2025). The default value is 0.4.

7.6 Stress k1 Ratio

The stress coefficient k1 represents the ratio of lateral stress to longitudinal stress within the ice jam. It indicates the jam's ability to transfer longitudinal stress into lateral stress against the channel banks (USACE 2025). The default value for k1 is 0.33.

7.7 Maximum velocity, V_{max}

The maximum velocity parameter, V_{max}, in HEC-RAS defines the upper limit of mean velocity permitted beneath an ice jam. In other words, this parameter limits the mean velocity under an ice jam to prevent the jam's thickness from increasing to such an extent that the entire flow area of the channel is obstructed. If the computed mean velocity exceeds V_{max}, the model reduces the ice thickness until the velocity falls back below this threshold (USACE 2025).

An analysis was conducted to assess how V_{max} influences the simulated ice jam. When V_{max} is set above the default value, the model allows high velocities under the jam, enabling the jam to overly thicken. Conversely, setting V_{max} below the default value results in artificially thinning the jam to increase the open flow area and thus maintaining velocities below the imposed threshold.

In this study, the probability of having the ice jam obstruct the flow area is almost non-existent. Thus, it was found that keeping V_{max} to its default value of 1.524 m/s provides realistic ice jam thicknesses and avoids artificial thickening or thinning of the jam.

7.8 Ice Jam Toe and Head Locations

The presence of islands, the meandering patterns and variations in channel width along the Mackenzie River contribute to ice jams formation. The toe of the ice jam is located at the downstream end of the jam while the head is located at the upstream. Satellite imagery was analyzed to identify the locations of the ice jam toe and head during the May 2021 ice-related flood event. A similar analysis was carried out for various winters to determine the range of possible toe and head positions to be used as an input in the Monte Carlo Simulation. These analyses are presented in more detail in Section 9.1.5.

8 ICE JAM MODEL CALIBRATION

The ice jam model's extent is the same as that from the open water model presented in Section 6.1. The main difference between the two models is the implementation of ice covers and ice jams.

8.1 May 20, 2021 and May 25, 2021 Ice Jam Calibration Events

The ice jam model was calibrated using two ice jam related events from 2021: the May 20 and May 25 events. These events were selected because water surface elevations, flows, and ice jam conditions can be estimated and implemented in the ice jam model. These two different events allowed the estimation of different ice Manning's n coefficients, which were useful for defining the parameter range to be applied in the Monte Carlo Simulation.

Figure 8-1 shows in blue the water surface elevations recorded at Station 10LD001 from WSC (2025) in CGVD13. As presented in Figure 8-1 the highest stage elevation has been recorded on May 25, 2021, at 17:30, corresponding to an elevation of 31.1 m. Nonetheless, a maximum flood level of 33.8 m has been estimated from the HWM level survey carried out by Ollerhead & Associates (2023). Because the WSC data appear to underestimate water levels, a correction factor of +2.7 m was applied to these data. The adjusted WSE values were used for calibration and are shown in red in Figure 8-1.

Table 8-1 also shows the difference between the two events (orange rectangles). On May 20, 2021, the water surface elevations remained relatively stable, with minor fluctuations in the flow and in the water surface elevations. In contrast, on May 25, 2021, the water surface elevation increased and decreased while the flow steadily decreased. These two orange rectangles represent the two events considered for the ice jam model calibration.

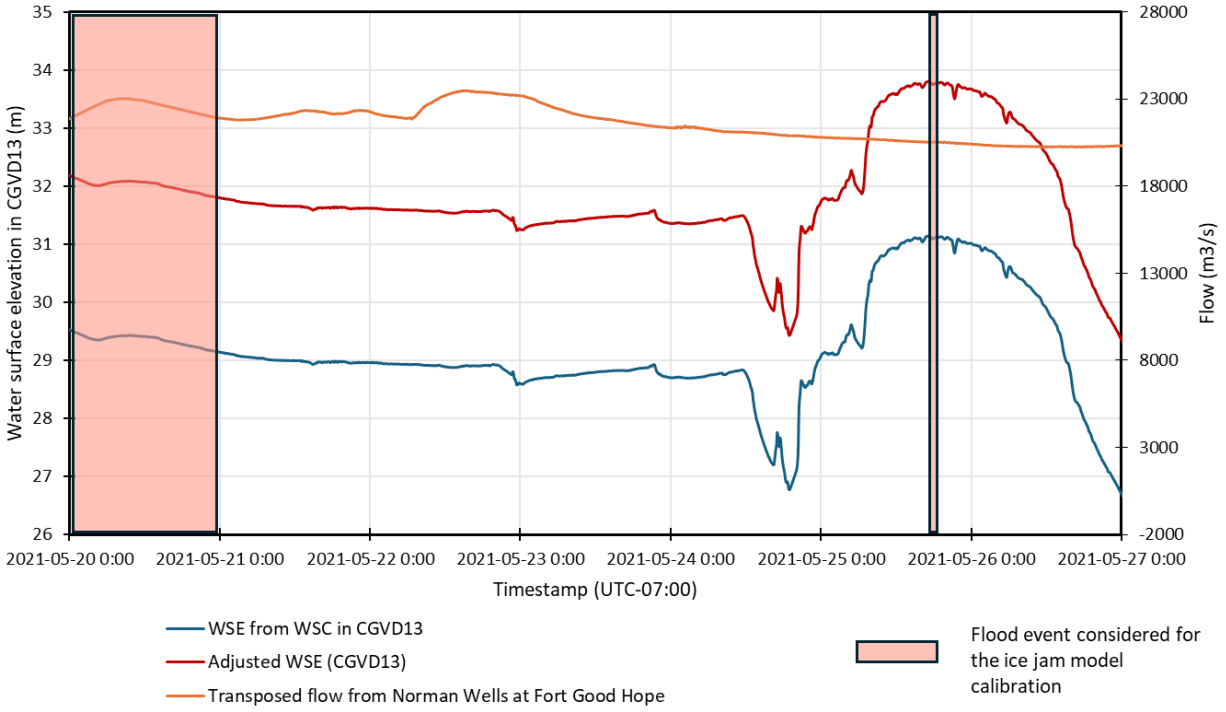

Figure 8-1: Measured WSE at Station 10LD001 in CGVD13, Adjusted WSE with Correction Factor Obtained from HWM Survey (Ollerhead & Associates 2023), and Fow Data from Station 10KA001 at Norman Wells Transposed at Fort Good Hope

Table 8-1 presents the original WSE as provided by WSC (2025), the adjusted WSE using the correction factor of +2.7 m, and the corresponding flows for May 20 and 25, 2021. This table also shows the difference between two timestamps: UTC-07:00 and UTC. No major difference was noted for the May 20 event, as the average of the day was taken, and no significant fluctuation occured in the water level.

However, some confusion might arise for the May 25, 2021 event since the maximum stage level occurs on May 25, 2021 at 17:10 using the UTC-07:00 timestamp, but on May 26, 2025 at 00:10 with the UTC timestamp.

Table 8-1: WSE from WSC (2025) in CGVD13, Adjusted WSE in CGVD13, and Corresponding Flows Used for the Ice Jam Model Calibration

Timestamp (UTC-07:00)	Time (UTC)	WSE from WSC in CGVD13 (m)	Adjusted WSE in CGVD13 (m)	Corresponding flow (m^3/s)
May 20, 2021	May 20, 2021	29.6	32.3	21,553
May 25, 2021 17:10	May 26, 2021 00:10	31.1	33.8	20,523

Figure 8-2 and Figure 8-3 show the RADARSAT images from NRCan of the ice conditions during the above-mentioned days.

Figure 8-2 shows an ice jam whose head is located at cross section 82748, about 1.6 km downstream of Manitou Island. The ice jam toe location was estimated to be at cross section 68216, which is around 2 km upstream of the 15 Mile Point Cabin. Appendix B shows photos of cross sections near these locations.

A longer ice jam is observed in Figure 8-3, where the ice jam head location is still at cross section 82748, but the ice jam toe location is further downstream, at around cross section 60908, located 4.7 km downstream of the 15 Mile Point Cabin.

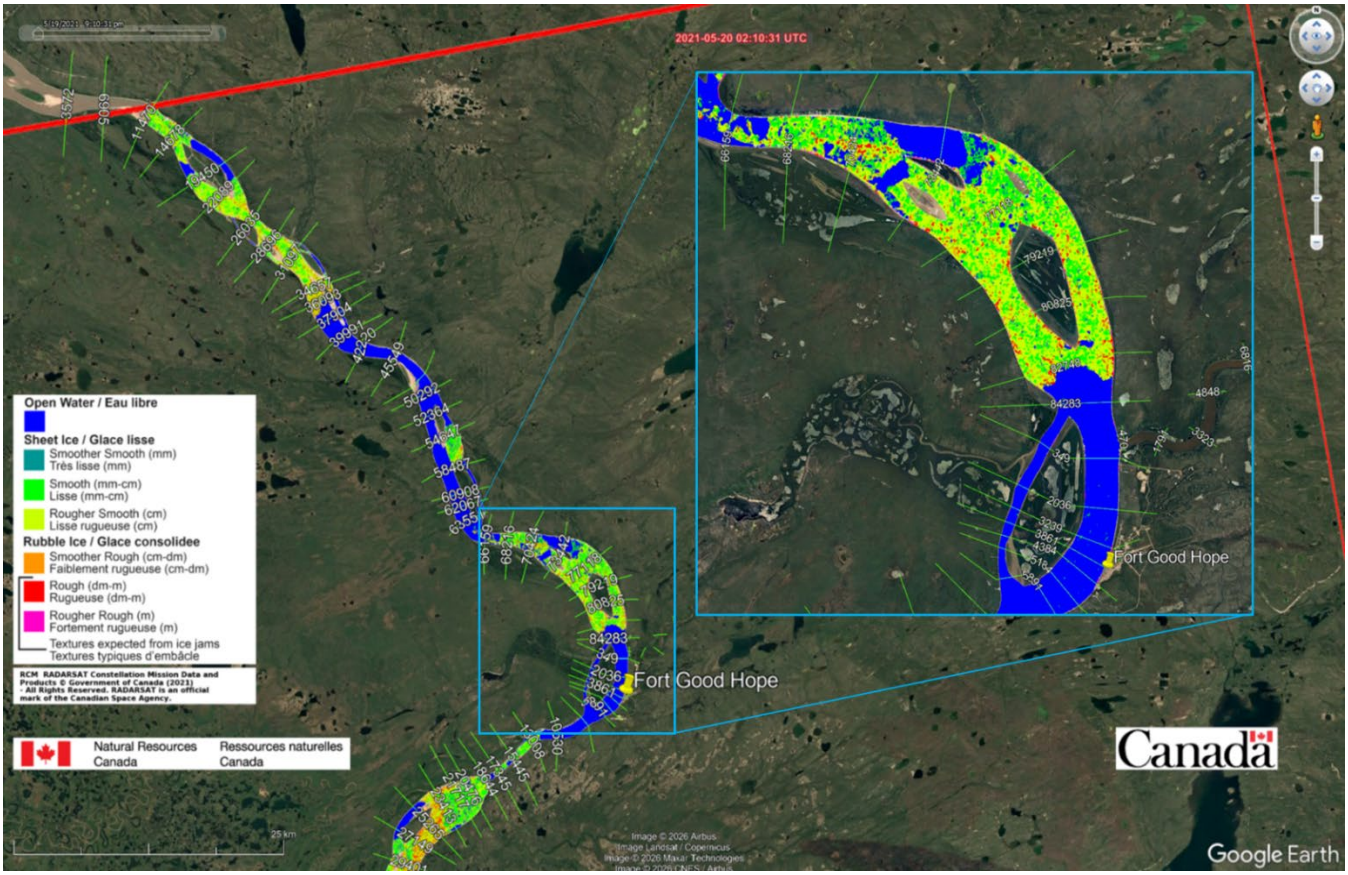

Figure 8-2: RCM RADARSAT Constellation Mission Data of the Ice Conditions on 2021-05-20 02:10:31 UTC near Fort Good Hope (NRCan 2021)

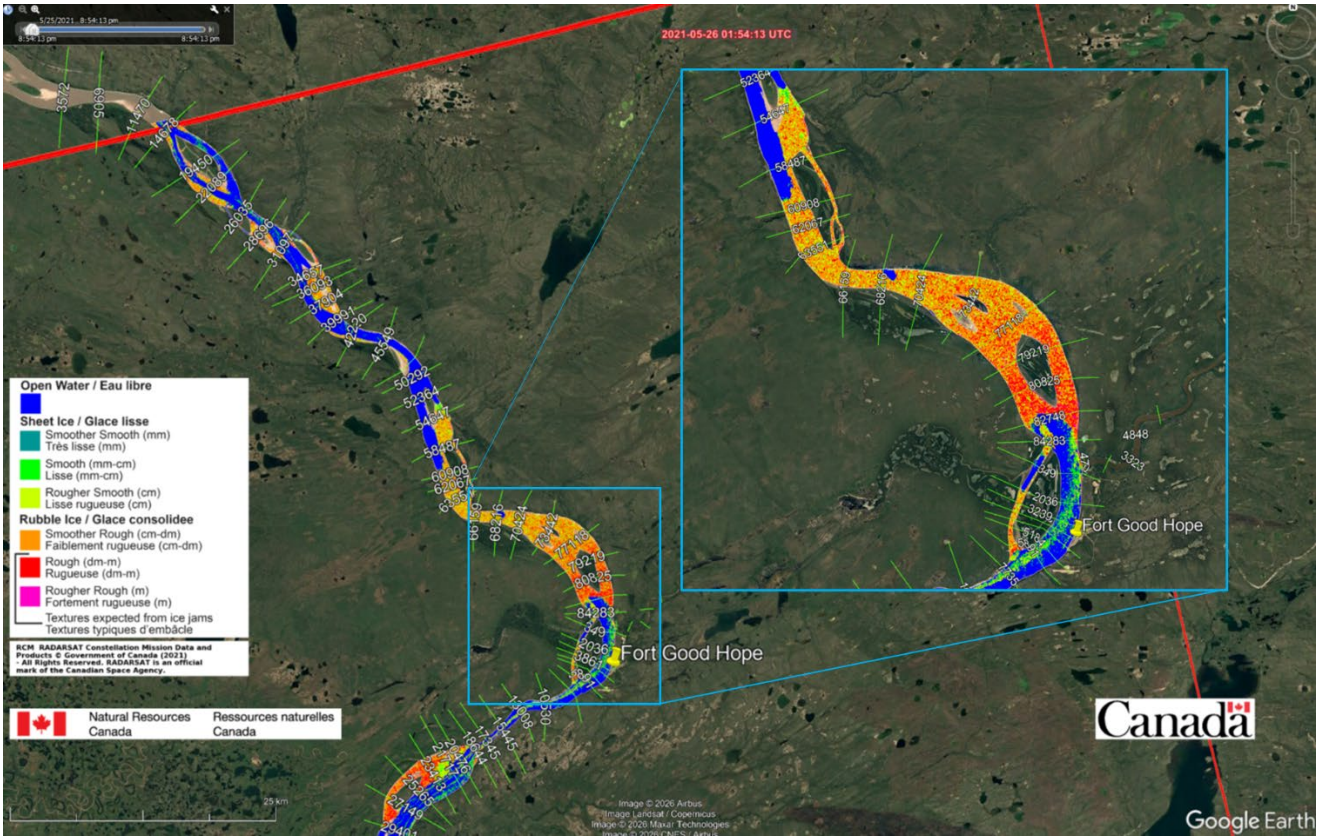

Figure 8-3: RCM RADARSAT Constellation Mission Data of the Ice Conditions on 2021-05-26 01:54:13 UTC near Fort Good Hope (NRCan 2021)

8.2 Ice Manning's n Coefficients from Calibration

The calibrated ice Manning's n coefficients for the May 20, 2021 and May 25, 2021 events were 0.06 and 0.08, respectively.

8.3 Calibration of the May 20, 2021 Flood Event

Figure 8-4 shows the calibration results where an ice Manning's n coefficient of 0.06 was used. The blue curve shows the water surface profile computed with HEC-RAS. The point in red depicts the observed water surface elevation on May 20th, 2021 (see Table 8-1), at Fort Good Hope, for which the computed water elevation by HEC-RAS matched the observed value of 32.3 m.

The blue points correspond to ice scars surveyed during the summer 2025 by WSP along the right and left banks, as well as on islands. The computed water profile lies within the range of these surveyed ice scars.

Furthermore, the orange points represent high water marks (HWMs) surveyed during the summer of 2025 by WSP on both banks and on islands. Downstream of the 15 Mile Point Cabin, the computed water surface profile aligns with the lower end of the HWMs. The higher HWMs downstream of the 15 Mile Point Cabin likely occurred after the ice jam released, a process not represented in this model. While the ice jam model was able to reproduce the upstream water level increase caused by the jam, it did not simulate the jam release or its downstream impacts.

The ice scars and the HWMs help validate the calibrated water surface profile and check whether it falls within what has been observed in the past, which it does.

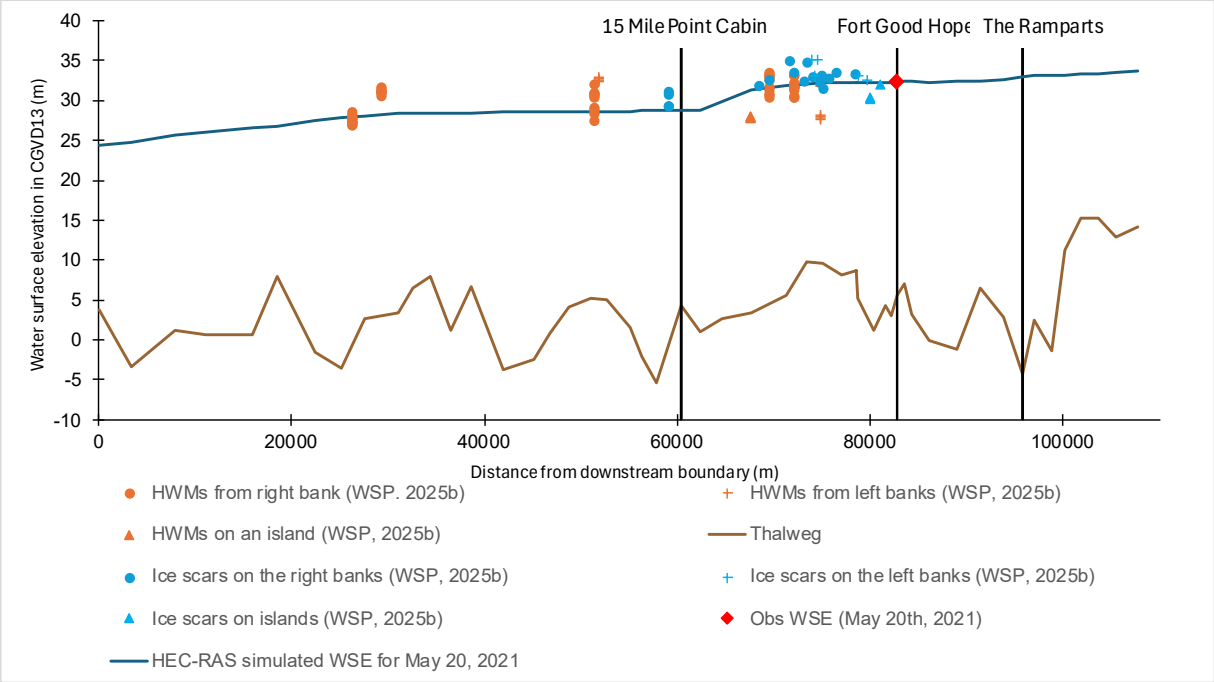

Figure 8-4: Calibration of the May 20, 2021 Ice Jam Flood Event

8.4 Calibration of the May 25, 2021 Flood Event

Figure 8-5 shows the calibration of the May 25, 2021 event for which an ice Manning's n coefficient of 0.08 was used. A higher water profile was obtained upstream of the 15 Mile Point Cabin for which the computed and observed water elevations were in agreement at 33.8 m at Fort Good Hope.

The water surface profile still falls within the surveyed ice scars and HWMs upstream of the 15 Mile Point Cabin. Downstream of it, the water surface profile is below the surveyed HWMs. As explained in the previous subsection, The HEC-RAS model simulated the water profile when there is presence of an ice jam downstream of Fort Good Hope. Thus, Figure 8-5 depicts the profile prior to the ice jam release. The HWMs downstream of 15 Mile Point Cabin could have resulted from the ice jam release, which is not modelled in this study.

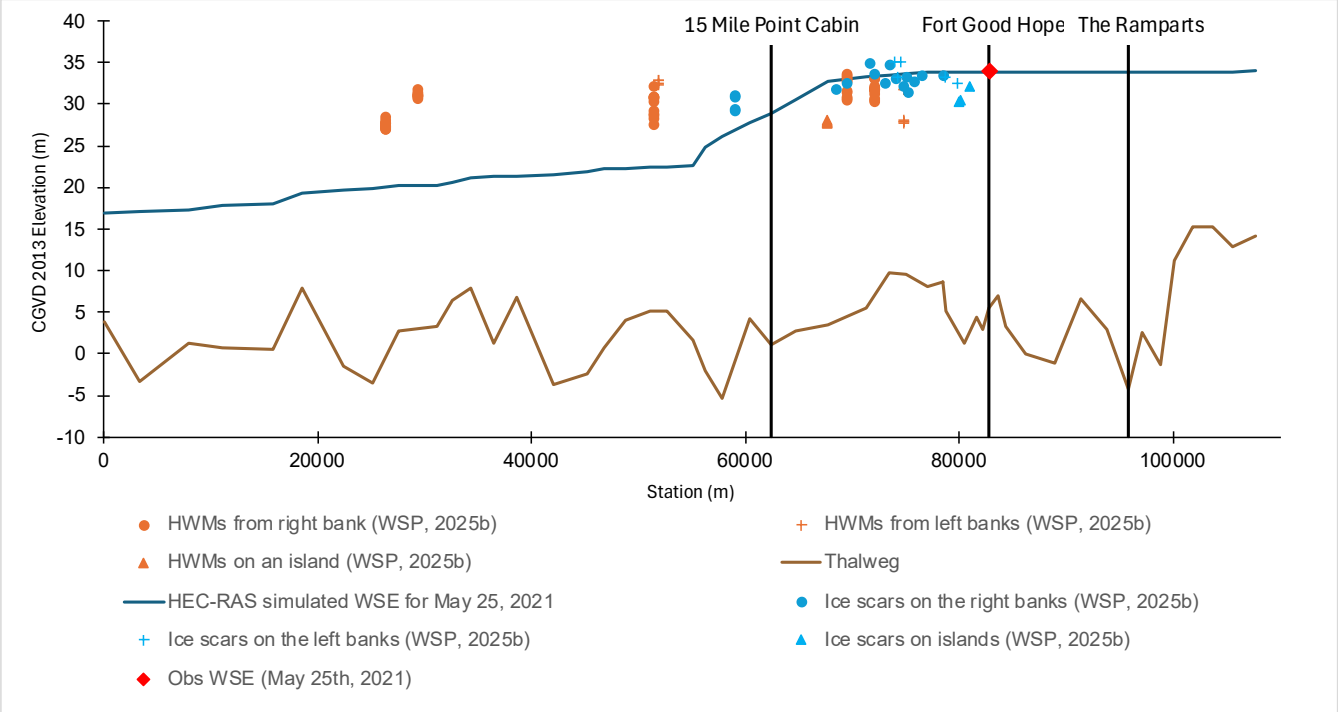

Figure 8-5: Calibration of the May 25, 2021 Ice Jam Flood Event

9 MONTE CARLO ANALYSIS

This section presents the Monte Carlo analysis that was used to estimate ice jam flood hazards. In this analysis, different random input values were implemented in the model to obtain a set of ice jamming scenarios. The HEC-RAS ice jam model ran all these scenarios sequentially and outputted water surface profiles along the Mackenzie River. Annual exceedance probability (AEP) water level profiles were then derived from the Monte Carlo simulations.

The Monte Carlo Analysis was performed several times, with parameters adjusted to produce AEP water profiles that correspond to flood levels, high water marks (HWMs), and ice scars surveyed along the Mackenzie River. The parameters presented in this section represent the finalized, calibrated values.

9.1 Monte Carlo Framework

In the Monte Carlo Analysis, the parameters that affect the ice jam configuration in the HEC-RAS ice jam model were modified for each scenario. Table 9-1 presents the description of each of these parameters. Historical observed values of flow and ice thickness were used to determine the frequency distribution and the range. In both cases, a GEV distribution was used.

Table 9-1: Distribution Types and Ranges of the Parameters used in the Monte Carlo Analysis (USACE 2025)

Variable	Description	Unit	Distribution	min	max	Comment
Q	Flow	m^3/s	GEV	3,922	23,707	Truncated from observed data
h	Ice thickness	m	GEV	0.8	1.3	From observed data
n_{ice}	Ice Manning's n coefficient	-	Uniform	0.06	0.08	HEC-RAS Hydraulic Reference Manual
A	Friction angle of ice	°	Uniform	43	46	(White 1999)
E	Porosity	-	Uniform	0.39	0.41	±0.01 from the HEC-RAS default value
K1	Lateral stress coefficient	-	Uniform	0.3	0.36	±0.03 from the HEC-RAS default value
Ice toe location	HEC-RAS Cross Section Number	-	Uniform	62067	77118	From RADARSAT and satellite images

9.1.1 Flow Distribution

The daily mean flows were obtained from Station 10KA001 at Norman Wells and transposed at Fort Good Hope. The flows corresponding to peak ice jam staging recorded at the Norman Wells gauge were used for this analysis because they were considered to be the best estimate to the peak ice jam break-up flows at Fort Good Hope, given the current available data.

Figure 9-1 presents the observed historical flows at Fort Good Hope and the GEV frequency distribution in blue. This GEV distribution was used to obtain 2,000 random values of flows that were used as input in the Monte Carlo Analysis. The minimum flow considered was 3,922 m^3/s and the maximum flow was 23,707 m^3/s.

The maximum threshold (23,707 m^3/s) was set at 10% above the flow event observed on May 20, 2021 (21,553 m^3/s), which was the maximum flow during the May 2021 ice jam event. While flows exceeding this threshold may have occurred at Norman Wells, the Ramparts could create a backwater effect that reduced the flows experienced at Fort Good Hope, especially in ice jam conditions. Furthermore, it is unlikely that the ice jam downstream of Fort Good Hope could withstand elevated flows. Because the HEC-RAS model cannot simulate the ice jam release, considering these higher flows could lead to an overestimation of water levels at Fort Good Hope. Moreover, there may be some uncertainties in the flow measurements at high discharges. The discharges at Norman Wells were derived from continuous water level records from the Norman Wells gauge. The backwater effect caused by the Ramparts could lead to an overestimation of flows because elevated water levels may be interpreted as higher discharges.

Additional investigations (Section 13) would be required to define with greater certainty the flow at Fort Good Hope during ice-affected conditions.

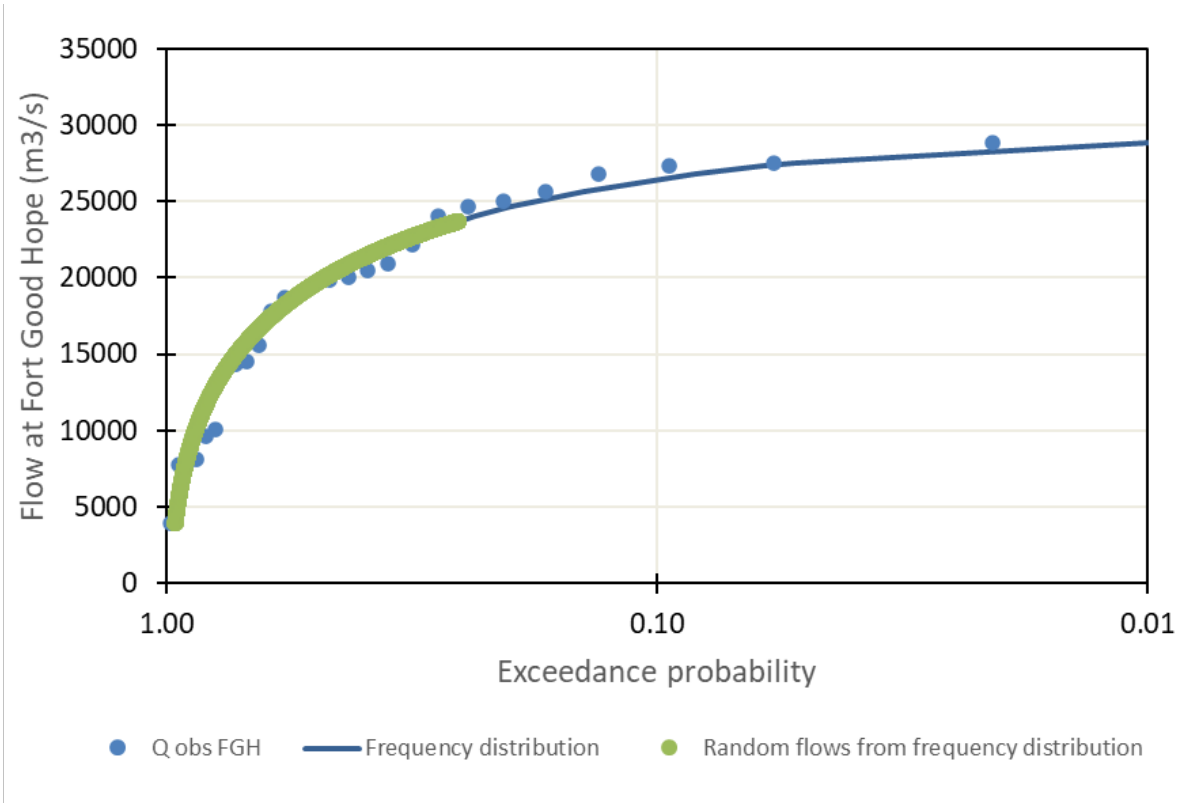

Figure 9-1: Frequency Distribution of Historical Flow Data at Fort Good Hope and the Random Flows Considered for the Monte Carlo Analysis

9.1.2 Ice Thickness Distribution

In a similar way, random values of ice thicknesses were obtained using a GEV distribution. This distribution was obtained using CDDF values and the Stefan equation presented in Section 7.1. Different values of ice-growth coefficient (α) were used to plot the GEV distributions presented in Section 9.2. The exceedance probability curve of ice thickness surveyed by the Original Ice Thickness Program is also plotted.

As the exceedance probability decreases, the observed ice thicknesses at Norman Wells become greater than the estimated ice thicknesses. It is important to note that these measurements were taken 15 to 20 days before the estimated date of ice jam release, during which ice thickness may decrease due to rising temperatures at the end of winter.

As explained in the global sensitivity analysis in Section 9.2, the ice thickness parameter does not have a great influence on the results compared to flow and ice Manning's n coefficient. Thus, for this study, an ice-growth coefficient of 0.20 was considered acceptable and was implemented in the Monte Carlo Analysis.

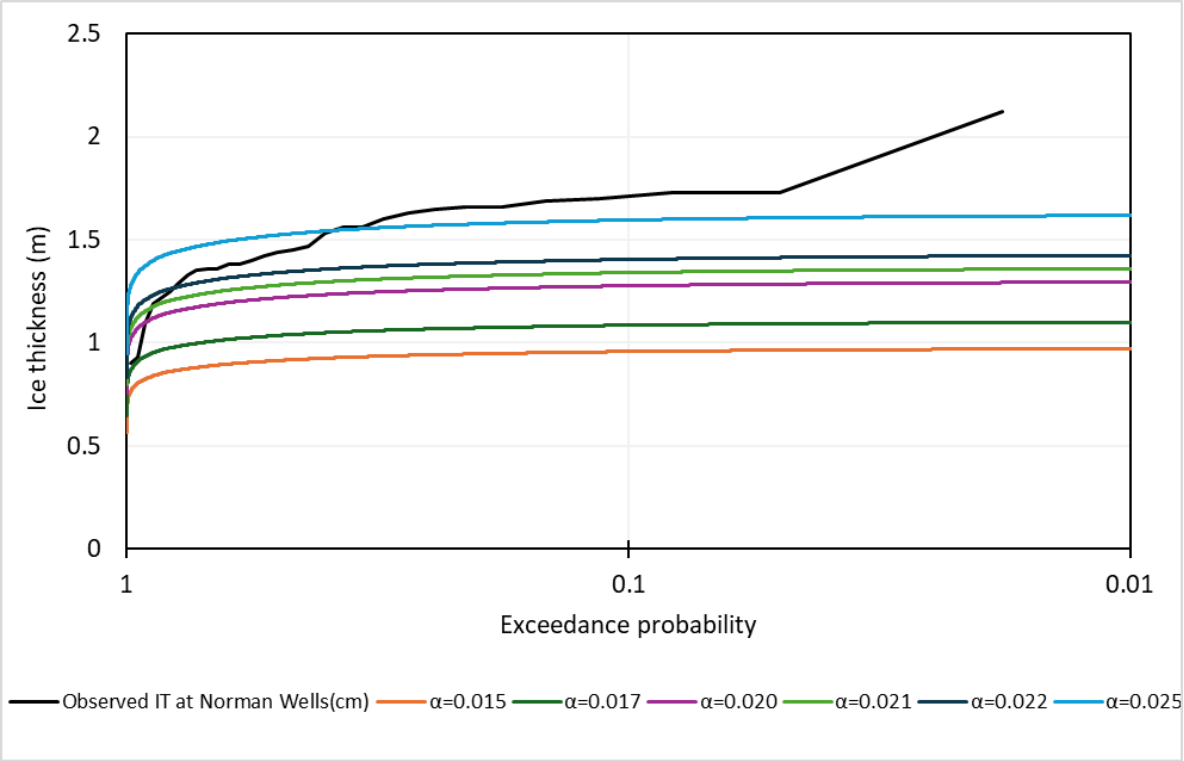

Figure 9-2: Ice Thickness Estimation from Historical CDDF for Different Ice-Growth Coefficient and Observed Ice Thicknesses at Norman Wells

9.1.3 Ice Manning's n Coefficient Distribution

As shown in Table 7-3, the suggested ice Manning's n coefficient of frozen frazil and sheet ice was 0.04 and 0.08 for a thickness of 1.0 m. These values changed to 0.06 and 0.09 for an ice thickness of 1.52 m.

Figure 9-3 shows some ice Manning's n coefficients proposed by different authors in the literature.

- May 19 and 29, 2020
- Beltaos (1978) used an approach combining elements of the Nezhikhovsky approach for two breakup ice jams on the Smoky and Wapiti Rivers (Alberta) for which an ice roughness (Manning's n coefficient) of 0.10 was obtained.
- Andres (1980) used a similar approach for the breakup ice jam that occurred in April 1978 on the Athabasca River in Alberta. Based on measured discharge, slope, and stage, an ice roughness (Manning's n coefficient) varying from 0.057 and 0.065 was obtained. The data obtained from this ice jam was later combined with additional 1977 and 1978 data and the ice roughness (Manning's n coefficient) was later updated to 0.072 (Andres and Doyle 1984).
- Knowles and Hodgins (1980) used the shear stress approach to estimate the ice roughness for two breakup jams on the Thames River in New Brunswick. They found an ice roughness (Manning's n coefficient) ranging from 0.01 to 0.015.
- Vogel and Root (1981) modeled breakup jams on the Missisquoi River in Vermont using an ice roughness (Manning's n coefficient) of 0.057.

- Rivard et al. (1984) modelled the May 1983 breakup ice jam on the Mackenzie River and used an ice roughness (Manning's n coefficient) of 0.045.
- An ice Manning's n coefficient of 0.060 was used by Tuthill and White (1997) to model a breakup jam on the Salmon River in Connecticut and by Korbaylo and Shumilak (1999) in modeling the 1986 Churchill River breakup jam.

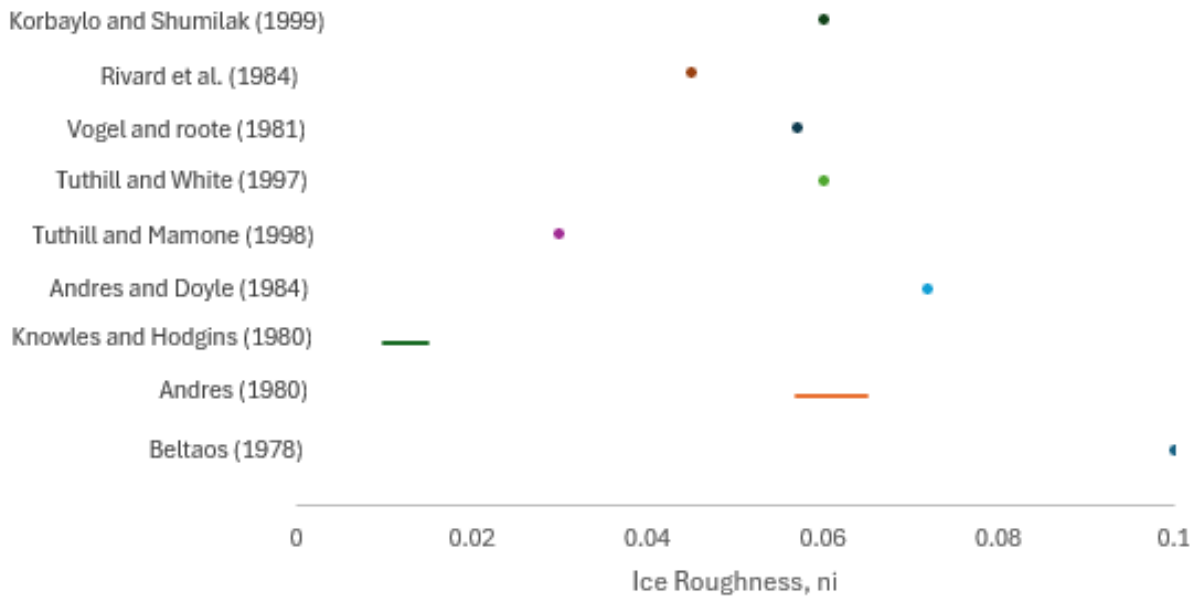

Figure 9-3: Ice Manning's n Coefficient for Breakup Ice Jams According to the Literature

During the calibration of the ice jam model for the May 20, 2021 and May 25, 2021 ice jam flood events, two ice Manning's n coefficients were obtained: 0.06 and 0.08, respectively. These two coefficients seem to agree with the majority of the proposed ice Manning's n coefficients proposed in Figure 9-3.

Iterations of the Monte Carlo Analysis have shown that the range of 0.06 to 0.08 for the ice Manning's n coefficients provide acceptable results of AEP water profiles. A uniform distribution is used for these values.

9.1.4 Friction Angle, Porosity, Lateral Stress Coefficient Distributions

The friction angle, porosity, lateral stress coefficients are represented using uniform distributions due to the lack of data on these parameters. The range defined for each parameter, presented in the Table 9-2, are centered around the default values provided by HEC-RAS.

Table 9-2: Boundaries of Uniform Distributions for the Friction Angle, Porosity, and Lateral Stress Coefficient

Parameter	Minimum	HEC-RAS Default Value	Maximum
Friction angle	43	45	46
Porosity	0.39	0.40	0.41
Stress k1	0.30	0.33	0.36

9.1.5 Ice Jam Toe and Head Location

RADARSAT images and satellite imagery of different years are analyzed to determine the general downstream ice jam toe and head locations, in the vicinity of Fort Good Hope. These images are presented in Table 9-3 and show the following dates:

- May 19 and 29, 2020
- May 20, 24, and 26, 2021
- May 11, 2023
- May 12 and 15, 2024
- May 15, 18, and 20, 2025.

Table 9-3: RADARSAT RCM-3 (NRCan 2021) and Satellite Imagery (Sentinel-Hub 2025) of Ice Conditions near Fort Good Hope at Different Years

May 19, 2020
RCM-3 derived ice cover conditions: ▪ An ice jam seems to form on the right part downstream of the cross section 82748 (1.6 km of Manitou Island) up to 68216 (2 km upstream of the 15 Mile Point Cabin) 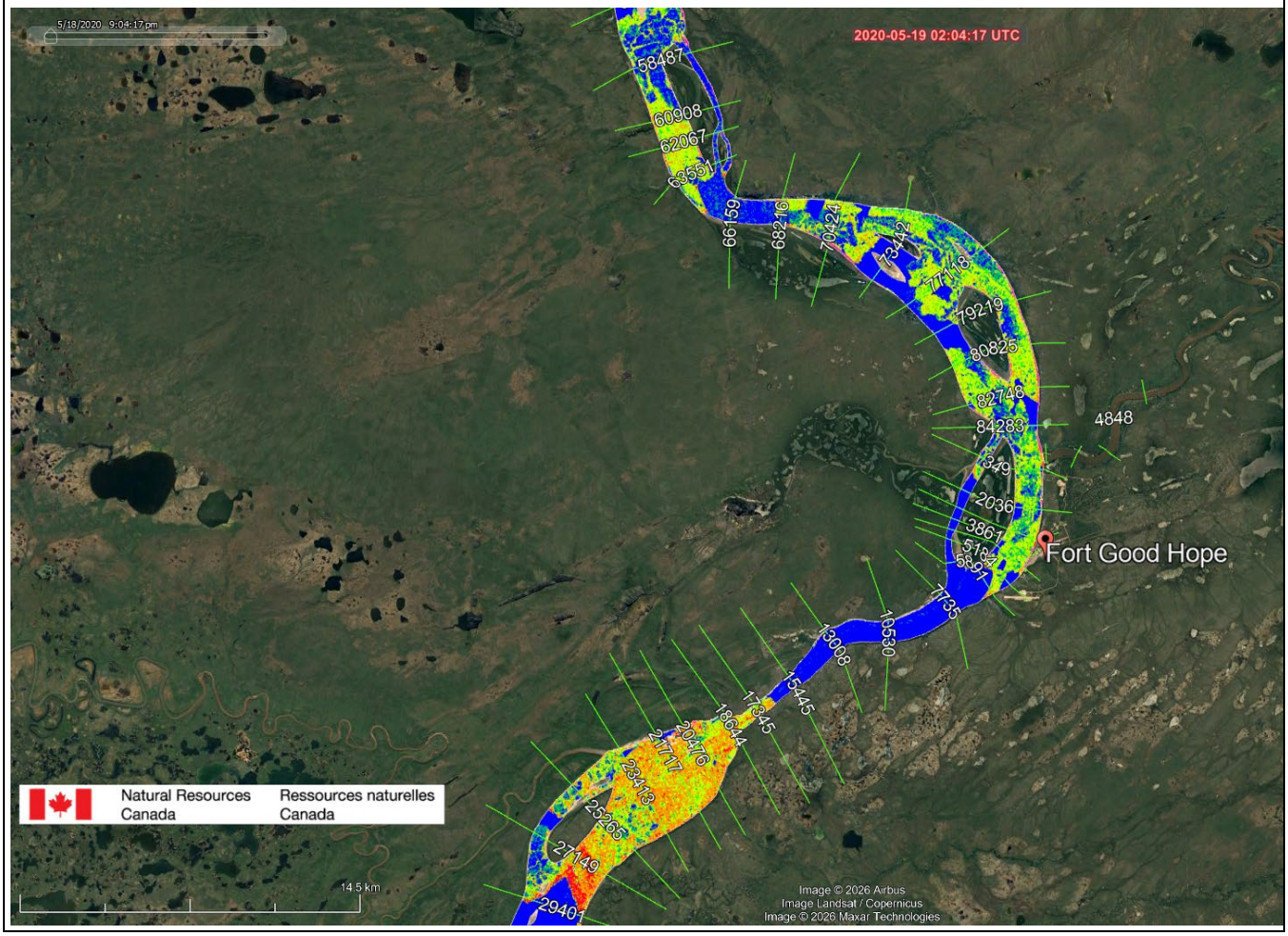

Table 9-3: RADARSAT RCM-3 (NRCan 2021) and Satellite Imagery (Sentinel-Hub 2025) of Ice Conditions near Fort Good Hope at Different Years

May 29, 2020
▪ No ice jam observed 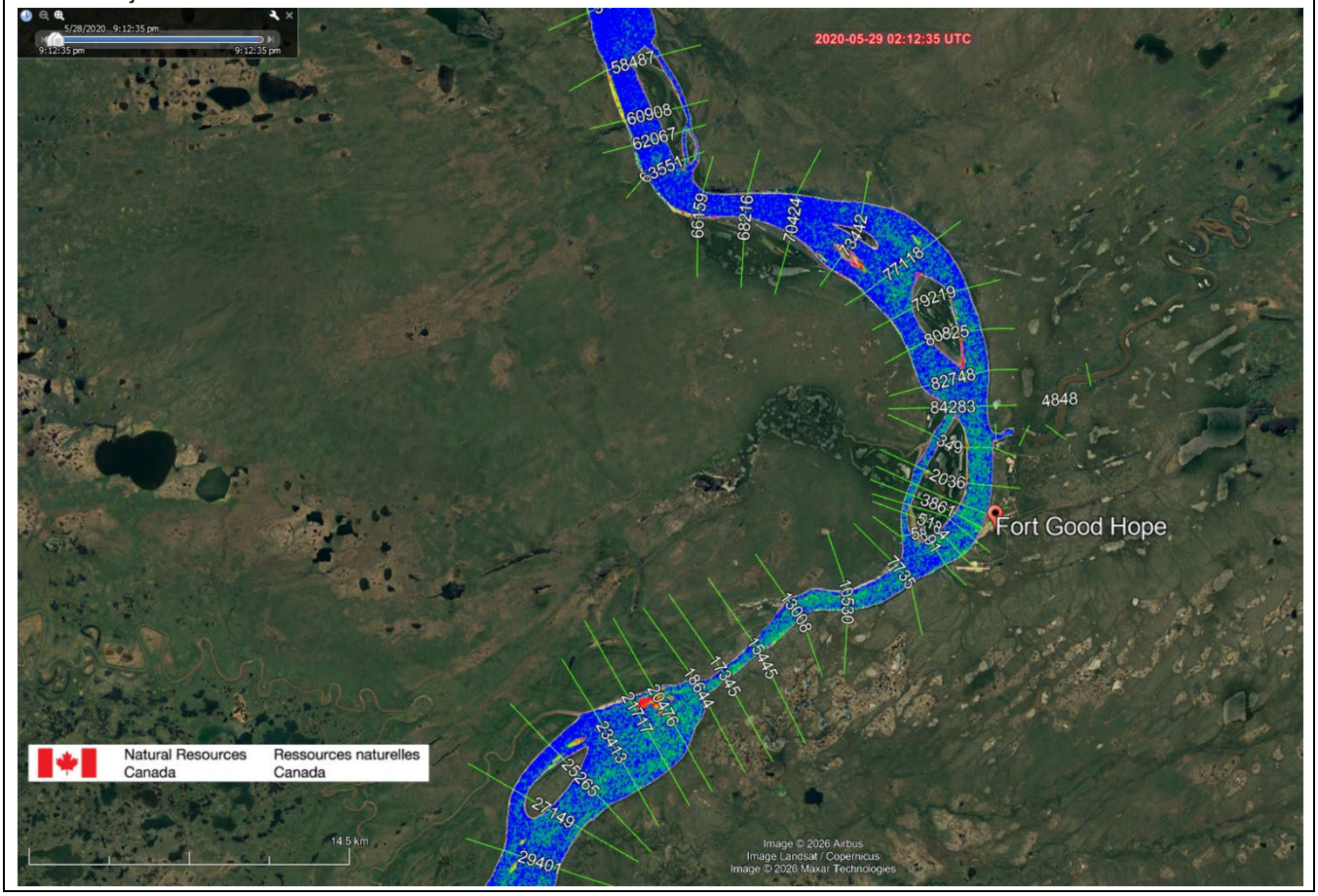

Table 9-3: RADARSAT RCM-3 (NRCan 2021) and Satellite Imagery (Sentinel-Hub 2025) of Ice Conditions near Fort Good Hope at Different Years

May 20, 2021
RCM-3 derived ice conditions: ▪ Ice jam head location: at cross section 82748 (1.6 km of Manitou Island) ▪ Ice jam toe location: around cross section 68216 (2 km upstream of the 15 Mile Point Cabin)

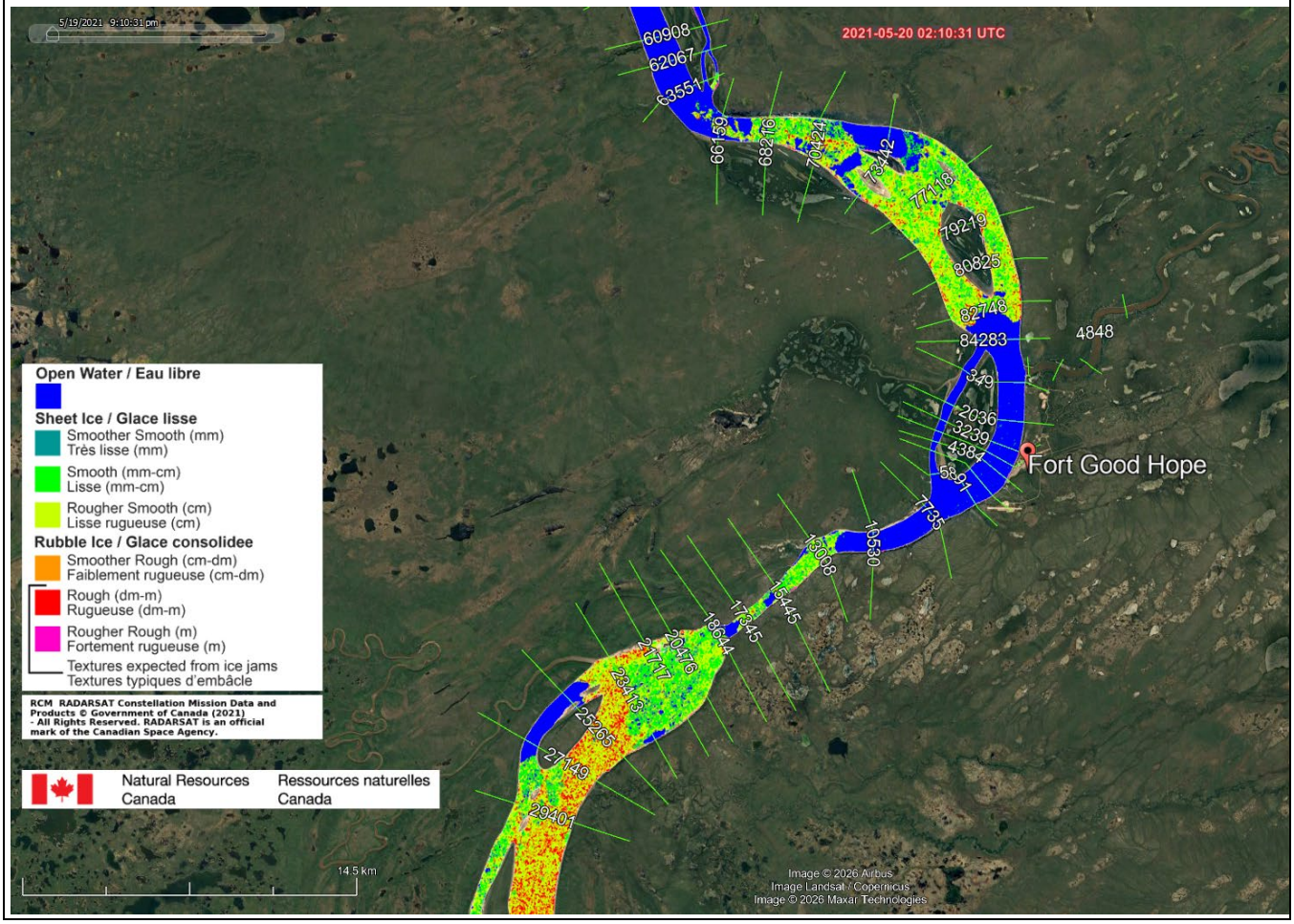

Table 9-3: RADARSAT RCM-3 (NRCan 2021) and Satellite Imagery (Sentinel-Hub 2025) of Ice Conditions near Fort Good Hope at Different Years

May 24, 2021
RCM-3 derived ice conditions: ▪ Ice jam head location: at cross section 82748 (1.6 km of Manitou Island) ▪ Ice jam toe location: 77118 (9.5 km upstream of the 15 Mile Point Cabin)

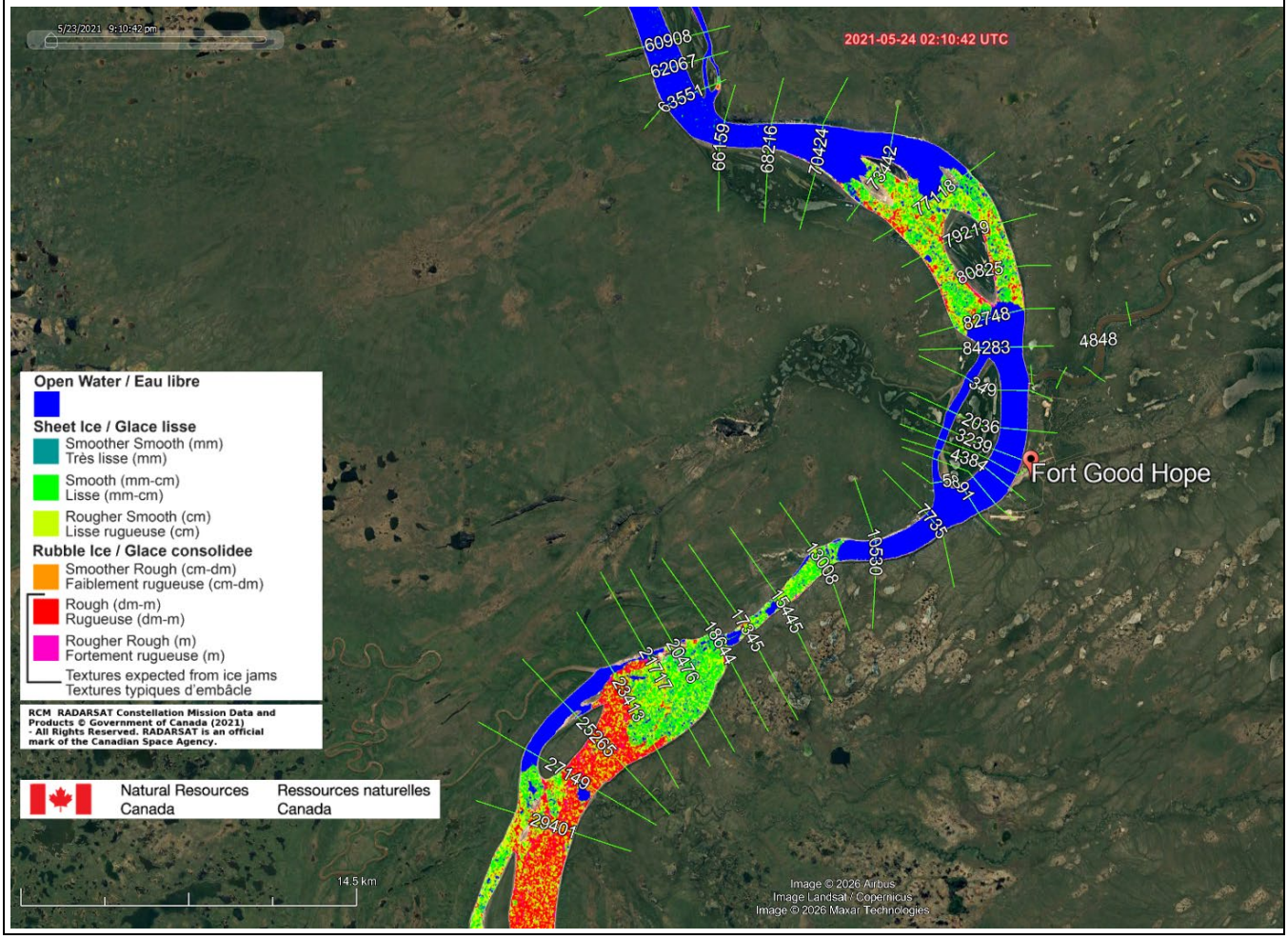

Table 9-3: RADARSAT RCM-3 (NRCan 2021) and Satellite Imagery (Sentinel-Hub 2025) of Ice Conditions near Fort Good Hope at Different Years

May 26, 2021
RCM-3 derived ice conditions: ▪ Ice jam head location: 82748 (1.6 km of Manitou Island) ▪ Ice jam toe location: 60908 (7 km downstream of the 15 Mile Point Cabin)

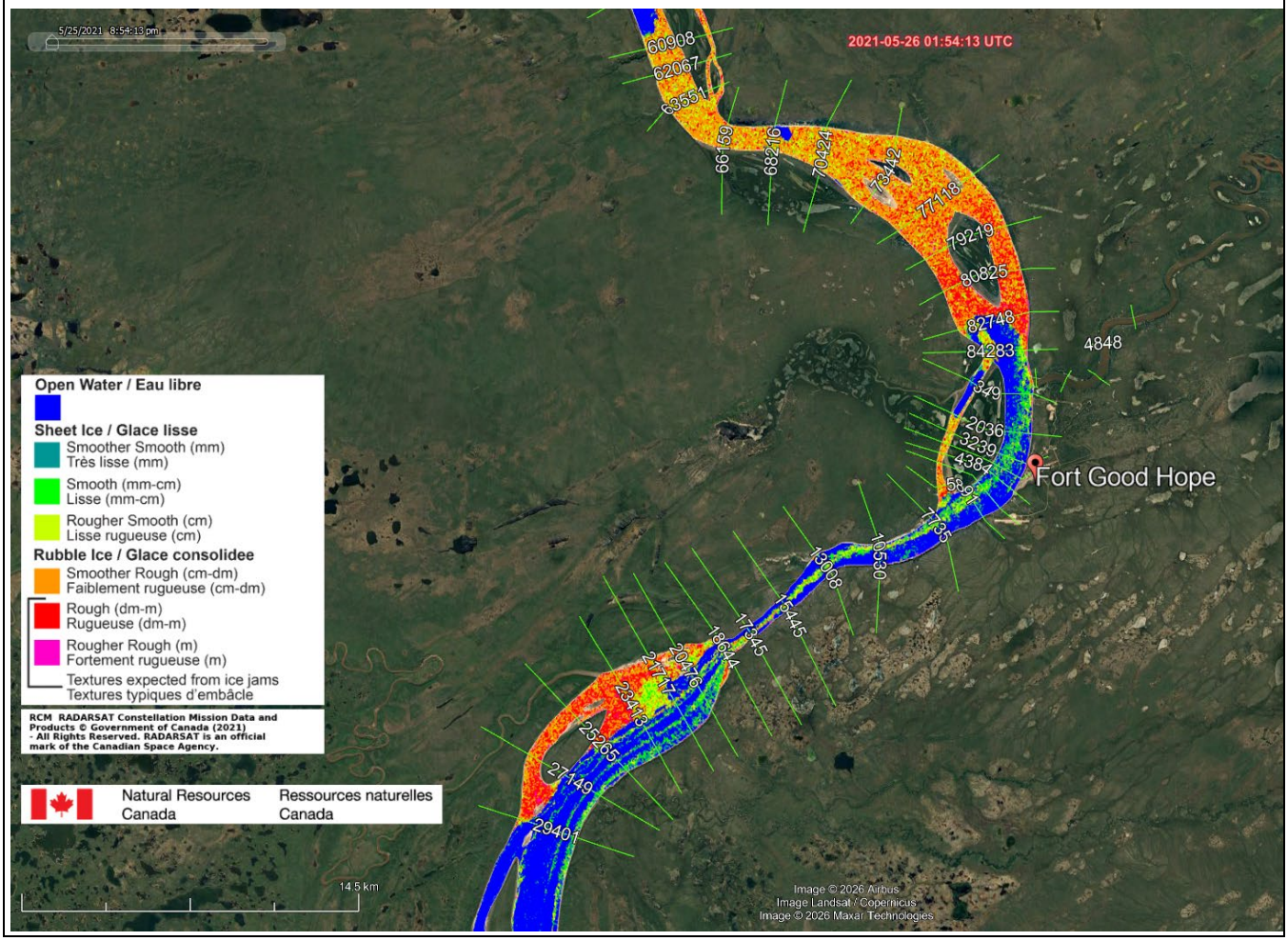

Table 9-3: RADARSAT RCM-3 (NRCan 2021) and Satellite Imagery (Sentinel-Hub 2025) of Ice Conditions near Fort Good Hope at Different Years

May 11, 2023
▪ Not necessarily an ice jam, but rather the ice cover is observed here 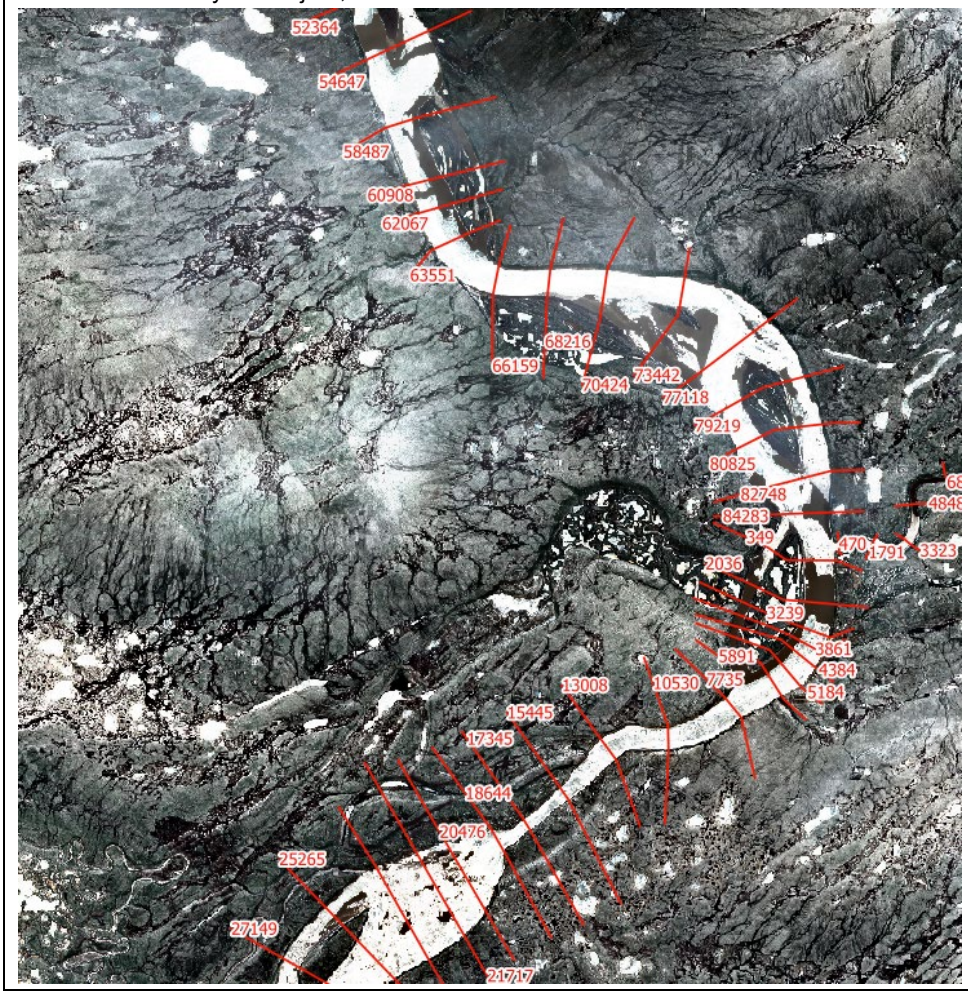

Table 9-3: RADARSAT RCM-3 (NRCan 2021) and Satellite Imagery (Sentinel-Hub 2025) of Ice Conditions near Fort Good Hope at Different Years

May 12, 2024
▪ Seems to be showing the ice cover melting 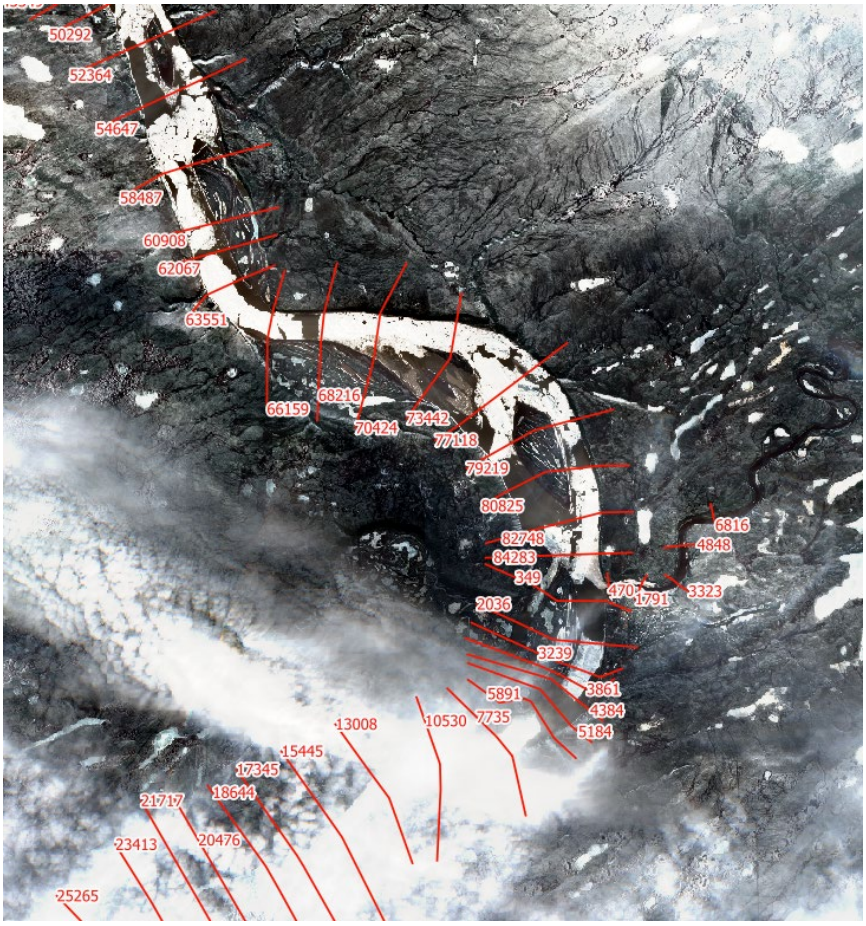

Table 9-3: RADARSAT RCM-3 (NRCan 2021) and Satellite Imagery (Sentinel-Hub 2025) of Ice Conditions near Fort Good Hope at Different Years

May 15, 2024
▪ This could be a small ice jam ▪ Ice jam head location: 79219 (5.5 km downstream of Manitou Island) ▪ Ice jam toe location: 68216 (2 km upstream of the 15 Mile Point Cabin)

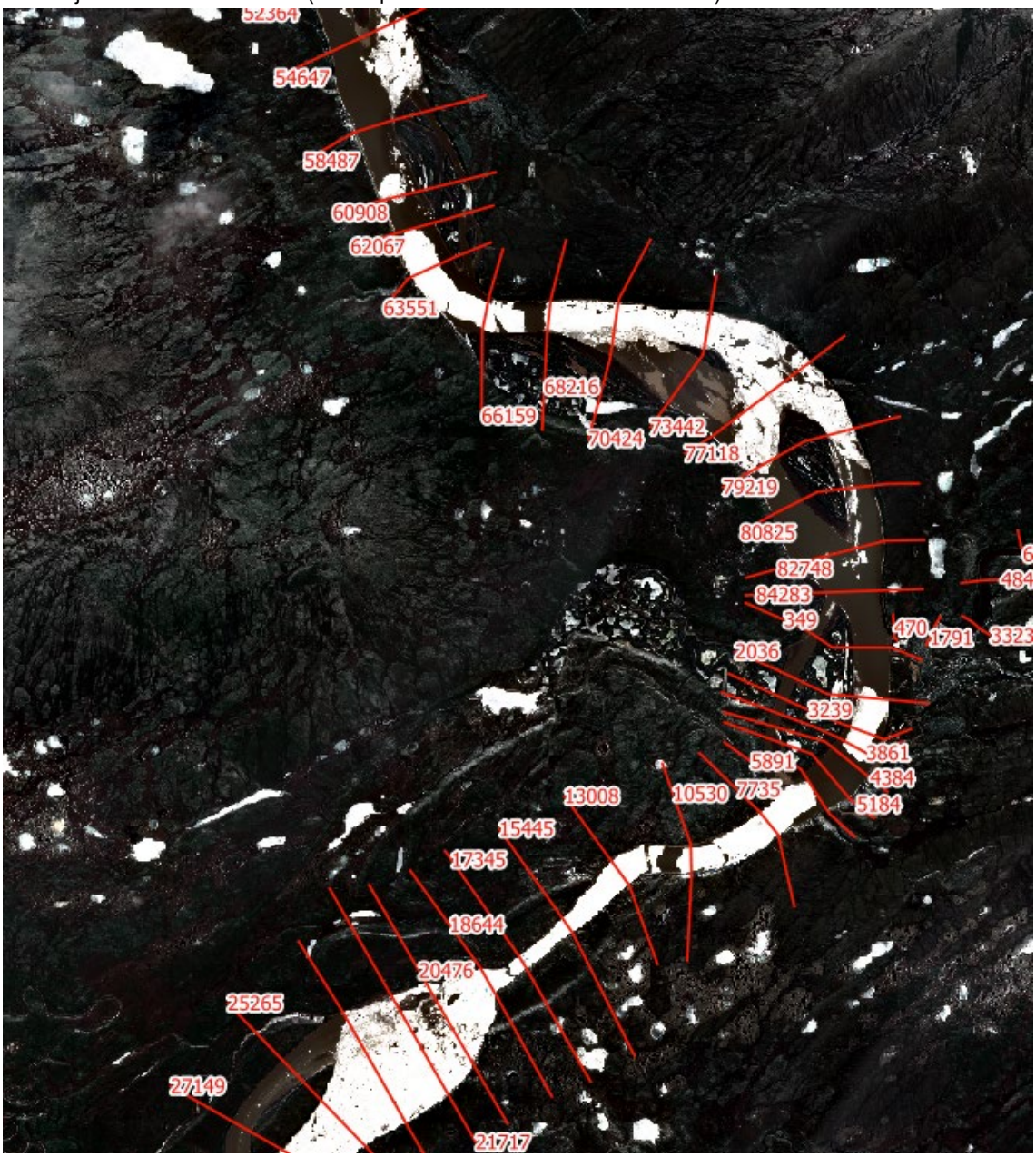

Table 9-3: RADARSAT RCM-3 (NRCan 2021) and Satellite Imagery (Sentinel-Hub 2025) of Ice Conditions near Fort Good Hope at Different Years

May 15, 2025
▪ This image seems to show the ice cover 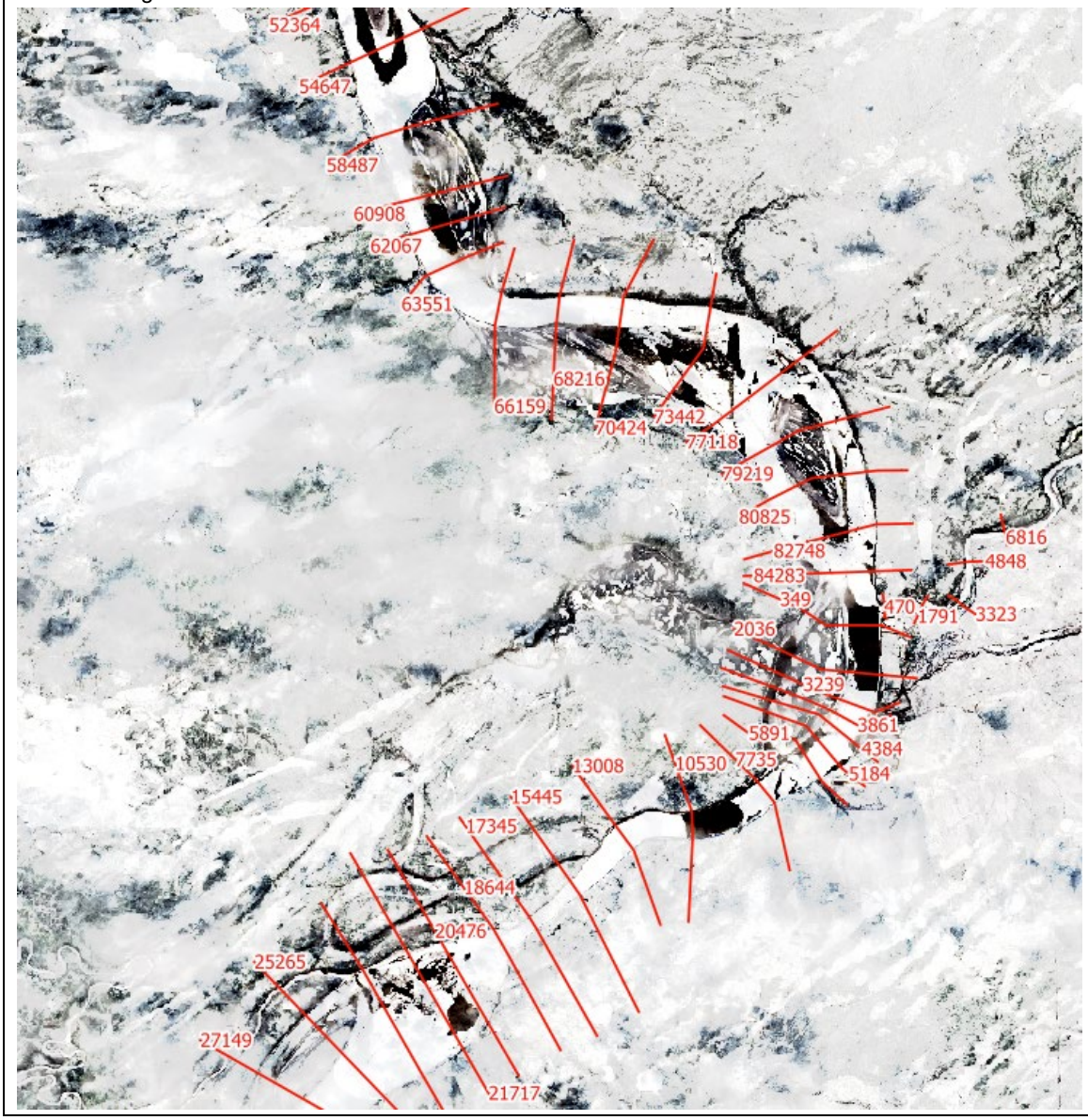

Table 9-3: RADARSAT RCM-3 (NRCan 2021) and Satellite Imagery (Sentinel-Hub 2025) of Ice Conditions near Fort Good Hope at Different Years

May 18, 2025
▪ In this image, it seems the ice cover is melting away 

Table 9-3: RADARSAT RCM-3 (NRCan 2021) and Satellite Imagery (Sentinel-Hub 2025) of Ice Conditions near Fort Good Hope at Different Years

May 20, 2025
This could be characterized as an ice jam ▪ Ice jam head location: 79219 (5.5 km downstream of Manitou Island) ▪ Ice jam toe location 54647 (10 km downstream of Manitou Island) 

An ice jam head location is usually observed at a constant location at cross section 82748 (1.6 km of Manitou Island). Ice jams seem to not occur upstream of this cross section, thus selecting cross section 82748 as a constant ice jam head location represents an acceptable choice.

The ice toe location exhibits significant day-to-day variability, typically forming either upstream or downstream of the meander. The furthest upstream ice toe has been observed at cross section 77118 (9.5 km upstream of the 15 Mile Point Cabin), while the furthest downstream occurred at cross section 54647 (10 km downstream of Manitou Island).

After multiple iterations of the Monte Carlo Analysis, an ice toe location varying from sections 62067 (3.6 km downstream of the 15 Mile Point Cabin) and 77118 (9.5 km upstream of the 15 Mile Point Cabin) were chosen.

Figure 9-4 illustrates the range of possible toe locations and the corresponding head position of the ice jam used in the Monte Carlo Analysis.

Figure 9-4: Position of Ice Jam Toe and Head Locations

9.2 Global Sensitivity Analysis

The global sensitivity analysis (GSA) was applied to determine which input parameters (listed in Section 9.1) will have a non-negligible impact on the results.

The steps below illustrate the methodology that will be used to determine the sensitivity of a given parameter (Φ_k):

1. Define a set of 10,000 randomly defined values for a given parameter (Φ_k). For example, random values of ice thickness could be obtained from a uniform distribution, or random values of flow could be obtained from a GEV distribution.
2. Run the calibrated HEC-RAS model with each of these values and obtain the water surface elevation (WSE). The dataset of all of these WSE is called the *A-priori set*.
3. Calculate the error from these calculated WSE with the observed WSE (for example, the observed WSE from the event on May 20, 2021).
4. Separate the *A-priori set* in two categories:
    a. Behavioral: the 10% of data having the least error
    b. Non-behavioral: the rest of the data
5. Get the cumulative distribution functions for the *A-priori, behavioral,* and *non-behavioral* sets, as shown in Figure 9-5.
6. Compare the three distribution functions and if there is a difference between the behavioral and non-behavioral CDF's greater than 5% of the average value, then the parameter can be considered a sensitive parameter.

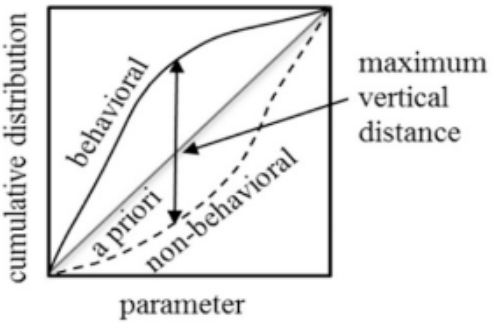

Figure 9-5: Example of the Cumulative Distribution Functions (CDF) of the Behavioral, Non-behavioral, and A-priori Sets for a Sensitive Parameter (Das and Lindenschmidt 2021)

Figure 9-6 shows the CDF obtained from the behavioural and non-behavioural data sets for the flow, ice thickness, porosity, friction angle, ice Manning's n coefficient, ice jam toe location, and stress ratio k1 parameters. The parameters that show highest discrepancy between the two curves are the flow, the ice Manning's n coefficient, and the ice jam toe locations. This indicates that the other parameters do not have as much influence on the water elevations.

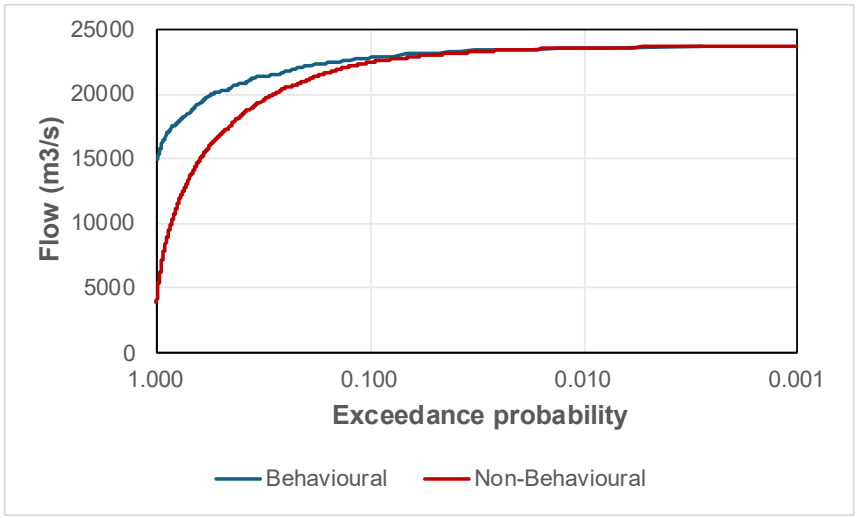

(c)

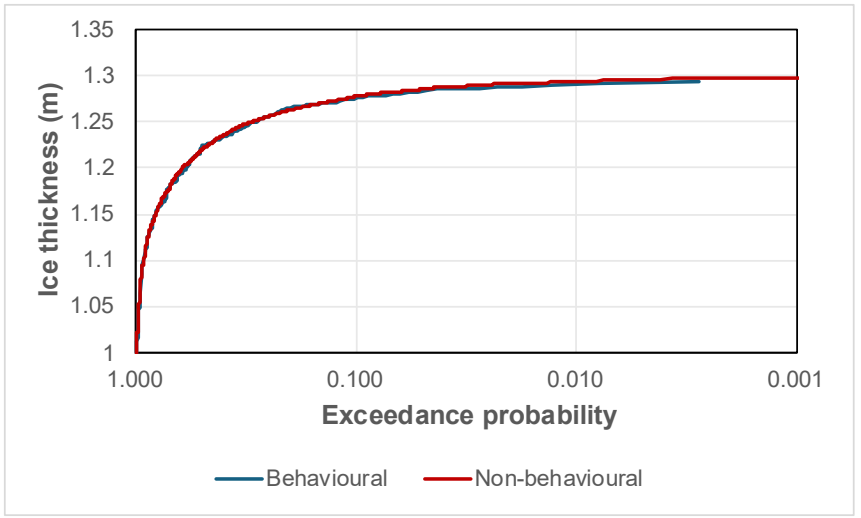

(b)

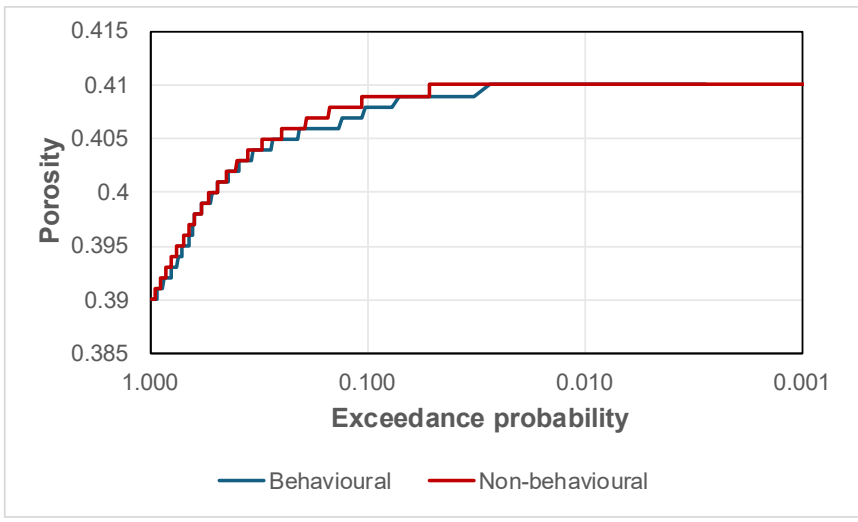

(c)

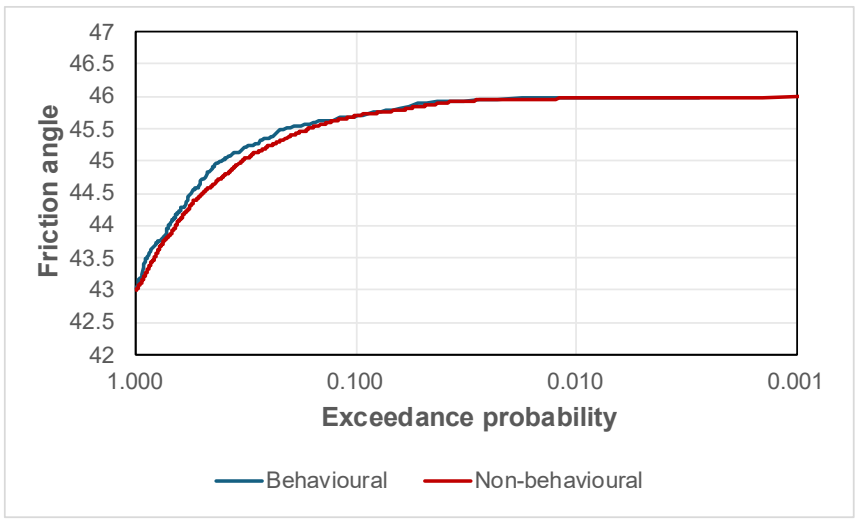

(d)

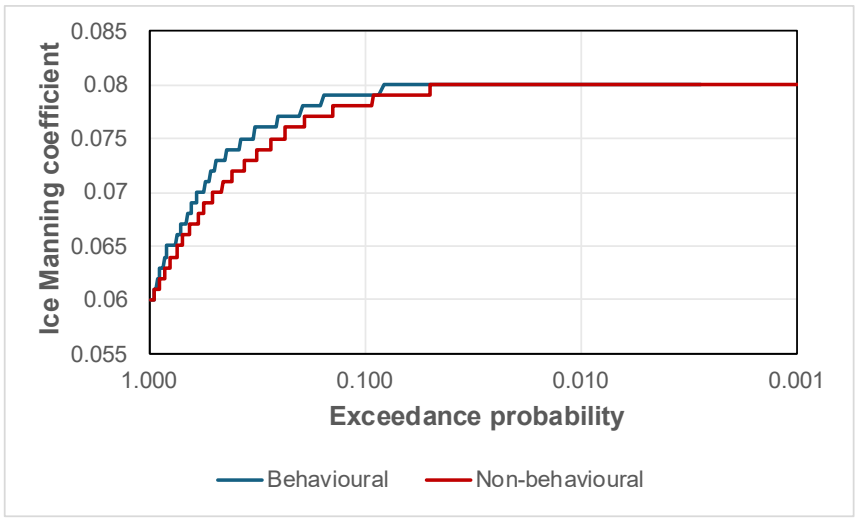

(e)

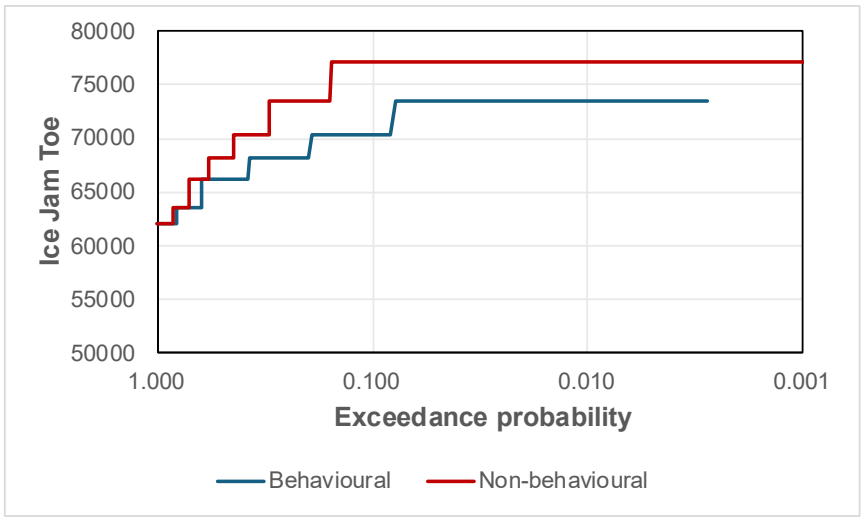

(f)

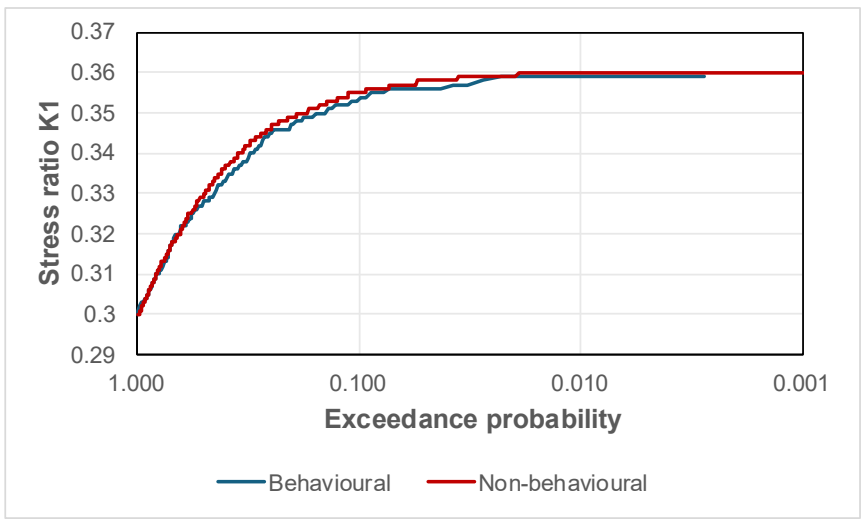

(g)

Figure 9-6: Cumulative Distribution Function (CDF) of: (a) Flow; (b) Ice Thickness; (c) Porosity; (d) Friction Angle; (e) Ice Manning's n Coefficient; (f) Ice Jam Toe Location; (g) and Stress Ratio k1, for Behavioural and Non-behavioural Data Sets

9.3 Joint Probability Analysis

The Joint Probability Analysis (JPA) examines the flood hazards resulting from the simultaneous occurrence of extreme values of multiple contributing drivers of ice jam flood events.

The methodology proposed by Hawkes (2008) involving Monte Carlo simulations uses a group of freely available computer programs designed for joint probability extremes analysis known as JOIN-SEA. The input data consists of many independent records of each flood-driving variable. Statistical distributions are fitted to the top few percent of each of the primary variables and their dependencies are modeled. Large samples of extreme values are then generated and analyzed to assess their joint exceedance probabilities.

The JPA proposed in this study is different to Hawkes' approach, mainly due to the lack of observational records for the relevant flood drivers. The analysis is similar to the Global Sensitivity analysis in which each variable of those listed in Section 9.1 is assigned a value that leads to "extreme" results. For most parameters, such as flow, initial ice thickness, and ice Manning's n coefficient, using the upper end values of the proposed intervals results in the highest water levels. Nonetheless, this is not the case for the friction angle parameter, for which a value of 45° generates the highest water levels. The hydraulic model simulates the case in which all variables produce maximum water levels, thus representing the case in which these extreme conditions occur simultaneously. The resulting water surface elevations then reflects the compound flood hazard under these joint extreme scenarios and is denoted as the maximum flooding profile in the Monte Carlo Simulation results.

For instance, for the current condition, a maximum flow of 23,707 m^3/s is selected for the JPA, along with a maximum initial ice thickness of 1.3 m and a maximum ice Manning's n coefficient of 0.08. Similarly, the friction angle, porosity, and stress ratio are set to the values generating maximum water levels, which are 45°, 0.41, and 0.36, respectively. On the other hand, the ice jam toe location is placed at the most possible downstream cross section (62067) to produce the longest ice jam. The resulting flood profile is shown as the maximum one – max (JPA) – in Figure 9-7 and represents the highest theoretical water levels attainable of 35.8 m. An exceedance probability of zero is assigned to this water surface profile.

9.4 Monte Carlo Simulation Results

Figure 9-7 shows the resulting AEP water surface profiles for the 2, 5 ,10, 20, 50, 100, 200, and 500-year floods. The minimum and maximum surface profiles are also shown which were taken when extreme minimum and maximum events occur simultaneously (joint probability analysis). The 25th and the 75th percentiles are also shown in the figure. The computed water surface profiles upstream of Fort Good Hope are compared to the observed water levels that occurred in May 2021 and to surveyed ice scars and HWMs.

The Monte Carlo Framework is designed to model ice jam flood conditions at Fort Good Hope. It is not intended to model ice jam flood levels downstream of 15-Mile Point. This explains why the computed water surface profiles downstream of 15-Mile Point are below the surveyed HWMs. These HWMs are most likely caused by the release of the ice jam or due to other ice jams formed further downstream, which are phenomena not accounted for in the current model.

The ice scars surveyed by WSP in 2025 upstream of the 15 Mile Point Cabin fall between the 25th percentile and the maximum water surface profile derived from the joint probability analysis. A larger concentration of ice scars aligns more closely with the 10-year flood profile. Furthermore, the surveyed HWMs upstream of the 15 Mile Point Cabin lie within the range defined by the 2-year and 50-year flood profiles.

Figure 9-8 shows the water elevations for different return periods at Fort Good Hope. The flooding level of 33.8 m observed on May 25, 2021 corresponds to about a 20-year flood. The water level estimated for May 11-14, 2005

is slightly lower, at 33.5 m, corresponding to a flood between the 10- and 20-year floods. Thus, considering these two flooding events, the result of the Monte Carlo was deemed acceptable. A water level of 34.8 m, 35.0 m, and 35.4 m are estimated for a 100-year, 200-year, and 500-year floods.

The 100, 200 and 500-year flood levels (34.8, 35.0 and 35.4 m) exceed the lower-chord elevation of the Jackfish Creek bridge (34.7 m) but do not exceed its deck elevation (35.8 m). In these conditions, the bridge is not overtopped but experiences pressured flow.

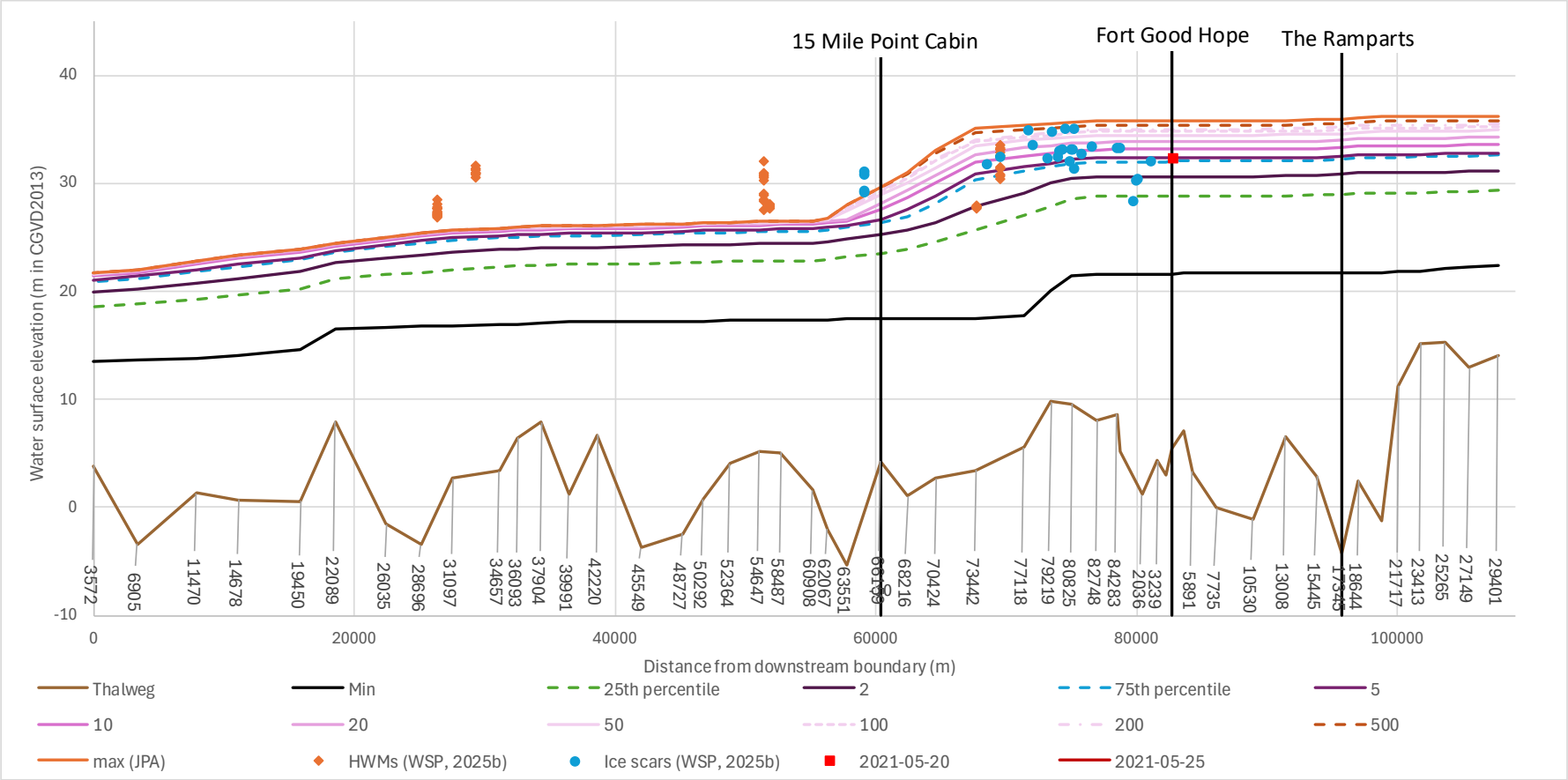

Figure 9-7: Water Surface Profile for Different AEP Floods (2, 5 ,10, 20, 50, 100, 200, and 500-year Floods) from the Monte Carlo Simulation – Ice Jam Profiles leading to Maximum Flood Conditions at Fort Good Hope – Results of the Monte Carlo + HEC-RAS Framework

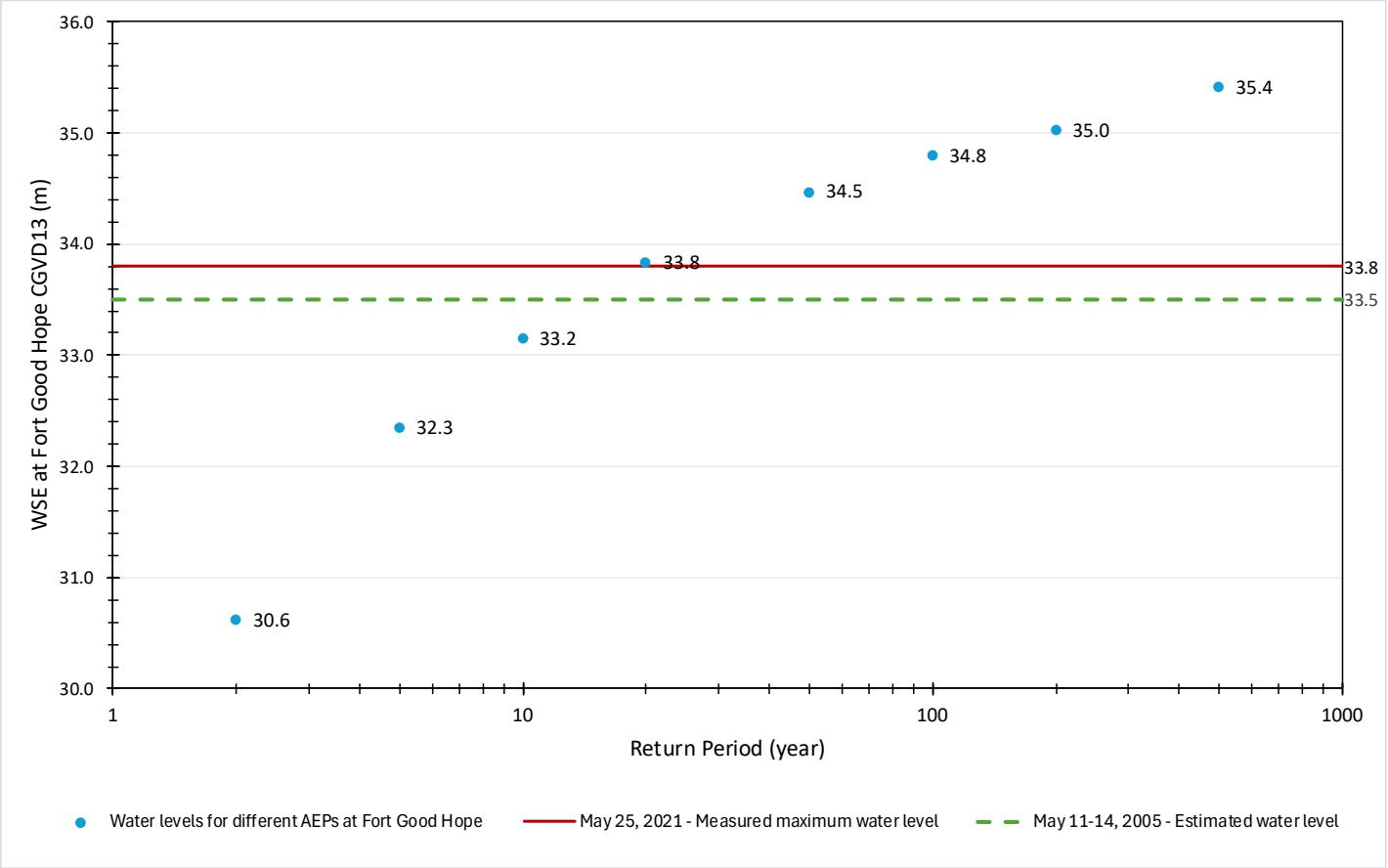

Figure 9-8: AEP Ice-Affected Water Levels at Fort Good Hope – Results of the Monte Carlo + HEC-RAS Framework

10 CLIMATE CHANGE

As climate change impacts the surrounding environment and the Mackenzie River watershed, these changes may influence ice jam flooding hazards at Fort Good Hope. The main factors influencing ice jam flood hazards in future include land cover changes in the Mackenzie River basin, changes in flows of the Mackenzie River and changes in river ice cover characteristics and behavior (e.g. timing, duration, and thickness). In the following sections, projections of climate change are used to understand how these factors may change in the future and to assess their influence on ice jam flooding.

10.1 Background and Data Sources

Climate model projections are an important tool for understanding how future climate is anticipated to change from today's climate to assess potential impacts. The Intergovernmental Panel on Climate Change (IPCC) is generally considered to be the definitive source of climate science and information on future climate change. The IPCC is a United Nations body responsible for assessing the science related to climate change and providing guidance to policymakers. Periodically, the IPCC issues assessment reports summarizing the current state of climate science. The Sixth Assessment Report (AR6; IPCC 2021) represents the most recent complete synthesis of information regarding climate change, including a range of possible greenhouse gas (GHG) emissions scenarios over the 21st century. Future climate projections presented in AR6 originate from the Coupled Model Intercomparison Project 6 (CMIP6), which includes results from approximately 100 distinct Global Climate Models (GCMs) developed by 49 different modelling groups around the world using a standardized set of modeling inputs. Compared to earlier iterations including the Fifth Assessment Report (AR5), informed by projections from the Coupled Model Intercomparison Project 5 (CMIP5), large scale patterns and projected trends in climate are consistent, and within the anticipated uncertainty of the projections (IPCC 2021, Chen et al. 2020).

GCMs are used to simulate the Earth's climate system through a mathematical representation of global land, sea, and atmosphere interactions. The Earth's climate system (atmosphere, ocean, land) is divided up into a set of grid cells (e.g., "boxes"), and the mathematical equations are solved within each grid cell for key climate variables. Examples include equations representing the conservation of momentum, mass, and energy to describe motion of the atmosphere and oceans. These equations describe how climate variables such as air temperature and total precipitation may change over time when atmospheric greenhouse gas (GHG) concentrations change due to natural and human induced emissions, represented through a set of GHG scenarios.

The IPCC recommends that climate change assessments use as many models and climate scenarios as possible, or a multi-model ensemble to delineate the probable range of results as no one climate model or scenario can be viewed as completely accurate. In this study, two ensembles of climate change projections are used for representing river flows and river ice thickness under climate change as outlined in Table 10-1.

River ice thickness projections are estimated in this study (see Section 10.3) and rely on an ensemble of statistically downscaled climate scenarios available from ClimateData.ca, which includes outputs from a total of 26 climate models each run for low (SSP1-2.6), moderate (SSP2-4.5 and SSP3-7.0) and high (SSP5-8.5) emissions scenarios as part of AR6, providing a total of 104 ensemble members (climate models x emissions scenarios). Climate variables available from this ensemble include daily total precipitation, minimum and maximum air temperature.

River flow projections were obtained from the MESH (Modélisation Environnementale Surface et Hydrologie – Surface and Hydrology Environmental Modelling) hydrological model, which was set up and calibrated by Elshamy et al. (2024a,b). The MESH model relied on a dynamically downscaled climate model ensemble from the Canadian Regional Climate Model (CanRCM4) – Large Ensemble for a high emissions scenario (RCP 8.5), driven

by the Canadian Earth System Model (CanESM) developed at a global scale as part of AR5. While this ensemble is based an earlier iteration of global climate projections (AR5), it represents the most recently updated dynamically downscaled climate projections available in Canada and included a larger set of climate variables at the spatial and temporal resolution required to drive the MESH modelling framework. Due to the level of complexity and run time associated with the MESH modelling framework, a subset of 15 future climate simulations was selected from a total of 50 available.

Table 10-1: Details of Climate Projection Ensembles used in this Study

	River Ice Thickness	River Flows
Climate Projection Ensemble	▪ ClimateData.ca Statistically Downscaled Climate Scenarios (CanDCS-M6)	▪ Dynamically Downscaled Canadian Regional Climate Model (CanRCM4) – Large Ensemble
IPCC Assessment Report	▪ Sixth Assessment Report	▪ Fifth Assessment Report
Emissions Scenarios	▪ SSP1-2.6 ▪ SSP2-4.5 ▪ SSP3-7.0 ▪ SSP5-8.5	▪ RCP 8.5
Ensemble Members	▪ Includes 26 climate models statistically downscaled to Canadian climate observations ▪ Total of 104 ensemble members (26 climate models x 4 emissions scenarios) used in this study	▪ Total of 50 ensemble members available based on perturbation of initial conditions from the Canadian Earth System Model (CanESM) ▪ Set of 15 members selected in Elshamy et al. (2024b) to reduce ensemble size while maintaining uncertainty from larger set

Discussion related to uncertainty associated with the multi-model ensembles of climate projections as it relates to the Monte Carlo framework used in this study is provided in Section 12.8.

10.2 Land Cover Changes

Within the MESH modelling framework climate change is linked to land cover, driving changes in vegetation, permafrost, and glacial retreat within the Mackenzie River Basin through its land surface model component. This component simulates vertical processes of heat and moisture transfer between the land surface and atmosphere using a deep soil profile to capture permafrost dynamics. Details regarding the MESH modelling framework and the coupling of climate change and land cover changes are outlined in Elshamy et al. (2024a,b). The climate projections within the MESH modelling framework are provided from CMIP5 (Elshamy et al. 2024a,b).

Modelling results from Elshamy et al. (2024b) indicate that with rising temperatures under climate change, most of the permafrost areas in the Mackenzie River Basin will disappear by the 2080s for a high emissions scenario. In addition, glaciers in the Rockies are projected to melt substantially, resulting in a reduction of summer river flows in headwater areas across the basin (Elshamy et al. 2024b). Despite major shifts in land cover including permafrost and melting glaciers, it was found that the overall effect of warmer temperatures and increased rainfall amounts projected under climate change may have a greater influence on river flows than changes in land cover.

10.3 River Ice Thickness Changes

Projected changes in river ice cover timing and thickness are estimated using Stephan's equation, which is an empirical relationship originating from heat transfer theory and is widely used in hydrology and cryospheric sciences (Stephan 1891), and future temperatures embedded in CDDF:

$$h = \sqrt{2k \cdot \frac{CDDF}{\rho L}} \quad \text{(Eq. 10-1)}$$

Where h is the ice thickness (m), k is the thermal conductivity of ice (W/m·K), $CDDF$ is the cumulative degree days of freezing (°C·days) – obtained from simulated temperatures under climate change scenarios, ρ is the density of ice (kg/m^3), and L is the latent heat of fusion (J/kg). In practice, a simplified version of this equation is often used:

$$h = C \cdot \sqrt{CDDF} \quad \text{(Eq. 10-2)}$$

Where C is an empirical coefficient, typically ranging from 1.5 to 2.5 cm/(°C·day)$^{-0.5}$ depending on local conditions including snow cover, water salinity, and wind (Ashton 1986). Over the modelled baseline period of 1980 to 2005, $CDDF$ is calculated for each climate model and emissions scenario to calibrate the C coefficient using ice thickness ADCP measurements at Norman Wells by Water Survey Canada (see Section 4.5). Using the calibrated C coefficient, ice thickness is estimated for each future period. Calibrated ice thickness projections are illustrated in Figure 10-1 for the baseline and future periods assessed, where the solid lines denote the median and the shaded regions denote the range of results across available climate models and emissions scenarios with the multi-model ensemble. With increasing air temperatures projected over the study area, ice thicknesses are projected to decrease. Notably, a wider spread of ice thicknesses is projected for periods further into the future, as climate model projections tend to diverge towards end-of-century.

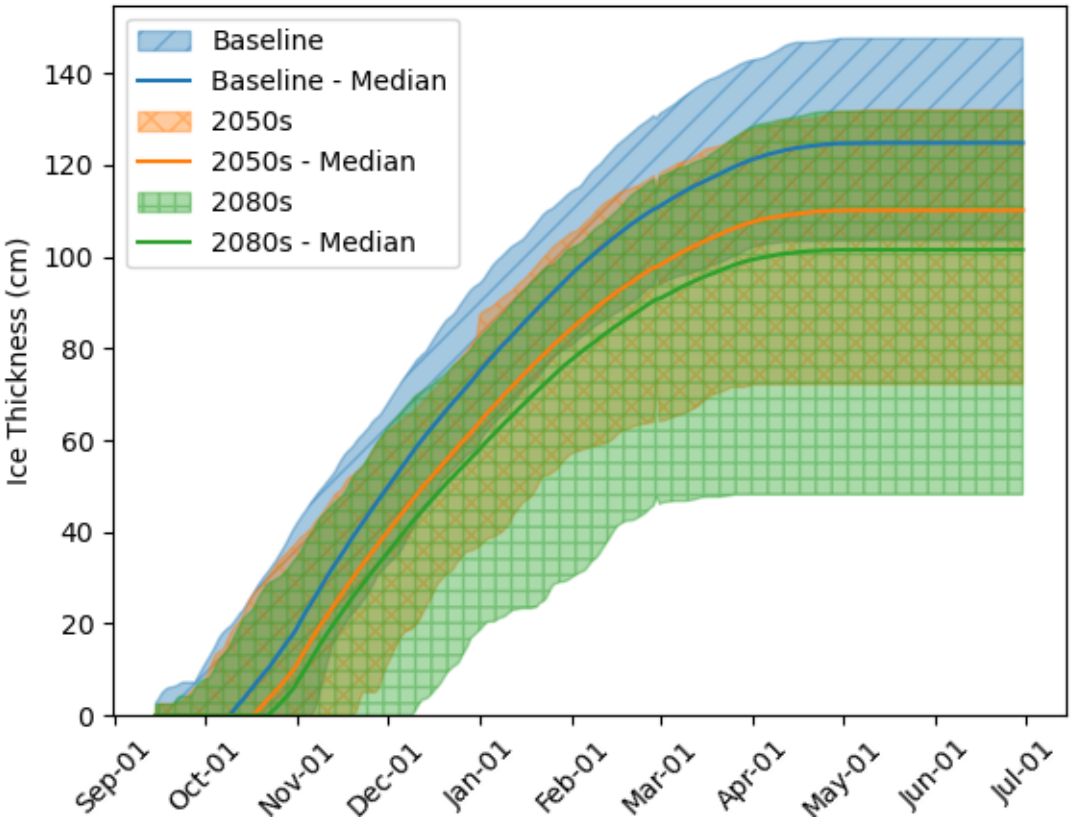

Figure 10-1: Calibrated Ice Thickness Projections for Baseline (1980 to 2005), Mid-Century (2050s), and End-of-Century (2080s) Future Periods

Peak ice thickness every year in each period is estimated prior to spring breakup, and a statistical distribution is fitted to describe peak ice thickness across climate models, emissions scenarios, and years. In Figure 10-2 the fitted statistical distributions are presented. Similar to Figure 10-1, peak ice thicknesses are generally projected to decrease with increasing air temperatures due to climate change, with a greater range projected for periods further into the future. Peak ice thicknesses are approximately normally distributed, with a slight left skew for the end-of-century period. This skew is likely due to the presence of “hot models” included in set of climate models evaluated, which are more sensitive to radiative forcing and project greater warming than others (Cannon 2024). For use in the Monte Carlo analysis, peak ice thickness is represented in terms of projected change, which is calculated on a model-to-model basis. This approach allows for baseline peak ice thicknesses to be scaled for climate change and avoids drawing from different climate models and emissions scenarios to represent baseline and future peak ice thickness. The resulting projected changes in peak ice thickness used for Monte Carlo analysis are illustrated in Figure 10-3, which follow an approximately lognormal distribution to capture greater left skew than the absolute peak ice thicknesses presented in Figure 10-2. The reason for greater left skew when presenting projected change in peak ice thickness is due to the presence of climate models that simultaneously represent greater peak ice thickness in the baseline and lower peak ice thickness in the future than others, resulting in a substantial decrease in peak ice thickness.

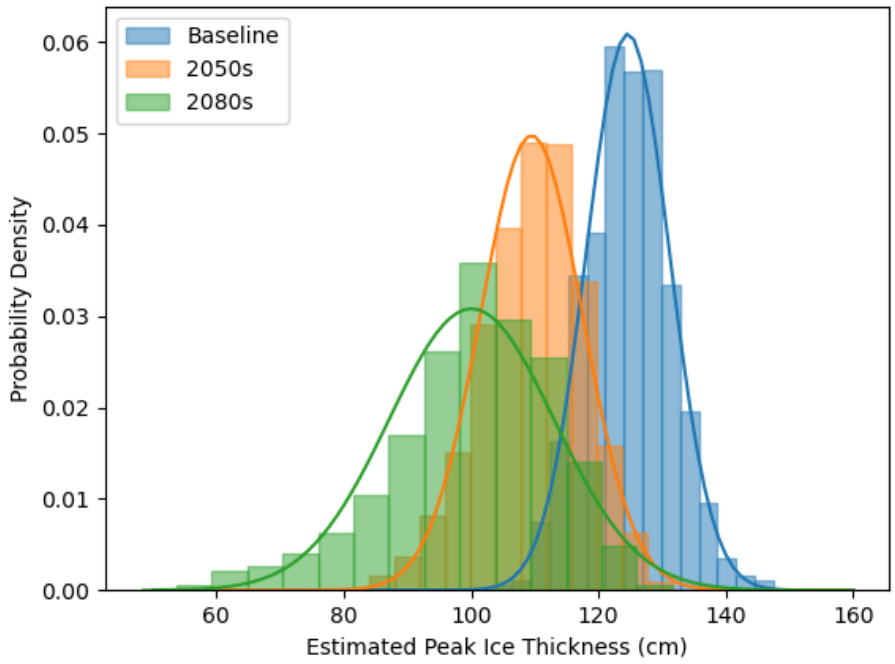

Figure 10-2: Future Projected Probability Distribution of Peak Ice Thickness for Baseline, Mid-Century (2050s), and End-of-Century (2080s) Future Periods

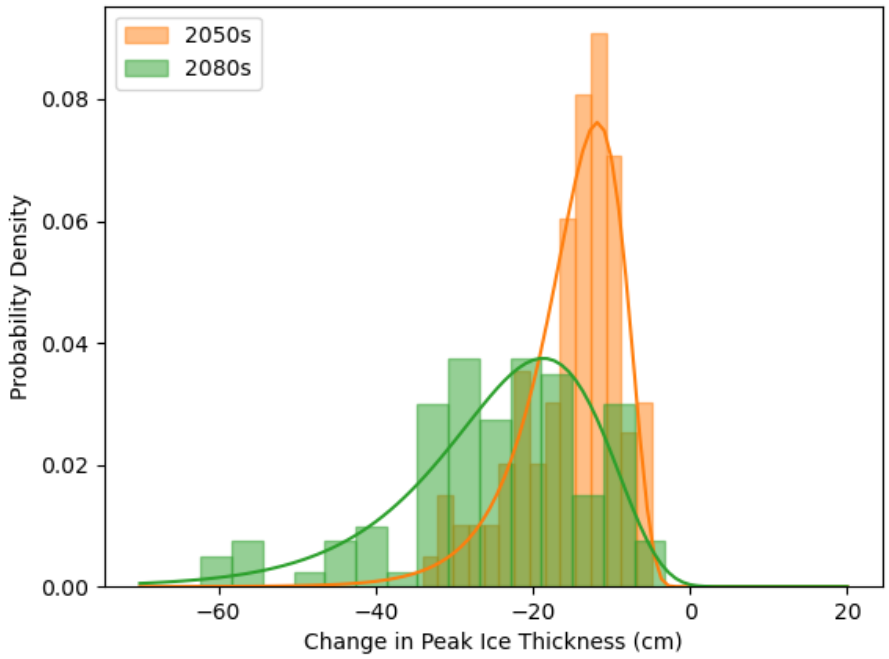

Figure 10-3: Future Projected Probability Distribution of Peak Ice Thickness Change from Baseline for Mid-Century (2050s), and End-of-Century (2080s) Future Periods

10.4 Shifts in Flows during Ice Jams

Future ice jam flood hazards influenced by climate change were assessed for the community of Norman Wells, located along the Mackenzie River about 180 km upstream of Fort Good Hope. These assessments relied on an empirical hydrological model (MESH) designed to estimate river discharge and water stage during ice jam events. The MESH hydrological model of the Mackenzie River basin (Elshamy et al. 2025a), which was used in another study to produce different models of historical and future daily flows (Elshamy et al. 2025b), is also used in this present study. To account for uncertainty and variability, the model was embedded within a Monte Carlo simulation framework, which uses randomly selected values for parameters and boundary conditions drawn from established frequency distributions.

A crucial aspect of the hazard analysis involved developing frequency distributions of daily mean river flows that corresponded to peak backwater levels observed during ice jam occurrences just downstream of the Norman Wells hydrometric gauge. The empirical model was calibrated using historical observational data to ensure its reliability, and simulations were conducted for two distinct future timeframes: the mid-century period (2040–2065), and the far future (2075–2100).

To simulate future flow conditions, data were extracted from MESH—a basin-scale hydrological model that incorporates climate projections from global circulation models (GCMs). These GCMs provided future air temperature scenarios, which were used to derive distributions of cumulative degree days of melting (CDDM). These distributions were aligned with the timing of maximum instantaneous water levels caused by ice breakup and jamming events. To correct for biases between historical and projected data, a delta adjustment was applied to the flow values, enabling more accurate projections of future ice jam flood conditions.

The results of the Elshamy et al. (2025b) study indicate a consistent increase in ice jam flood hazard across all future periods, suggesting that climate change will likely exacerbate flood risks in the region over the coming decades. Elshamy et al. (2025b) assessed future changes in the Mackenzie River Basin using a physically based cryo-hydrological model driven by an ensemble of regional climate projections and found that climate warming will alter river flow timing, magnitude, and ice-related processes, leading to higher ice-jam flood hazard. The study showed that warmer air temperatures and increased spring precipitation will cause snowmelt-driven peak flows to occur earlier and with greater magnitude, increasing the likelihood of mechanical ice breakup rather than gradual thermal decay. At the same time, widespread permafrost thaw is projected to increase winter baseflow leading to more rapid spring runoff which creates conditions that favor ice accumulation and jamming during breakup. The methodology to determine shifts in ice jam flood hazard at Norman Wells due to climate change has been adapted from Dehghani Sanij et al. (submitted) and Lindenschmidt et al. (2025). The method uses flows simulated from a hydrological model and the cumulative degree days of melting (CDDMs) are used to find the timing when ice jamming occurs. The key steps of the workflow are:

1) Historical CDDM distribution
2) Randomized peak ice jam dates
3) Historical flow frequency
4) Bias correction
5) Future projections

Step 1: Historical CDDM calculation and distribution

Future air temperature scenarios for different GCM's were obtained from Elshamy et al. (2024b). The cumulative degree days of melting (CDDM) were computed from these scenarios to examine the thermal energy buildup that causes ice breakup events. The CDDM were determined to measure the amount of ice melting during the pre-breakup to breakup period (March 1 – May 31) using:

$$CDDM = \sum_{i=D_1}^{D_n} (T_{Di} + 5) \qquad \text{(Eq. 10-3)}$$

where D_1 is the starting day for calculating CDDM, T represents the daily mean air temperature (from the meteorological station at Norman Wells). Included in this equation, is an additional 5°C that is added to T_{Di} to account for the contribution of solar radiation to ice melting. CDDM curves were calculated for each year from 1 March for the years 1980 to 2022 (Figure 10-4). The timing for the CDDMs was identified by first assembling and preparing a continuous daily mean air temperature record from Norman Wells, focusing on the months of March through June. The analysis defined March 1 of each year as the starting point for accumulating degree-days. From this date onward, cumulative degree-days were calculated by summing only the portion of each day's mean temperature that exceeded a threshold of –5 °C, a threshold selected to account not only for above-freezing air temperatures but also for the impingement of solar radiation to the ice cover which also promotes pre-breakup weakening of river ice. Once the CDDM curves were generated, the actual timing of ice jam peak backwater stages (Wpeak), determined from the historical instantaneous ice jam peak water levels recorded at the Norman Wells gauge, was used to determine the CDDM value corresponding to each peak date.

Then, the CDDM values at peak ice jam staging were used to create a density function of CDDMs, which was best represented by a log-normal distribution, as indicated in Figure 10-5.

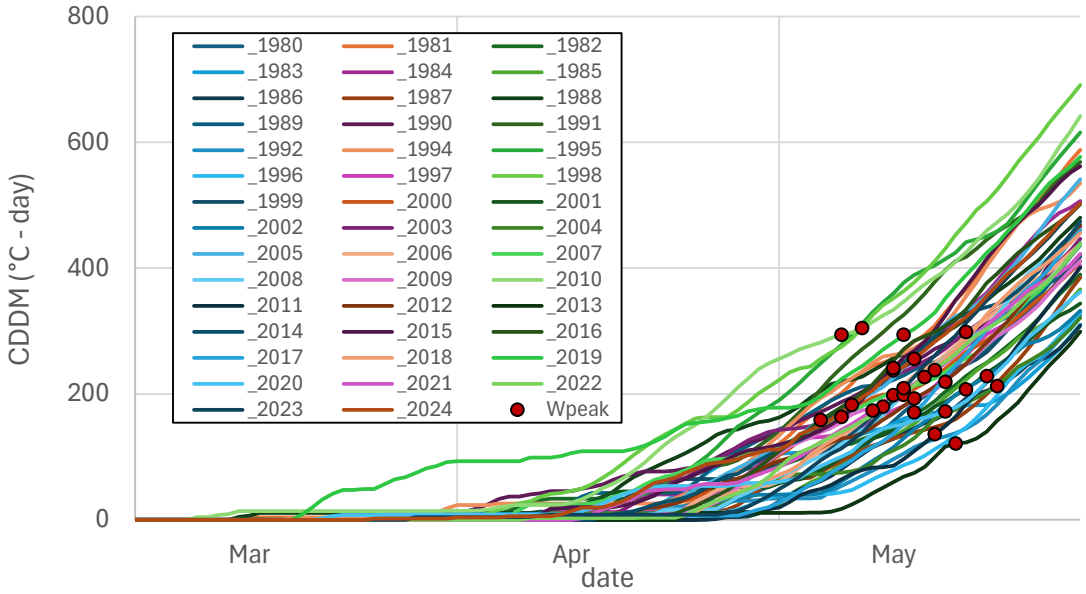

Figure 10-4: Cumulative Degree Days of Melting Beginning 1 March to the end of May for the Years 1980 to 2022 (Wpeak dots indicate the date of peak ice jam staging at Norman Wells)

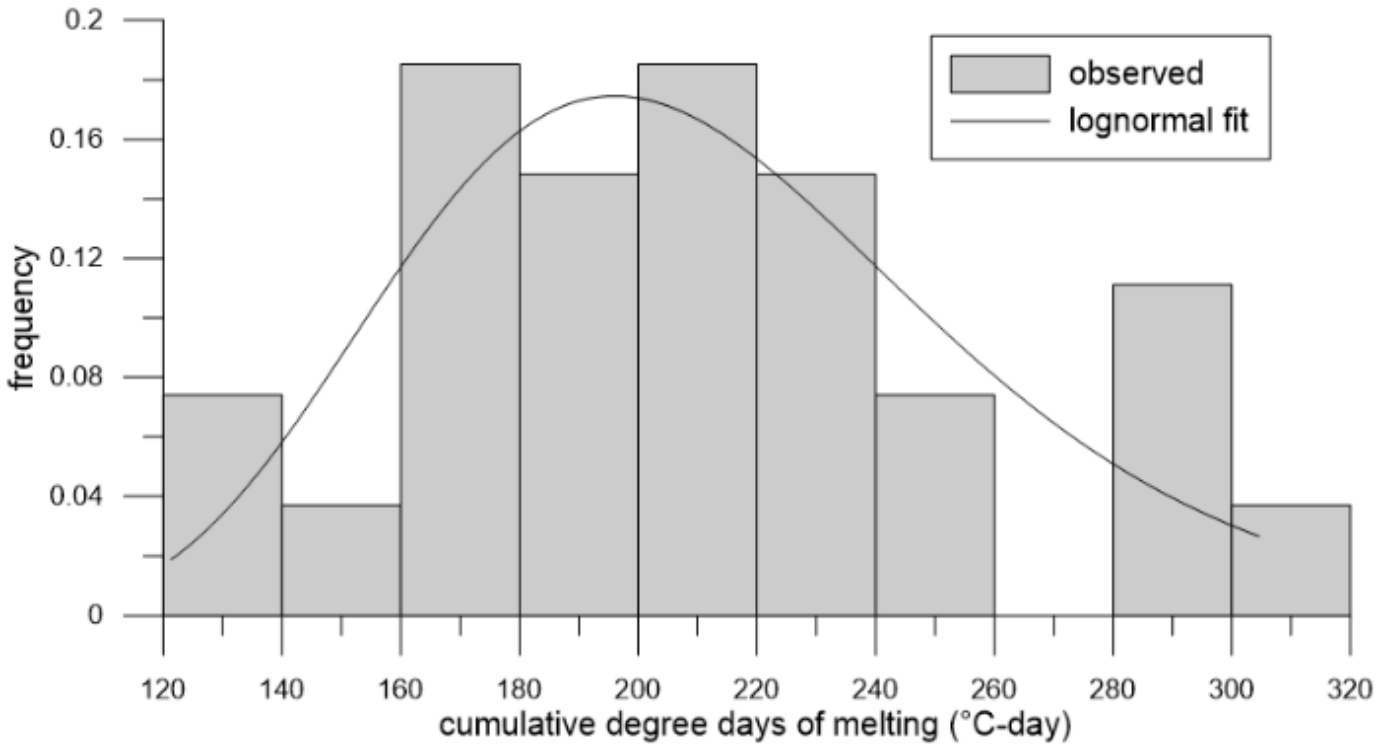

Figure 10-5: Log-normal Distribution Fit to Observed Cumulative Degree Days of Melting, Beginning 1 March, until Peak Ice Jam Staging for the Years 1980 to 2022

Step 2: Randomized dates of peak ice jam staging

Random values of the historic CDDM's were extracted from the theoretical log-normal distribution shown in Figure 10-5. Using daily mean air temperatures for Norman Wells from the CanRCM4-ESM2 climate change data, a date of the peak ice jam staging for a particular year corresponding to the timing required to attain the randomly generated CDDM for that year.

The method assumes that the cumulative degree-days of melting accumulated from March 1 until the historical peak-ice day represent the same amount of melt energy that will be required in future scenarios. While the CDDM values themselves are treated as unchanged between the historical and the future, the actual timing at which those same CDDM totals are reached will shift because future daily temperatures differ from historical ones. This will cause breakup dates to advance due to earlier increases in seasonal air temperatures in the future.

The timing for the period 1980 to 2100, which includes the simulated historical period (1980 – 2005) and the future period (2006 – 2100) are shown for one randomization in Figure 10-6. These time periods are set by the climate change scenarios for CMIP5. A trend to earlier dates of ice jam staging can be observed throughout this century.

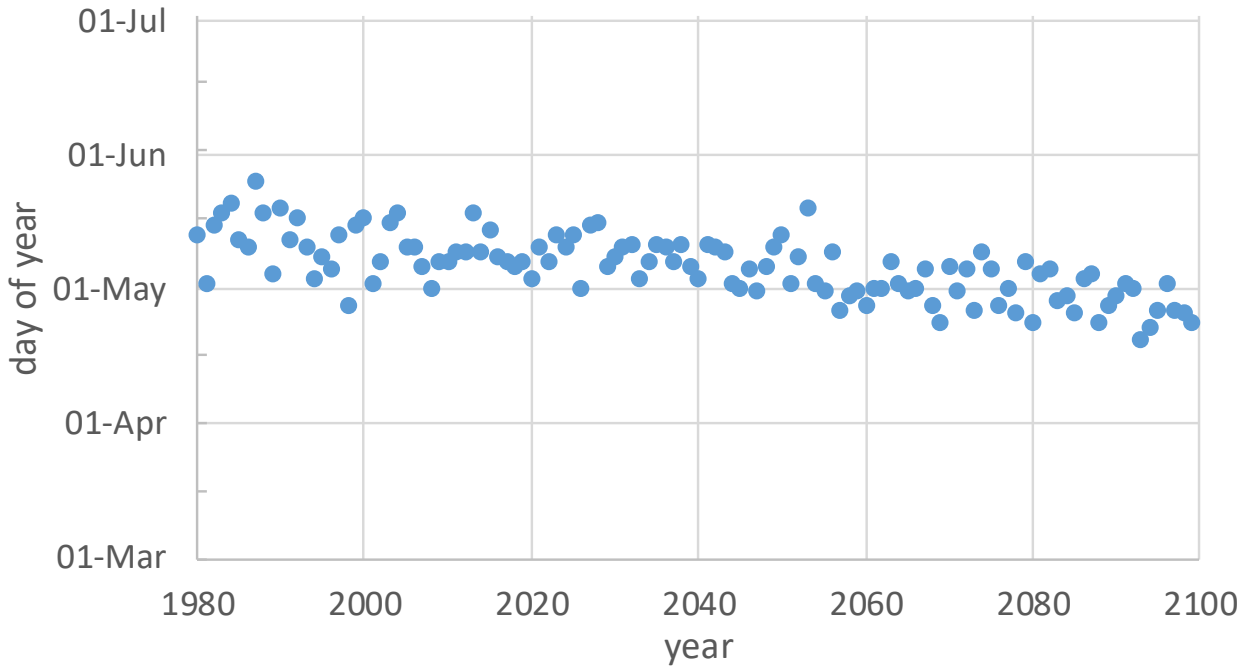

Figure 10-6: One Randomized Series of Dates of Peak Ice Jam Staging each Year from 1980 to 2100

Step 3: Historical flow frequency distributions

A daily mean flows corresponding to the CDDM dates were then extracted from a hydrological model of the Mackenzie River basins for all the years 1980 to 2100. The hydrological model is MESH (Modélisation Environnementale Surface et Hydrologie – Surface and Hydrology Environmental Modelling) model, which was set up and calibrated by Elshamy et al. (2024a, b). The modelling incorporated a 15-member ensemble of the Canadian Regional Climate Model (CanRCM4) downscaled from the Canadian Earth System Model (ESM2) and resulted in 15 sets of flow data. This adjustment was based on comparing all simulated flows from the 15 modelled flows with the observed flows for 1980 to 2005. A Gumbel distribution of the flows was fitted to Gringorton plotting positions (Gringorton 1963) for the historical period 1980 to 2005 and compared to the Gumbel distribution of the observed flows for the same time period when peak ice jam staging was recorded at the Norman Wells gauge. The maximum flow from all 15 members using the corresponding average air temperatures of all members provided the closest fit of its flow frequency to the observed flow frequency distribution, as shown in Figure 10-7.

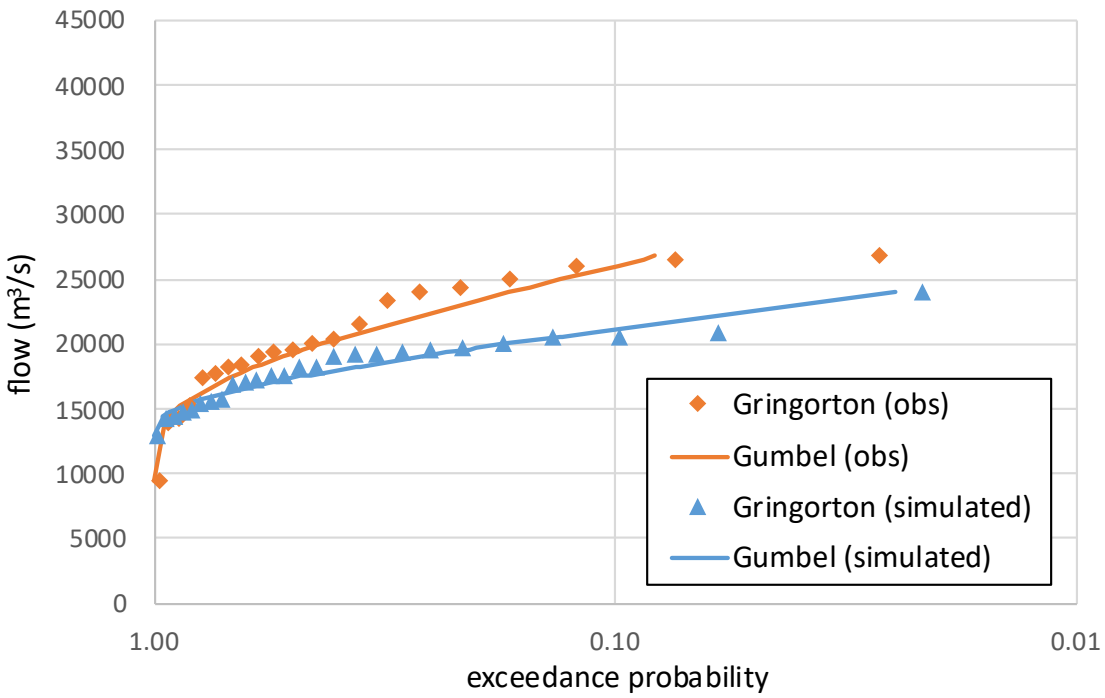

Figure 10-7: Simulated and Observed Flow Frequency Distributions for the Historical Period 1980 – 2005

Step 4: Bias Correction

In order to better fit the simulated to the observed flow frequency distribution in Figure 10-7, two adjustments were carried out to remove the bias: (i) the location and scale parameters of the CDDM distribution were slightly adjusted (location from 5.33 to 5.0; scale from 0.227 to 0.4); and (ii) a delta (× 1.3) was introduced to the flows to linearly augment them. The bias corrected distribution is shown in Figure 10-8, which now coincides with the observed flow frequency distribution.

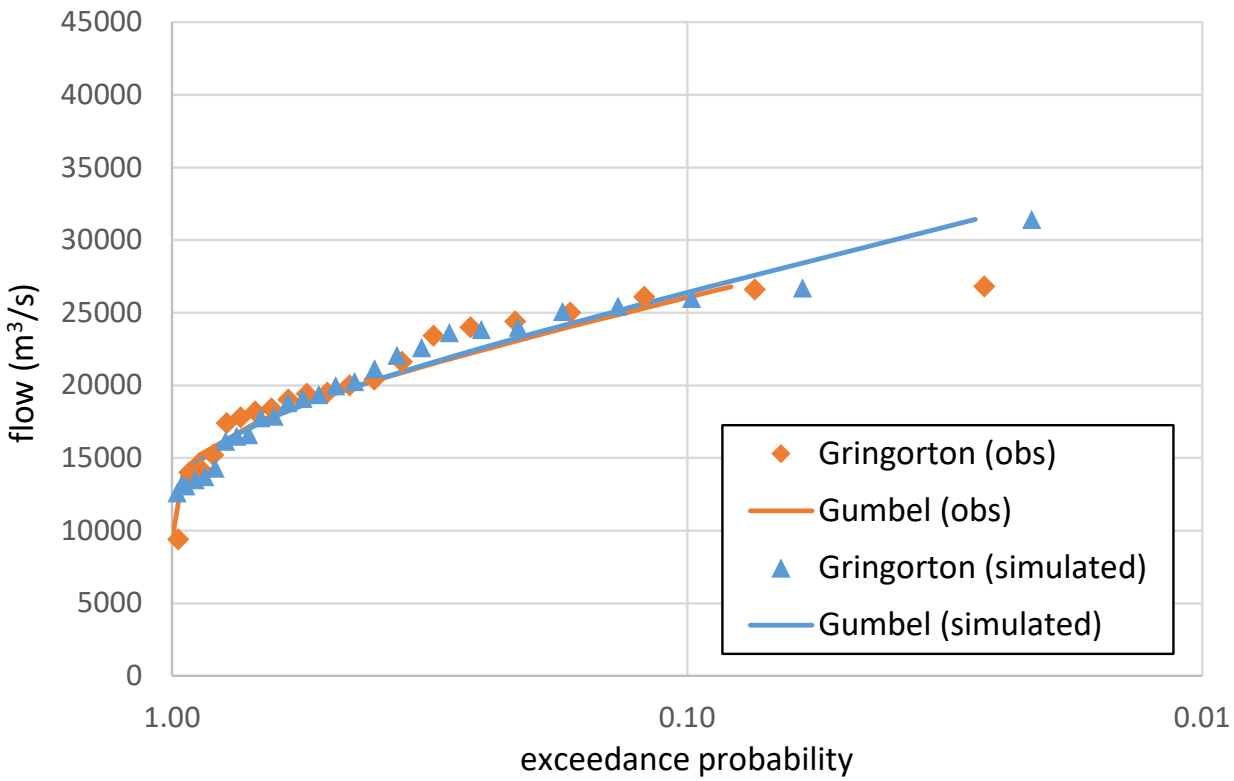

Figure 10-8: Simulated and observed flow frequency distributions for the historical period 1980 – 2005

Step 5: Future projections of flow frequency distributions

Future flow frequency distributions at ice-jam peak staging were estimated using a temperature-driven stochastic approach that links cumulative degree days of melting (CDDM) with hydrological model output rather than by directly extrapolating historical flow statistics. The bias-adjusted historical CDDM distribution was projected into the future and used as a thermal threshold, meaning that random CDDM values were sampled from it and applied to future simulated air temperature time series to determine the timing of peak ice-jam staging in each future year. Once the future peak staging date was identified from the air temperature data, the corresponding simulated river flow from the hydrological model was extracted. The process was repeated across all years.

Future daily temperatures were obtained from the downscaled climate model projections (CanRCM4-ESM2) for two different time periods: mid-future (2040-2065), and far future (2075-2100). First, the future CDDMs were calculated for each year's daily air temperature timeline starting from March 1 averaged over all 15 climate change model runs. The flow frequency distributions for two future periods: mid future (2040-2065), and far future (2075-2100), are provided in Figure 10-9.

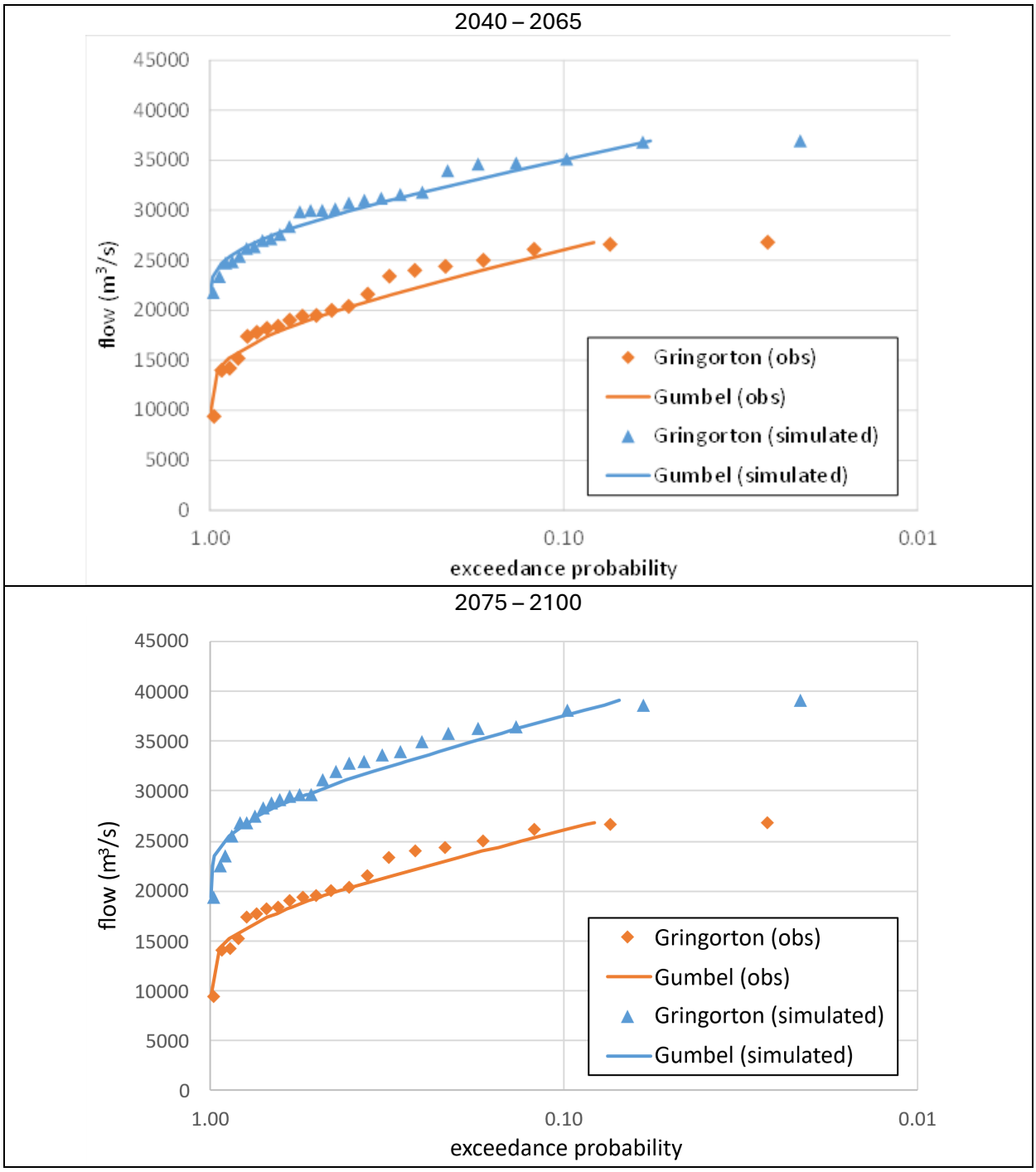

Figure 10-9: Flow Frequency Distributions for the Mid-future (top panel) and Far Future (bottom panel)

10.5 Ice Jam Flood Profiles with Climate Change

10.5.1 Approach to Water Surface Profiles Under Climate Change Conditions

In Section 9.1.1, for current conditions (when no climate change is yet considered), a maximum flow threshold is set to account for the unlikeliness of the ice jam downstream of Fort Good Hope to withstand elevated flows and the limitation of the HEC-RAS model to simulate ice jam release. A maximum threshold of 10% above the highest recorded flow on May 20, 2021 was defined.

The incoming flow is expected to increase under climate change conditions, but defining a maximum threshold for such conditions is more complicated. Thus, to avoid underestimating incoming flow in climate change conditions, no maximum threshold is imposed and flows from the whole distribution are considered. As a means of comparison, the Monte Carlo Simulation without climate change is once more performed but without a maximum threshold.

The differences in water levels between conditions with and without climate change for all flows are then calculated and used to define the water surface profiles in climate change.

Equations 10-4 and 10-5 shown below are defined to provide a better explanation of the afore-mentioned approach:

$$\Delta WL = WSE_{CC}^{AF} - WSE^{AF} \quad \text{(Eq. 10-4)}$$

Where ΔWL is the difference in water levels between scenarios with and without climate change, WSE_{CC}^{AF} are the water surface elevations with climate change when all flows are considered, and WSE^{AF} are the water surface elevations without climate change when all flows are considered.

$$WSE_{cc}^{MT} = \Delta WL + WSE^{MT} \quad \text{(Eq. 10-5)}$$

In equation 10-5, WSE_{CC}^{MT} denotes the corresponding water surface elevations under climate change conditions when a maximum threshold is defined (as explained in Section 9.1.1), ΔWL is the difference in water surface elevations as defined in equation 10-5, and WSE^{MT} defines the water surface elevations without climate change when a maximum threshold is defined.

10.5.2 Ice Jam Volume Under Climate Change Conditions

As explained in Section 10.3, the ice thickness is expected to reduce with climate change and Table 10-2 shows the percentage reduction in comparison to the scenario without climate change. A greater reduction in ice thicknesses is obtained with higher exceedance probabilities.

Table 10-2: Ice thickness percentage reduction for mid-century and end-of-century climate change scenarios – Results of the Monte Carlo + HEC-RAS Framework

Return Period	Exceedance Probability	Ice Thickness Percentage Reduction (%)	
		Mid-Century Climate Change (2050s)	End-Of-Century Climate Change (2080s)
2	0.5	-12.6	-19.9
5	0.2	-10.3	-14.3
10	0.1	-9.1	-11.9
20	0.05	-8.1	-9.9
50	0.02	-7.1	-7.4
100	0.01	-6.5	-6.3
200	0.005	-5.9	-4.9
500	0.002	-4.4	-3.7

In the HEC-RAS calculations, the user simply specifies the location of the ice jam: cross section numbers for the toe and the head of the jam. The ice thicknesses and ice volume within the ice jam are computed directly by the HEC-RAS model. These parameters are affected by the river flow. At higher flow, the computed ice jam will grow bigger (thicker ice and larger ice volume) and the upstream water levels affected by the jam will increase.

As the flow is expected to increase in climate change, the ice jam volume computed by HEC-RAS is greater under climate change conditions. This volume increase might not be representative of reality since HEC-RAS does not consider other parameters affected by climate change nor does it simulate ice jam release.

If the Ramparts keeps acting as an obstruction to ice floes in the Mackenzie River, it can be assumed that ice availability downstream is limited. Therefore, considering the projected reduction in ice thickness under climate change conditions, it is reasonable to hypothesize that future ice jams would decrease in volume.

To account for this decrease in ice volume, the ice jam head location is moved one cross section downstream, as shown in Figure 10-10. Head location 1 (cross section 82748) refers to the ice jam head location used in the Monte Carlo Simulation in current conditions (when climate change was not considered). This head location will also be evaluated under climate change conditions. Head location 2 is the new ice jam head location considered for climate change (cross section 80825) considered to evaluate its impact on water elevations.

The blue-marked area shown on Figure 10-10 represents the maximum ice jam extent for head location 2; between cross sections 62067 and 80825 (18-km long).

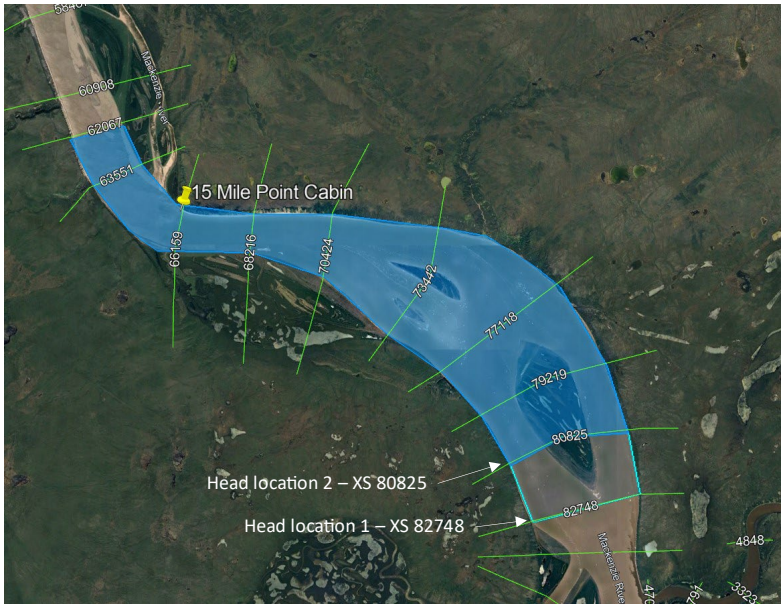

Figure 10-10: Ice Jam Head Locations 1 and 2 considered for Climate Change Scenarios. The blue-marked area represents the maximum ice jam extent for Head Location 2.

The percentage change in ice jam volume when considering head locations 1 and 2 are presented in Table 10-3.

Table 10-3: Percentage change in ice jam volume under climate change scenarios at mid-century (2040-2065) and at end-of-century (2075-2100) – Results of the Monte Carlo + HEC-RAS Framework

Return Period	Percentage Change of Ice Jam Volume (%)			
	Climate Change Scenario 2040-2065		Climate Change Scenario 2075-2100	
	Head Location 1	Head Location 2	Head Location 1	Head Location 2
2	29.0	-	32.7	-
5	17.2	-2.3	19.4	-0.6
10	10.5	-7.8	12.8	-5.9
20	8.9	-9.1	10.8	-7.6
50	6.7	-10.3	9.0	-8.5
100	6.0	-11.2	9.2	-8.2
200	4.9	-12.0	9.0	-9.0
500	3.6	-12.7	9.1	-9.5

As expected, an increase in ice jam volume is obtained when the ice jam head location is kept constant (Head Location 1). A greater increase is obtained when considering the end-of-century climate change scenario compared to mid-century climate change scenario because higher flows are anticipated.

When the ice jam head location is changed to Head Location 2, a decrease in ice jam volume is obtained (negative percentages). A smaller decrease in ice jam volume is projected for the end-of-century climate change scenario, mainly due to the anticipated higher flows.

These decrease in ice jam volume are slightly higher than the ice thickness percentage reductions presented in Table 10-2.

10.5.3 Water Levels in Climate Change Scenarios

The corresponding changes in water levels between the climate change scenarios and the current conditions were computed (ΔWL) and added to the water elevations found in Figure 9-8 (WSE^{MT}) to obtain the water levels WSE_{CC}^{MT}, as per Eq. 10-2. The flood extent difference between the ice jam head locations 1 and 2 for the 100-year flood are shown in Figure 10-11 and Figure 10-12. When the ice jam head location is kept constant, an elevation of 36.6 m is obtained at Fort Good Hope for the mid-century climate change scenario while an elevation of 37.4 m is obtained for the end-of-the-century one. When the ice jam's volume is reduced by changing the head location to Head Location 2, the water elevations are reduced to 35.7m and 36.4 m, respectively. Changing the ice jam location from location 1 to 2 reduces water levels for about 1 meter. The flooded area that connects Jackfish River to the Mackenzie River is a low-lying part of the community enclosed by relatively steep slopes on both sides. As a result, a 1-m rise in water level does not seem to have a substantial effect in the overall flood extent.

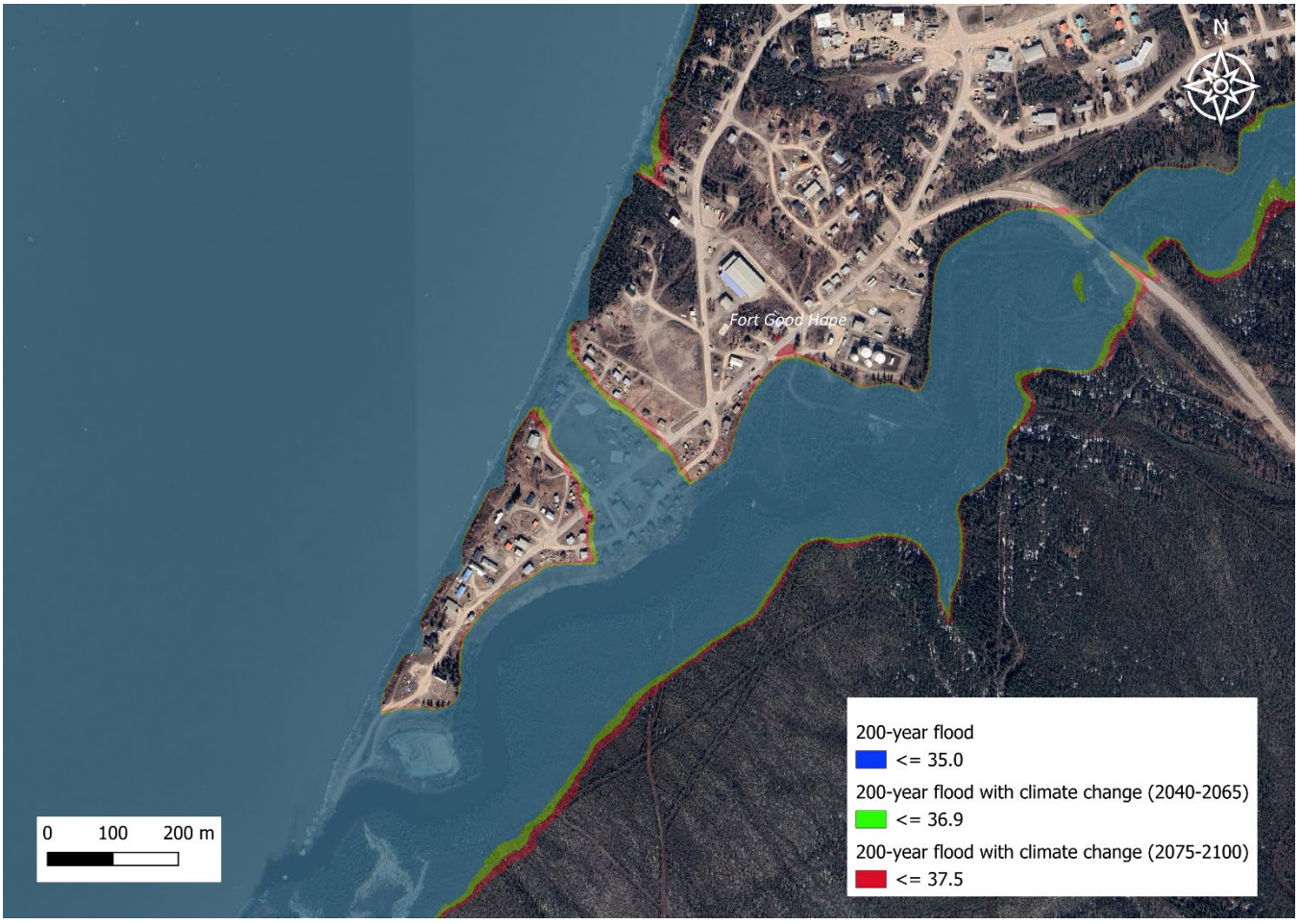

Figure 10-11: Flood extent comparison between scenarios with and without climate change for a 200-year flood when the ice jam head is kept at Head Location 1 – Results of the Monte Carlo + HEC-RAS Framework

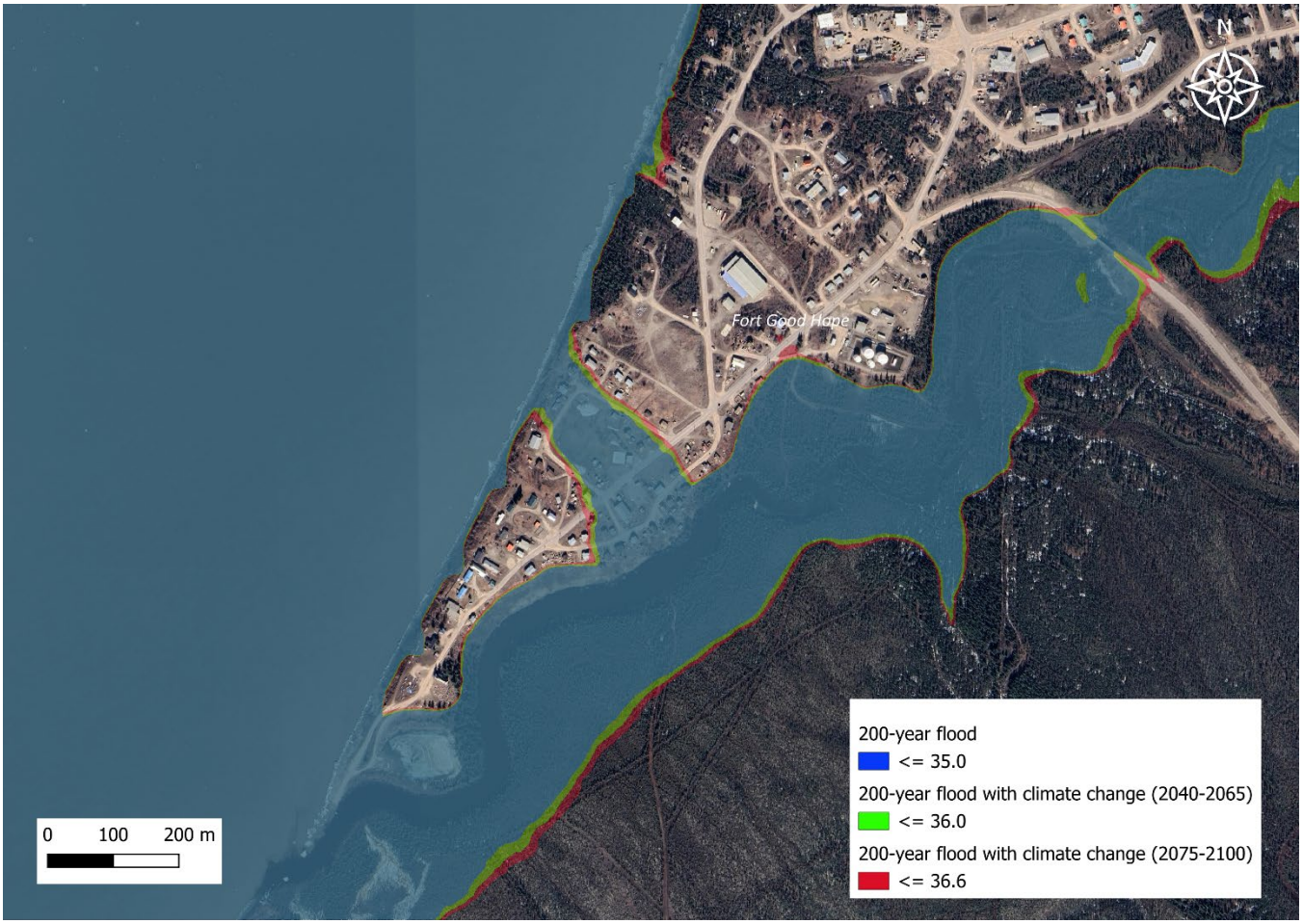

Figure 10-12: Flood extent comparison between scenarios with and without climate change for a 200-year flood when the ice jam head is changed to Head Location 2 – Results of the Monte Carlo + HEC-RAS Framework

WSP considers the flood extent shown in Figure 10-11 to be reasonable and conservative without being overly so. While a reduction in ice jam volume under climate change is a possibility, other factors affecting ice jam formation may not be fully accounted for. Therefore, to avoid artificially reducing the ice jam volume in the modelling, WSP recommends using the water levels obtained when ice jam head location is kept constant in climate change scenarios.

The recommended water surface elevations at Fort Good Hope under climate change conditions for the 100-year and 200-year floods are presented in Table 10-4.

Table 10-4: Water surface elevation at Fort Good Hope in CGVD13 for mid-century and end-of-century climate change scenarios for the 100 and 200-year floods – Results of the Monte Carlo + HEC-RAS Framework

Return Period	Water Surface Elevation in CGVD13 (m)		
	Current Conditions	Climate Change Scenario 2040-2065	Climate Change Scenario 2075-2100
100	34.8	36.6	37.4
200	35.0	36.9	37.5

Results of the Framework indicate that the ice jam flood magnitude will increase significantly in the future mainly due to the significant river flow increase at time of breakup. Results show that the reduction in ice thickness, or in downstream ice jam volume, in future conditions would not compensate for this flow increase.

Freeze-up level, winter discharge and ice transport at the Ramparts will be affected in the future by warmer weather, thus changing the behavior of downstream jams that drive ice jam flooding at the Community. This context of uncertainty calls for caution when assessing flood level under climate change scenarios.

Flood inundation and hazard mappings showing the water surface elevations for these two AEPs under the mid-century and end-of-century climate change scenarios are provided in Appendix E and F.

Considering that Jackfish Creek bridge's deck elevation is 35.8 m, the bridge would be overtopped in 100 and 200-year floods conditions, for both climate change scenarios.

11 FLOOD MAPPING

Key deliverables for this study include flood inundation mapping and flood hazard maps for Fort Good Hope.

11.1 May 2021 Flood Maps

The May 2021 flood inundation maps were developed to represent peak water levels during the ice jam event. This flood event was described in Section 4.2 and in the flood chronology report WSP (2026). High water marks from the May 2021 flood surveyed in Fort Good Hope were used to develop a river centerline profile and interpolated to produce the flood inundation area.

The May 2021 flood inundation maps are provided in Appendix D. Details of the three sets of flood inundation maps are provided in Table 11-1; the maps contain the same results but are shown at three different map scales.

Table 11-1: May 2021 Flood Map Details

Map Title	Map Scale	Number of Map Sheets in the Study Area
2021 Flood Inundation Map Fort Good Hope (Rádéyı́lı̨ Kóé)	1:15,000	3
2021 Flood Inundation Map Fort Good Hope (Rádéyı́lı̨ Kóé)	1:5,000	1
2021 Flood Inundation Map Fort Good Hope (Rádéyı́lı̨ Kóé)	1:2,000	1

Ollerhead (2023) surveyed the high water marks associated to the May 2021 flood at Fort Good Hope. Figure 11-1 shows the locations of the surveyed points (17) and the surveyed high water mark elevations in CGVD2013 datum. All points are in the low-lying part of the community.

Figure 11-1: May 2021 High Water Marks Surveyed by Ollerhead (2023). Elevations in CGVD2013 datum

Seventeen (17) points were surveyed by Ollerhead (2023), with elevations (CGVD2013) ranging between 33.22 and 34.2 m, with an average value of 33.63 m.

WSP estimated the maximum flood water level in the community by comparing the LiDAR elevations and the aerial images captured on May 25, 2021. Flood extent on LiDAR surface and images were compared for various water levels, and a value of 33.8 m was retained. Figure 11-2 presents the result of this comparison in the low-lying part of the community.

For flood inundation mapping of the May 2021 ice jam flood, WSP estimated the slope of Mackenzie River near Fort Good Hope based on the Digital Surface Model (DSM) published by Natural Resources Canada. Figure 11-3 illustrates the river reach used to calculate the river slope.

The surface slopes derived from the DSM are 0.004% from km 0 to km 20 and 0.018% below km 30. Station 10LD001 (Fort Good Hope) is located at km 12.8, in reference to Figure 11-3.

The slope used to prepare the draft May 2021 flood maps next to the community (0.00004 m/m) is similar, but slightly lower slope, than the one used in the Monte-Carlo Analysis (0.0001 m/m; Section 9). This lower slope used for flood mapping has no impact on flood extent at the community and led to water levels few centimetres higher outside the community.

To generate the flood extent along the river, the water level of 33.80 m in Fort Good Hope was projected using the surface slopes above. Thus, the following water levels along the river were developed:

- km 0.0 (Ramparts): 34.31 m
- km 12.8 (Gauge 10LD001): 33.80 m [Reference gauge]
- km 16.8 (Rabbit Skin River): 33.64 m
- km 30.0: 33.11 m
- km 40.0: 31.31 m

Figure 11-4 presents a comparison between the aerial image and the draft flood zone near the outlet of Rabbit Skin River.

(a) Aerial image

(b) Flood inundation zone

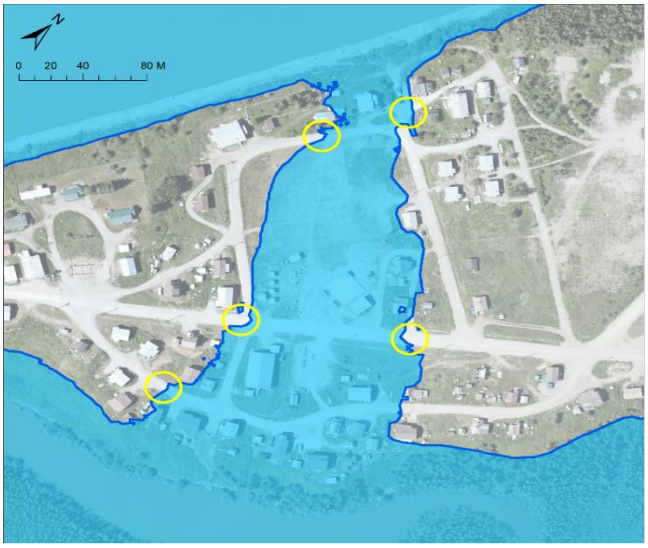

Figure 11-2: Comparison Between Flood Zones on May 25, 2021 in Low-lying Part of the Community: (a) Aerial Image; and (b) Flood Inundation Zone. Yellow Circles Indicate Comparison Points

Figure 11-3: River Profile Used to Estimate the Slope of Mackenzie River Near Fort Good Hope

(a) Aerial image

(b) Flood inundation zone

Figure 11-4: Comparison Between Flood Zones on May 25, 2021 Near Rabbit Skin River: (a) Aerial Image; and (b) Flood Inundation Zone. Yellow Circle Indicates a Comparison Point

11.2 Current Condition Flood Maps

From the AEPs included in the hydraulic model (50%, 20%, 10%, 5%, 2%, 1%, and 0.5%), two AEP floods were chosen to develop flood hazard maps in consultation with GNWT: 1% and 0.5% AEPs. The 1% AEP (100-year flood) and 0.5% AEP (200-year flood) flood hazard maps are intended to support community and land use planning. The floodway and flood fringe have been delineated for these two AEP floods based on ice jam model results.

Water surface elevation and flood depth grids were created to support delineation of the floodway. Flood water depths at Fort Good Hope governed the development of the ice-affected floodway based on output from the HEC-RAS model and Monte Carlo simulation results of flood water levels. Water levels from the AEP flood at each model cross-section were used to interpolate a TIN surface between cross-sections using Arc-GIS Pro software. Flood water level surfaces were compared with the terrain to obtain flood water depth for each AEP.

Based on guidance from GNWT (2026), the ice-affected floodway is defined as "*the river channel and parts of the flood hazard area where the water depth is greater than 1 metre, or that are exposed to moving ice, during an ice-affected flood*". The ice-affected flood fringe is defined as: "*parts of the flood hazard area where the water depth is less than 1 metre, and that are not exposed to moving ice, during an ice-affected flood* ".

The criteria used to define the floodway in this flood study include:

- Flood water depth exceeding 1 m. When the governing flood is an ice jam flood, depth is the dominant criteria.
- Any "islands" above the flood level smaller than 100 m^2 were screened out of the flood inundation and floodway.
- The floodway always includes the main channel. Any areas that were flooded but that were not connected to the main channel were also removed.
- Areas in the floodway within the main channel such as small islands are included in the floodway, with exceptions made for larger islands with extensive dry areas.

Areas within the ice-affected floodway are more hazardous as they have water depths of at least 1 metre or are exposed to moving ice. The floodway spans fully across the Mackenzie River channel. Any areas within the mapped floodway that do not exceed the floodway 1 m depth criteria, such as small islands are considered in the floodway. A previous flood study presented flood inundation areas, but no floodway was mapped. No engineered flood control structures are known to exist in the study area.

Details of the two sets of flood inundation maps and two sets of flood hazard maps are provided in Table 11-2; these maps are shown at two different map scales. Flood inundation maps for the 1% and 0.5% AEPs are provided in Appendix E, and the corresponding flood hazard maps are provided in Appendix F.

Table 11-2 Current Conditions Flood Map Details

Map Title	Map Scale	Number of Map Sheets in the Study Area
Flood Inundation Maps (Appendix E)		
100-Year Flood Inundation Map Fort Good Hope (Rádéyíłı Kóé)	1:15,000	3
100-Year Flood Inundation Map Fort Good Hope (Rádéyíłı Kóé)	1:3,000	1
200-Year Flood Inundation Map Fort Good Hope (Rádéyíłı Kóé)	1:15,000	3

Map Title	Map Scale	Number of Map Sheets in the Study Area
200-Year Flood Inundation Map Fort Good Hope (Rádéyílı Kóé)	1:3,000	1
Flood Hazard Maps (Appendix F)		
100-Year Flood Hazard Map Fort Good Hope (Rádéyílı Kóé)	1:15,000	3
100-Year Flood Hazard Map Fort Good Hope (Rádéyílı Kóé)	1:3,000	1
200-Year Flood Hazard Map Fort Good Hope (Rádéyílı Kóé)	1:15,000	3
200-Year Flood Hazard Map Fort Good Hope (Rádéyílı Kóé)	1:3,000	1

Flood maps are limited spatially to the study area defined by GNWT (Figure 1-1) as the ice jam model is set up using the locations of historical ice jams downstream of Fort Good Hope and simulates the backwater at the community. Model results obtained further downstream of the study area do not accurately represent ice jam conditions and would likely underestimate water levels in those areas. In the same way, model result outside the study area near the Ramparts may also be inaccurate.

The areas within the community susceptible to ice jam flooding include the same low-lying areas between the Mackenzie River and Jackfish Creek that flooded in May 2021, though the flooded extents are slightly larger. Floodway isolates the westernmost portion of the community including the RCMP building. During the 200-year flood, at least 16 buildings are within the floodway and the bridge over Jackfish Creek is overtopped.

11.3 Climate Change Flood Maps

Flood inundation and flood hazard maps for the mid-century and far-future climate change time periods were developed to provide an indication of future ice jam flood conditions at Fort Good Hope. These maps have higher uncertainty than those representing current conditions which will be discussed in more detail in Section 12. Methods used to develop these maps from HEC RAS and Monte Carlo modelling results were the same as for the current conditions flood maps described in Section 11.2, but used the climate change results described in Section 10.5.

Climate change flood inundation maps for the 1% and 0.5% AEPs are provided in Appendix G, and the corresponding flood hazard maps are provided in Appendix H. Details of the two sets of flood inundation maps are provided in Table 11-3; the maps are shown at two different map scales.

Table 11-3: Climate Change Flood Map Details

Map Title	Map Scale	Number of Map Sheets in the Study Area
Flood Inundation Maps (Appendix G)		
100-Year Flood Inundation Map (Climate Change 2040-2065) Fort Good Hope (Rádéyílı Kóé)	1:15,000	3
100-Year Flood Inundation Map (Climate Change 2040-2065) Fort Good Hope (Rádéyílı Kóé)	1:3,000	1
100-Year Flood Inundation Map (Climate Change 2075-2100) Fort Good Hope (Rádéyílı Kóé)	1:15,000	3
100-Year Flood Inundation Map (Climate Change 2075-2100) Fort Good Hope (Rádéyílı Kóé)	1:3,000	1
200-Year Flood Inundation Map (Climate Change 2040-2065) Fort Good Hope (Rádéyílı Kóé)	1:15,000	3

Map Title	Map Scale	Number of Map Sheets in the Study Area
200-Year Flood Inundation Map (Climate Change 2040-2065) Fort Good Hope (Rádéyı́lı̨ Kóé)	1:3,000	1
200-Year Flood Inundation Map (Climate Change 2075-2100) Fort Good Hope (Rádéyı́lı̨ Kóé)	1:15,000	3
200-Year Flood Inundation Map (Climate Change 2075-2100) Fort Good Hope (Rádéyı́lı̨ Kóé)	1:3,000	1
Flood Hazard Maps (Appendix H)		
100-Year Flood Hazard Map (Climate Change 2040-2065) Fort Good Hope (Rádéyı́lı̨ Kóé)	1:15,000	3
100-Year Flood Hazard Map (Climate Change 2040-2065) Fort Good Hope (Rádéyı́lı̨ Kóé)	1:3,000	1
200-Year Flood Hazard Map (Climate Change 2040-2065) Fort Good Hope (Rádéyı́lı̨ Kóé)	1:15,000	3
200-Year Flood Hazard Map (Climate Change 2040-2065) Fort Good Hope (Rádéyı́lı̨ Kóé)	1:3,000	1

12 UNCERTAINTY AFFECTING ICE JAM MODELLING

This section discusses potential sources of uncertainty in the hydraulic modelling and results. Details are discussed in the following subsections.

12.1 Water Level Readings at Fort Good Hope

The peak water elevation measured at Station 10LD001 and provided by Water Survey Canada on the May 25, 2021 event was 31.14 m. Nonetheless, surveyed high water observations by Ollerhead & Associates Ltd. on 2023 show that water levels as high as 33.8 m were surveyed at Fort Good Hope. A high discrepancy is observed between these two values. It is highly probable that the water gauge at Fort Good Hope has been affected by the ice movements on the Mackenzie River. This adds some uncertainties on the water levels provided by Water Survey Canada, including for the May 20, 2021 calibration value.

12.2 Jave Analysis

Satellite imagery spanning an eight-year period from 2017 to 2024 was analyzed to assess whether a jave, a surge of water and ice caused by the release of an ice jam at the Ramparts, could contribute to enhanced backwater staging of an ice jam located at or just downstream of Fort Good Hope. The analysis suggests that this phenomenon likely occurred during the 2021 ice jam flood event. Furthermore, there is some indication that a similar effect may have taken place during the ice jamming associated with the 2023 spring breakup. If these two instances are representative, the preliminary probability of a jave augmenting ice jam flood staging would be approximately 25 percent, based on two occurrences within eight observed years (2/8 = 0.25).

However, this estimate carries significant uncertainty for several reasons. First, cloud cover during critical observation periods obscured key stretches of the river, making it difficult to confirm whether ice cover persisted in certain locations. Second, shifts in gauge positioning may have distorted water level recordings, further complicating interpretation. Additionally, the eight-year dataset represents a relatively short time frame for deriving a robust probability of staging enhancement caused by javes. For example, imagery from a critical date during the 2025 event (May 23, 2025) could dramatically alter the assessment if evidence emerges that staging was either

influenced or unaffected by a jave. This underscores the need for a longer observation period and more reliable data to improve confidence in these findings.

12.3 Flows at Norman Wells

As mentioned in Section 2.3, hydrometric stations on the Mackenzie River have commonly had data gaps during ice-breakup periods and this is the case for Norman Wells also. Flow data are also derived from continuous water level records and backwater calculations or shifts based on winter gauged discharge values and open water conditions stage-discharge rating curves. Measurement of discharge is not safe during ice-break up so there is a lack of data during a critical period. Flows change relatively rapidly during break-up and gauge conditions may alternate between ice-affected and open-water and backwater varies. While hydrometric data records are thoroughly reviewed and corrected each year to the extent possible, periods with high uncertainty may either be removed from the public record or remain on the record but with high uncertainty in flows especially during ice-breakup.

12.4 Flows at Fort Good Hope

Discharge is not monitored at the Fort Good Hope station, only water levels. There have been occasional flow measurements at this station in the past, such as on July 27, 2010, but it is not systematically gauged. Flows at Fort Good Hope were estimated for this study from flows at Norman Wells, which are in turn, most uncertain during the ice-break period, as discussed above. The Ramparts also creates a back water affect at Norman Wells and creates a water storage effect upstream of Fort Good Hope.

12.5 Break-up Mechanism

The frequency of thermal versus mechanical ice break-up at Fort Good Hope is not well documented. This must be interpreted from photos at the hydrometric gauge, and/or aerial or remote sensing imagery. The documented sudden water level rise and fall during break-up at Norman Wells infers that mechanical ice break-up is dominant (Section 4.3 and Appendix C). Similar data is not available at Fort Good Hope due to data gaps.

Most years it is assumed there is an ice jam downstream and/or at the Ramparts though the impact on flooding at Fort Good Hope varies each year. For example, no flooding is expected during break-up years with lower flows and thin ice. Early in the winter, the ice cover likely freezes thicker at the Ramparts (secondary consolidation), and this ice cover persists later in the spring. This could be verified by physical measurements in future, or the increased roughness of ice surface at the Ramparts may be visible on radar imagery Sentinel-1 during the winter.

12.6 River Ice Thickness

Ice thickness before break-up may not be the same as ice thickness at break-up as ablation occurs, so these values may be overestimated.

12.7 Ice Jam Head and Toe Locations

The uncertainty in ice jam head and toe locations was tested in the analysis provided in Section 9.1.5.

12.8 Climate Change Projections

Climate change projections carry an inherent degree of uncertainty related to the use of multi-model ensembles (climate model outputs from multiple models and emissions scenarios) to assess climate change impacts. In Section 10.1 this uncertainty is described in further detail including four main sources: (1) natural variability in the climate system, (2) differences in climate model structure and response to radiative forcing, (3) the future trajectories of greenhouse gases (Charron 2016; IPCC 2021) and (4) downscaling methods applied.

Data sources for climate change projections used in the river ice thickness and river flow components of this study were described in Section 10.1. The use of multi-model ensembles used in this study include uncertainties described above and were assessed through the Monte Carlo framework. In the case of river ice thickness projections (estimated from the Can-DCS-M6 ensemble), the use of multiple climate models and emissions scenarios captures uncertainties related to climate model structure and future trajectories of greenhouse gases. For river flows (provided by Elshamy et al. (2025b) based on the CanRCM4 ensemble), the use of multiple sets of initial conditions represents uncertainty related to natural variability in the climate system. Incorporating both climate model ensembles in this study captured uncertainty in downscaling methods applied, as the Can-DCS-M6 ensemble is statistically downscaled while the CanRCM4 ensemble is dynamically downscaled.

These sources of uncertainty were carried through this study by considering the range of climate projections evaluated using statistical distributions as input to the Monte Carlo framework to simulate the associated range of projected climate change impacts through flood hazard mapping.

12.9 Future Flows

Based on Elshamy et al. (2025b), future flows stemming from MESH, used for the future ice jam flood hazard assessment, carry uncertainties that arise primarily from climate-model forcing, land-cover change assumptions, and changes in the cryosphere.

The simulations for the Mackenzie River Basin rely on bias-corrected and downscaled regional climate model forcings, and these introduce uncertainty because different climate models vary in their projections of temperature, precipitation, and snowmelt timing. These variations propagate directly into hydrological outputs such as the magnitude and timing of flow increases in spring.

The representation of permafrost thaw adds another layer of uncertainty, since the rate at which permafrost disappears influences subsurface connectivity, groundwater flow, and baseflow levels, and these processes depend on assumptions about soil thermal properties, projected warming rates, and how MESH parameterizes deep subsurface storage.

Land-cover change scenarios incorporated at discrete time steps create uncertainties because the timing and magnitude of vegetation shifts such as greening, shrubification, or forest-tundra transitions and are themselves difficult to predict. These changes modify evapotranspiration, snow accumulation, and surface energy balance, all of which influence modelled discharge. In addition, structural uncertainty arises from the way MESH represents cryospheric and hydrologic processes, including parameterisations of organic soils, snow dynamics, and groundwater pathways, which may not fully capture landscape heterogeneity across a large, complex basin.

Observational uncertainty in the datasets used for validation (e.g., discharge, snowpack, permafrost measurements) contributes to residual uncertainty in how confidently the model reproduces current conditions and, therefore, robustly it can project future flows.

13 RECOMMENDATIONS

Analysis of May 2021 geodetic water levels at Fort Good Hope has revealed a major discrepancy between ECCC recordings (Station 10L001) and high-water mark surveys. ECCC recordings (once converted to geodetic using the official conversion factor) underestimates the May 2021 maximum flood level by 2.7 m. The exact source of this error is unknown. The prevalence of this error of also unknown; and perhaps it could have affected other high-level readings. WSP suggests using great care when dealing with geodetic data coming from this station and continuing the discussions with ECCC to improve the reliability of Station 10LD001.

Hydrometric data at Fort Good Hope during break-up have been limited since the station operated by Environment and Climate Change Canada (10LD001) was seasonally-operated until 2024, though this will be improved going forward with the change to year-round operation. The gauge location also makes it vulnerable to ice-induced damages. WSP recommends adding a hydrometric station about 200 to 800 m from the mouth of Jackfish Creek to monitor Mackenzie River backwater levels . The new station could not be placed at the location of former Station 10LD002, as it is too far from the mouth and thus not representative of the Mackenzie River flood levels. Placing a gauge in the creek, instead of along the Mackenzie riverbank, would protect it against the ice and thus ensuring that it can record reliable water levels even during breakup season. A simple pressure sensor could be installed as soon as this winter (2026) below the ice cover, to acquire data during next breakup.

WSP also recommends monitoring the ice conditions at the entrance of the Ramparts, especially during ice jam and ice breakup seasons. We recommend installing a water level gauge and a trail camera to monitor the ice movement and get a better understanding of the release mechanisms and ice jam timings. A similar monitoring system (camera and gauge) is also recommended downstream of the Community. It could be placed next to an existing cabin, for easy access.

An enhanced hydrometric surveillance system of the Mackenzie River near Fort Good Hope would help understand and quantify important ice phenomena that currently can not be fully assessed, due to the scarcity of data and observations. Such a system would help understanding the conditions leading to ice jam formation upstream and downstream of the Community, as well as monitoring the passage of ice jam wave (jave).

14 SUMMARY

This report includes a summary of all aspects of the Fort Good Hope flood study and references data collected during previous studies at Fort Good Hope as well as reports and memorandums completed as part of this study, including:

- Valuable information was provided by the Sahtu Breakup Reports and the above-mentioned data sources to develop the May 2021 flood chronology report (WSP 2026b).
- Phase 1 study report (WSP 2025) with a summary of background information reviewed, flood history and hydrology, and describes development of the 2021 ice jam flood inundation maps (Appendix D).
- Fort Good Hope flood study survey memorandum (WSP 2026a) that summarizes the methods and results used to collect bathymetry data in July 2025.
- Flood chronology memorandum (WSP 2026b) that summarizes historical flood events at Fort Good Hope.

Highlights from the data review outlined in WSP (2025) included the following:

- A discrepancy was identified between the WSC gauge 10LD001 stage after converting to water surface elevation in CGVD2013 vertical datum and the observed 2021 peak water surface elevations during the ice jam event that were based on LiDAR and the high water mark survey.
- The potential for reviewing additional high water marks from the 2021 flood based on numerous drone and camera videos, photos, WSC gauge photos, aerial photos that are available has expanded the high water mark record for Fort Good Hope during the field survey in July 2025

Key results from the open water flood assessment include:

- Flood peaks observed on the Mackenzie River at the Arctic Red River gauge, being downstream of Norman Wells, were generally larger than the corresponding peak observed at Norman Wells except for the four largest peaks when the opposite occurred; in the latter cases this is likely due to attenuation of the extreme high flows due to constriction at the Ramparts.
- Using the flood frequency analysis results for the Norman Wells and Arctic Red River gauges, a regional flood frequency curve for the Mackenzie River was developed by plotting flood frequency results against drainage area and from this, results were obtained for Fort Good Hope.
- Flood magnitude and frequency results for the Rabbit Skin River and Jackfish Creek are based on existing relatively short records. These records could not be extended due to sparse hydrometric data in the region.

Highlights from the ice jam flood hazard assessment include:

- The empirical approach of non-dimensional discharge and stage was successfully implemented to estimate the ice jam flood hazard at the gauged community of Norman Wells. With a preliminary analysis of javes, this in turn allowed a successful extrapolation of the hazard assessment to the community of Fort Good Hope where only an open-water season gauge is installed.
- There is evidence from an analysis of the 2021 ice jam flood event that additional staging occurred at Fort Good Hope from ice jamming induced by an ice jam release wave (jave).

Draft May 2021 flood inundation maps were developed to support the community engagement activities planning in February 2025. The flood extent was confirmed based on 17 high water marks surveyed by Ollerhead (2023), with values ranging between 33.22 and 34.2 m (though the latter may be an outlier), and an average value of 33.63 m. The maximum flood water level was obtained by comparing the LiDAR elevations and the aerial images captured on May 25, 2021. The flood extent on LiDAR surface and images was compared for various water levels, and a value of 33.8 m was selected. During the engagement meetings, community members corroborated the flooded areas provided in the inundation maps and provided observations of potential high water mark locations that were visited in July 2025 and used in the hydraulic model calibration.

The 2021 flood chronology memorandum describes what led to the May 2021 flood in Fort Good Hope, observations made, and chronology of the event as it unfolded (WSP 2026b). Findings included:

- The winter of 2020-21 was one of the coldest since 1999 which resulted in thicker and more competent ice cover on the Mackenzie River.
- Freeze-up and winter water levels on the river prior to break-up were historically high and this may have contributed to more stable ice jams than at lower elevations.
- From May 18 to 24 (7 days), ice had cleared in front of Fort Good Hope but ice jams were still present upstream of the community at the Ramparts and downstream, below the Rabbit Skin River confluence. The ice jam at the Ramparts was very long. A series of ice jams and releases occurred.
- On May 24, 2021 at the end of the day, the ice jam upstream started to break. Initially river water levels rapidly decreased before starting to rise suddenly at the Fort Good Hope gauge.
- The maximum recorded water level was 33.8 m (CGVD13) on May 25, 2021 at 17:10. This was about 10 m higher than the average level over the gauge period of record.

- A series of ice jams and releases occurred between May 20 to 25, 2021 on the Mackenzie River near Fort Good Hope, which led to historical flood levels in the community and an evacuation order on May 25, 2021. The ice jam downstream of the community also caused flooding and damages at some cabins along the river.

This report summarized the bathymetric survey completed in July 2025 with support from the Guardians that provide improved river bathymetry, high water marks and ice scars that were used to calibrate the ice jam model (WSP 2026a).

This report outlines the modelling approach for ice jam flood analysis:

- Ice-specific model parameters are presented and include the ice thickness, the ice Manning's n coefficient, the ice specific gravity, the friction angle, the porosity, the stress k1 ratio, the maximum velocity, and the ice jam toe and head locations.
- The ice jam model is calibrated using two events observed on May 20, 2021 and 25, 2021. Calibration results compare the simulated and observed water elevations. The peak water level experienced in May 2021 at Fort Good Hope (33.8 m CGVD2013) corresponds approximatively to a 5% AEP (1 in 20 years average return period).
- The Monte Carlo Analysis used to estimate ice jam flood hazards is presented. Random values for each of the ice-specific model parameters are obtained within a defined range using statistical distributions. These distributions are either based on historical observed data or are obtained from literature. The Monte Carlo Analysis is performed several times to adjust these parameters. The results of the Monte Carlo Analysis are presented with water surface profiles for different floods (2, 5, 10, 20, 50, 100, 200 and 500-year floods).

Climate change data, methods and results used in this study were summarized in Section 10. To simulate future flow conditions, data were extracted from MESH—a basin-scale hydrological model that incorporates climate projections from global circulation models (GCMs). Simulations are conducted for two distinct future timeframes: the mid-century period (2040–2065), and the far future (2075–2100). An increase in flow discharges in the Mackenzie River is foreseen for these scenarios from the model projections. Furthermore, a trend to earlier dates of ice jam staging can be observed throughout this century.

Flood inundation maps for the 1% and 0.5% AEPs as well as the two climate change scenarios, are provided in Appendix E. The AEP maps are different than the event-based flood extent map (the 2021 flood inundation map) as the AEP maps represent a probabilistic event and not an actual event that really occurred. Results show limited expansion of the flooded area with increasing flood magnitudes.

Flood hazard maps for the 1% and 0.5% AEPs are also provided and can be found in Appendix F, along with flood hazard maps for the mid-century climate change scenario. Flood hazard maps include an ice-induced floodway and flood fringe areas. Flood impacts during the current condition 1% and 0.5% AEPs include:

- the same low-lying areas between the Mackenzie River and Jackfish Creek that flooded in May 2021, though the flooded extents are slightly larger;
- the westernmost portion of the community including the RCMP building are isolated from the rest of the community
- the low chord of Jackfish Creek Bridge is reached which could cause damage to the bridge. This bridge is important infrastructure as it is the only access between the community and the local airport.

Climate change flood hazard maps were also developed for the mid-century time period (Appendix H) and show increased water levels and slightly larger flood extents from current conditions. These maps show Jackfish Creek Bridge is overtopped for both the 0.5% and 1% AEP floods. Climate change results have higher uncertainty.

15 STUDY LIMITATIONS

WSP prepared this report solely for the use of the intended recipient, GNWT, in accordance with the professional services agreement between the parties. In the event a contract has not been executed, the parties agree that the WSP General Terms for Consultant shall govern their business relationship which was provided to you prior to the preparation of this report.

The report is intended to be used in its entirety. No excerpts may be taken to be representative of the findings in the assessment.

The conclusions presented in this report are based on work performed by trained, professional and technical staff, in accordance with their reasonable interpretation of current and accepted engineering and scientific practices at the time the work was performed.

The content and opinions contained in the present report are based on the observations and/or information available to WSP at the time of preparation, using investigation techniques and engineering analysis methods consistent with those ordinarily exercised by WSP and other engineering/scientific practitioners working under similar conditions, and subject to the same time, financial and physical constraints applicable to this project.

WSP disclaims any obligation to update this report if, after the date of this report, any conditions appear to differ significantly from those presented in this report; however, WSP reserves the right to amend or supplement this report based on additional information, documentation or evidence.

WSP makes no other representations whatsoever concerning the legal significance of its findings.

The intended recipient is solely responsible for the disclosure of any information contained in this report. If a third party makes use of, relies on, or makes decisions in accordance with this report, said third party is solely responsible for such use, reliance or decisions. WSP does not accept responsibility for damages, if any, suffered by any third party as a result of decisions made or actions taken by said third party based on this report.

WSP has provided services to the intended recipient in accordance with the professional services agreement between the parties and in a manner consistent with that degree of care, skill and diligence normally provided by members of the same profession performing the same or comparable services in respect of projects of a similar nature in similar circumstances. It is understood and agreed by WSP and the recipient of this report that WSP provides no warranty, express or implied, of any kind. Without limiting the generality of the foregoing, it is agreed and understood by WSP and the recipient of this report that WSP makes no representation or warranty whatsoever as to the sufficiency of its scope of work for the purpose sought by the recipient of this report.

In preparing this report, WSP has relied in good faith on information provided by others, as noted in the report. WSP has reasonably assumed that the information provided is correct and WSP is not responsible for the accuracy or completeness of such information.

The nature of the work undertaken is stochastic with substantial inherent uncertainly around any given data points. The reader acknowledges that the uncertainty associated with any projections or forecasts is increased with how far into the future the projected period extends and is subject to future developments or intervening acts which may manifest in the interim period.

The information in this report was prepared using published data and information, technical journals, articles as well as professional judgment and experience.

Benchmark and elevations used in this report are primarily to establish relative elevation differences between the specific testing and/or sampling locations and should not be used for other purposes, such as grading, excavating, construction, planning, or development.

Flood maps are limited spatially to the study area defined by GNWT (Figure 1-1) as the ice jam model is set up using the locations of historical ice jams downstream of Fort Good Hope and simulates the backwater at the community. Model results obtained further downstream of the study area do not accurately represent ice jam conditions and would likely underestimate water levels in those areas. In the same way, model result outside the study area near the Ramparts may also be inaccurate.

.

Signature Page

WSP Canada Inc.

PREPARED BY:

Andréa Mellado, M.Sc.
Hydraulic and River Ice Support

Karl-Erich Lindenschmidt, Ph.D.
Academic Research Collaborator

Ed Hunt, P.Eng. (NT/NU)
Bathymetry and Survey Lead

Patrick Breach, Ph.D.
Climate Change Advisor

Jaime Hogan, M.Sc.
Hydrologist

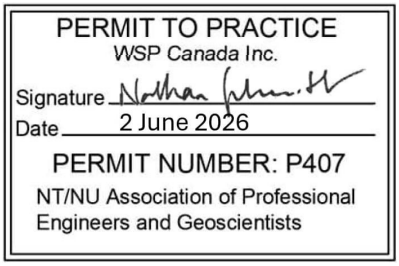

REVIEWED BY:

Martin Lacroix, M.Sc.
Principal Water Resource Consultant

Nathan Schmidt, Ph.D., P.Eng. (NT/NU)
Senior Principal Water Resources Engineer

Janya Kelly, Ph.D.
Lead Advisor – Climate Risk and Resilience

Simon Nolin, M.Sc.
Hydraulic Engineer & Ice Expert

16 REFERENCES

Andres DD. 1980. The breakup process and the documentation of the 1978 ice jams on the Athabasca River at Fort McMurray. In *Proceedings, Workshop on Hydraulic Resistance of River Ice, 23-24 September 1980, Burlington, Ontario*, p.143-161.

Andres DD, Doyle PF. 1984. Analysis of breakup and ice jams on the Athabasca River at Fort McMurray, Alberta. *Canadian Journal of Civil Engineering,* 11: 444-458.

Ashton GD. 1986. River and Lake Ice Engineering. Water Resources Publications, Colorado, USA. ISBN: 0-918334-59-4.

Beltaos S. 1978. Field investigations of river ice jams. In *Proceedings, IAHR Symposium on Ice Problems, 7-9 August 1978, Lulea, Sweden,* vol. 2, p. 355-371.

Brackenbury M. 2021a. May 25, 2021. State of emergency declared in Fort Good Hope as flood waters rise. Cabin Radio. **State of emergency declared in Fort Good Hope due to flooding**

Brackenbury M. 2021b. May 26, 2021. Water recedes in Fort Good Hope, community remains alert. Cabin Radio. **https://cabinradio.ca/63895/news/environment/water-recedes-in-fort-good-hope-community-remains-alert/**

Cannon AJ. 2024. The Impact of “Hot Models” on a CMIP6 Ensemble Used by Climate Service Providers in Canada: Do Global Constraints Lead to Appreciable Differences in Regional Projections? Journal of Climate, 37(6), 2141-2154. doi: 10.1175/JCLI-D-23-0459.1.

CBC News, May 18, 2021. Fort Good Hope remains on flood watch as water levels waver. **https://www.cbc.ca/news/canada/north/fort-good-hope-flood-watch-1.6030809**

Charron I. 2016. A Guidebook on Climate Scenarios: Using Climate Information to Guide Adaptation Research and Decisions, 2016 Edition. Ouranos, 94p. ISBN: 978-2-923292-21-2.

Chen H, Sun J, Lin W, Xu W. 2020. Comparison of CMIP6 and CMIP5 models in simulating climate extremes. Science Bulletin Vol 65 pp1415 – 1418.

ClimateData.ca. 2025. Climate Data for a Resilient Canada: Download. Available at: **https://climatedata.ca/download/**

Copernicus Browser. 2025. **https://browser.dataspace.copernicus.eu/**

Das A, Lindenschmidt K.-E. 2021. Evaluation of sensitivity of hydraulic model parameters, boundary conditions and digital elevation models on ice jam flood delineation. *Cold Regions Science and Technology*. **https://doi.org/10.1016/j.coldregions.2020.103218**

Dehghani Sanij M, Lindenschmidt K-E, Elshamy M. (submitted) Shifts in ice jam flood hazard due to climate change along the Mackenzie River. *Canadian Water Resources Journal*.

DFO. 2024. *CHS Nautical Charts 6421 and 6422.* **https://www.charts.gc.ca/charts-cartes/purchase-achat/index-eng.html**

DFO. 2025. *CHS NON-Navigational (CHS NONNA)*. **https://data.chs-shc.ca/dashboard/map**

Elshamy ME, Pomeroy J, Pietroniro A, Wheater H, Abdelhamed M, Davison B. 2024a. Land Surface Hydrological Modelling of the Mackenzie River Basin: Parametrization to Simulate Streamflow and Permafrost Dynamics. *Journal of Hydrology*. https://doi.org/10.2139/SSRN.4791947

Elshamy ME, Pomeroy JW, Pietroniro A, Wheater H, Abdelhamed MS. 2024b. The impact of climate and land cover change on the cryosphere and hydrology of the Mackenzie River Basin, Canada. *Water Resource Research*. https://doi.org/10.22541/essoar.173082837.77691678/v1

Elshamy ME, Pomeroy J, Pietroniro A, Wheater H, Abdelhamed M, Davison B. 2025a. Land Surface Hydrological Modelling of the Mackenzie River Basin: Parametrization to Simulate Streamflow and Permafrost Dynamics. *Journal of Hydrology*. https://doi.org/10.1016/j.jhydrol.2025.133134

Elshamy ME, Pomeroy JW, Pietroniro A, Wheater H, Abdelhamed MS. 2025b. The impact of climate and land cover change on the cryosphere and hydrology of the Mackenzie River Basin, Canada. *Water Resource Research*. https://doi.org/10.1029/2024WR039276

ECCC (Environment and Climate Change Canada). 2024a.. Hydrometric Data Search. Available at : Daily Water Level Graph for MACKENZIE RIVER AT FORT GOOD HOPE (10LD001) [NT] - Water Level and Flow - Environment Canada.

ECCC (Environment and Climate Change Canada). 2024b. Ice thickness data. Ice Thickness Program Collection, 1947 to 2002. https://www.canada.ca/en/environment-climate-change/services/ice-forecasts-observations/latest-conditions/archive-overview/thickness-data.html

GNWT (Government Northwest Territories). 2014. Sahtu Region Hazard Identification Risk Assessment (HIRA) – Annex D. Municipal and Community Affairs. https://www.maca.gov.nt.ca/sites/maca/files/resources/hira-sahtu_final.pdf

GNWT (Government Northwest Territories). 2024. NWT Water Monitoring Bulletin – May 18, 2024 at 17:00. https://www.gov.nt.ca/ecc/sites/ecc/files/resources/ecc_spring_break_up_report_2024_05_18.pdf

GNWT (Government Northwest Territories). 2025. Be Ready for Floods. Municipal and Community Affairs, Government of Northwest Territories. Webpage accessed March 2026. Available at: https://www.maca.gov.nt.ca/en/services/be-ready-emergencies/be-ready-floods.

GNWT (Government Northwest Territories). 2026. Planning in Flood Hazard Areas. A Guide for NWT Community Governments on the Community Plan Review Process. February 2026, 27p. Available at: https://www.maca.gov.nt.ca/sites/maca/files/resources/planning_in_flood_hazard_areas_guide_1.pdf

Gringorten II. 1963. A plotting Rule for Extreme Probability Paper. Journal of Geophysical Research. Vol. 68, No. 3. 813-814pp.

Hawkes PJ. 2008. Joint probability analysis for estimation of extremes. *Journal of Hydraulic Research.* Vol. 46. Extra Issue 2. pp.246-256. International Association of Hydraulic Engineering and Research.

HRD Alaska, Inc. Ice Processes in the Susitna River Study. Study Plan Section 7.6. 2014-2015 Study Implementation Report. Appendix B. Technical Memorandum: River1D Model – Initial Open Water Calibration and Validation. Prepared for Alaska Energy Authority. Prepared by: HDR Alaska, Inc., University of Alberta. October 2015. https://susitna-watanahydro.org/wp-content/uploads/2015/11/07.6_ICE_ISR_PartD.pdf

IPCC (Intergovernmental Panel on Climate Change). 2021a. Climate Change 2021: The Physical Science Basis. Contribution of Working Group I to the Sixth Assessment Report of the Intergovernmental Panel on Climate Change. Cambridge University Press, Cambridge, United Kingdom and New York, NY, USA, 3949 pp.

Knowles WL, Hodgins DB. 1980 Evaluation of ice jam roughness, Thames River, Ontario. In Proceedings, Workshop on Hydraulic Resistance of River Ice, 23-24, September 1980, Burlington, Ontario, p. 281-294.

Korbaylo BW, Shumilak BE. 1999. A case study: Lower Churchill River water level enhancement weir project. In Proceedings, 10th Workshop on River Ice, 9-11 June 1999, Winnipeg, Manitoba, p. 135-149.

Lamberink L., 2021. State of emergency declared in Fort Good Hope as flood waters rise. CBC News. https://www.cbc.ca/news/canada/north/flooding-alarm-fort-good-hope-1.6039536

Lindenschmidt K-E, Coles A, Saade Jad. 2024a. Reach-Based Extrapolation to Assess the Ice Jam Flood Hazard of an Ungauged River Reach along the Mackenzie River, Canada. *Water* **2024**, *16,* 1535. https://doi.org/10.3390/w16111535

Lindenschmidt K-E, 2024b. River Ice Processes and Ice Flood Forecasting – A Guide for Practitioners and Students (pp. 285-343). Switzerland AG: Springer Nature.

Lindenschmidt K-E, Gomez S, Saade J, Perry B, Das A. 2025. Empirical modelling of ice jam flood hazards along the Mackenzie River in a changing climate. *Water* **17**: 2288. https://doi.org/10.3390/w17152288 McElhanney Ltd. 2021. NWT Flood Mapping: Fort Good Hope Data Capture & Processing Report. Submitted to Government of Northwest Territories. March 11, 2021. 10 p.

Loney, D. A., 2021. Calibration, Validation, and Sensitivity Approach. Reclamation, Technical Service Center. https://deltacouncil.ca.gov/pdf/science-program/presentations/2023-09-12-wtmp-final-peer-review-cal-val-sens-approach.pdf

McElhanney Ltd. (2021). NWT Flood Mapping: Fort Good Hope, Data Capture and Processing Report. Submitted to GNWT March 11, 2021. 10 p.

Michel B. 1971. Winter regime of rivers and lakes. USACE CRREL Monograph M III-B1a, Hanover, NH, 131 p.

Northwest Hydraulic Consultants Ltd. 2025. Kátłodeh (Hay River) Flood Hazard Mapping Study Summary Report. Prepared for Government of Northwest Territories, May 15, 2025. NHC Reference No. 1008469. 76p.

NRCan. 2021. RCM RADARSAT Constellation Mission Data and Products. Government of Canada. https://search.open.canada.ca/openmap/5e6b40bf-299f-4e05-87c8-d10b9c8210f9

NRCan. 2025. High Resolution Digital Elevation Model HRDEM) - CanElevation Series. Available at: High Resolution Digital Elevation Model (HRDEM) - CanElevation Series - Open Government Portal.

Ollerhead & Associates Ltd. 2021. Spring 2021 flood level mapping in the communities of Fort Simpson and Jean Marie River, Northwest Territories. Whitehorse: Ollerhead & Associates Ltd.

PlanIt North, 2023. Field notes to inform a flood level survey to document 2023 and 2021 high water levels in Fort Good Hope. Report last updated 10 October, 2023. Field work by Christine Wenman and Twyla Edgi. Compilation by Tineke Kippers and Christine Wenman.

Rivard G, Kemp T, Gerard RL. 1984. Documentation and analysis of the water level profile through an ice jam, Mackenzie River, Northwest Territories. In *Proceedings, Workshop on the Hydraulics of River Ice, 20-21 June 1984, Fredericton, New Brunswick,* p.141-157.

Saade, Jad. 2025. Email sent by Jad Saade entitled RE: February Progress Meeting to WSP on March 4th, 2025.

Stephan J. 1891. Über die Theorie der Eisbildung. Monatshefte für Mathematik und Physik, 1: 1-6. https://doi.org/10.1007/BF01692459.

Turcotte B, Saal S. 2022. Flooding in Dawson: Exposure analysis and risk reduction recommendations. Presented to the Infrastructure Branch of the Department of Community Services, Government of Yukon, YukonU Research Centre, Yukon University, 90 p.

Tuthill AM, Mamone AC. 1998. Structural ice control alternatives for middle Mississippi River. *ASCE Journal of Cold Regions Engineering,* 12(4): 202-220.

U.S. Army Corps of Engineers (USACE). 2024. HEC-RAS River Analysis System, User's Manual Version 6.6. Davis, CA. **https://www.hec.usace.army.mil/confluence/rasdocs/rasum/latest**

U.S. Army Corps of Engineers (USACE). 2025. HEC-RAS User's Manual. **https://www.hec.usace.army.mil/confluence/rasdocs/rasum/latest**

Vogel RM, Roots MJ. 1981. The effect of floating ice jams on the magnitude and frequency of floods along the Missisquoi River in Northen Vermont. In *Proceedings, IAHR International Symposium on Ice, 27-31 July 1981, Quebec City, Canada,* vol. 1, p. 347-359.

WSC (Water Survey Canada). 2025. Vertical datum information for 10LD001 **https://wateroffice.ec.gc.ca/report/datum_e.html?stn=10LD001&mode=Graph**

WSP (WSP Canada Inc.). 2025. Government of Northwest Territories Fort Good Hope Flood Inundation and Hazard Mapping Study. Phase 1: Hydrology and Hydraulics Report. Final Report Submitted June 12, 2025. 102 p.

WSP. 2026a. Summary of Bathymetry and Topographic Surveys at Fort Good Hope. Final Report. Prepared for the Government of Northwest Territories, March 27, 2026. 9 p.

WSP. 2026b. Fort Good Hope 2021 Breakup Chronology. Prepared for Government of Northwest Territories, March 26, 2026. 18 p.